AGU PUBLICATIONS

Reviews of Geophysics

REVIEW ARTICLE
10.1002/2015RG000500

Key Points:
- The fast-developing Asia has suffered severe air pollution problem
- Aerosol affects the Asian monsoon
- Aerosol-monsoon interactions dictate the climate change in the region

Correspondence to:
Z. Li,
zli@atmos.umd.edu

Citation:
Li, Z., et al. (2016), Aerosol and monsoon climate interactions over Asia, *Rev. Geophys.*, *54*, 866–929, doi:10.1002/2015RG000500.

Received 29 JUL 2015
Accepted 6 SEP 2016
Accepted article online 10 SEP 2016
Published online 15 NOV 2016

Aerosol and monsoon climate interactions over Asia

Zhanqing Li[1,2], W. K.-M. Lau[2], V. Ramanathan[3], G. Wu[4], Y. Ding[5], M. G. Manoj[2], J. Liu[2], Y. Qian[6], J. Li[1], T. Zhou[4], J. Fan[6], D. Rosenfeld[7], Y. Ming[8], Y. Wang[9], J. Huang[10], B. Wang[11,12], X. Xu[13], S.-S. Lee[2], M. Cribb[2], F. Zhang[1], X. Yang[1], C. Zhao[1], T. Takemura[14], K. Wang[1], X. Xia[4], Y. Yin[12], H. Zhang[5], J. Guo[13], P. M. Zhai[13], N. Sugimoto[15], S. S. Babu[16], and G. P. Brasseur[17]

[1]State Key Laboratory of Earth Surface Processes and Resource Ecology and College of Global Change and Earth System Science, Beijing Normal University, Beijing, China, [2]Department of Atmospheric and Oceanic Science and ESSIC, University of Maryland, College Park, Maryland, USA, [3]Department of Atmospheric and Climate Sciences, University of California, San Diego, California, USA, [4]Institute of Atmospheric Physics, Chinese Academy of Sciences, Beijing, China, [5]National Climate Center, China Meteorological Administration, Beijing, China, [6]Pacific Northwest National Laboratory, Richland, Washington, USA, [7]Institute of Earth Sciences, Hebrew University, Jerusalem, Israel, [8]Geophysical Fluid Dynamic Laboratory, NOAA, Princeton, New Jersey, USA, [9]Jet Propulsion Laboratory, California Institute of Technology, Pasadena, California, USA, [10]College of Atmospheric Sciences, Lanzhou University, Lanzhou, China, [11]Department of Atmospheric Sciences, University of Hawaii, Honolulu, Hawaii, USA, [12]School of Atmospheric Physics, Nanjing University of Information Science and Technology, Nanjing, China, [13]Chinese Academy of Meteorological Sciences, Beijing, China, [14]Research Institute for Applied Mechanics, Kyushu University, Fukuoka, Japan, [15]National Institute for Environmental Studies, Tsukuba, Japan, [16]Space Physics Laboratory, Vikram Sarabhai Space Centre, Thiruvananthapuram, India, [17]Max Planck Institute for Meteorology, Hamburg, Germany

Abstract The increasing severity of droughts/floods and worsening air quality from increasing aerosols in Asia monsoon regions are the two gravest threats facing over 60% of the world population living in Asian monsoon regions. These dual threats have fueled a large body of research in the last decade on the roles of aerosols in impacting Asian monsoon weather and climate. This paper provides a comprehensive review of studies on Asian aerosols, monsoons, and their interactions. The Asian monsoon region is a primary source of emissions of diverse species of aerosols from both anthropogenic and natural origins. The distributions of aerosol loading are strongly influenced by distinct weather and climatic regimes, which are, in turn, modulated by aerosol effects. On a continental scale, aerosols reduce surface insolation and weaken the land-ocean thermal contrast, thus inhibiting the development of monsoons. Locally, aerosol radiative effects alter the thermodynamic stability and convective potential of the lower atmosphere leading to reduced temperatures, increased atmospheric stability, and weakened wind and atmospheric circulations. The atmospheric thermodynamic state, which determines the formation of clouds, convection, and precipitation, may also be altered by aerosols serving as cloud condensation nuclei or ice nuclei. Absorbing aerosols such as black carbon and desert dust in Asian monsoon regions may also induce dynamical feedback processes, leading to a strengthening of the early monsoon and affecting the subsequent evolution of the monsoon. Many mechanisms have been put forth regarding how aerosols modulate the amplitude, frequency, intensity, and phase of different monsoon climate variables. A wide range of theoretical, observational, and modeling findings on the Asian monsoon, aerosols, and their interactions are synthesized. A new paradigm is proposed on investigating aerosol-monsoon interactions, in which natural aerosols such as desert dust, black carbon from biomass burning, and biogenic aerosols from vegetation are considered integral components of an intrinsic aerosol-monsoon climate system, subject to external forcing of global warming, anthropogenic aerosols, and land use and change. Future research on aerosol-monsoon interactions calls for an integrated approach and international collaborations based on long-term sustained observations, process measurements, and improved models, as well as using observations to constrain model simulations and projections.

1. Introduction

The earliest description of the summer monsoon phenomenon on record may date back to some 4000 years ago in the era of Chinese King Shun (~22–23th centuries B.C.) in a Chinese ancient poem called "Southerly Wind" [*Zeng*, 2005; *An et al.*, 2015]:

Gently blows the southerly wind,
That eases my people's resentment,

Timely comes the southerly wind,
That makes my people's wealth grow.

The earliest literature about the winter monsoon can be found in a poem entitled "Northerly Wind" [*An et al*., 2015] in the Book of Odes (the earliest Chinese poetry anthology, Shi Jing) about 3000 years ago:

Cold blows the northerly wind,
Thickly falls the snow....
The northerly wind whistles,
The snow falls and drifts about the snow white.

Ye et al. [1958] noted two abrupt seasonal changes in general atmospheric circulation in June and October over the Northern Hemisphere. The monsoon, originally defined as the seasonal reversal in prevailing winds [*Ramage*, 1971; *B. Wang et al*., 2010], now refers to more general seasonal changes in multiple meteorological variables, especially the strong seasonal contrast in precipitation [*Webster*, 1987; *Wang*, 1994; *Webster et al*., 1998; *Wang and Ding*, 2008]. It is ultimately driven by the seasonal variation in incoming solar radiation reaching the Earth's surface [*Lau and Li*, 1984; *Krishnamurti*, 1985; *Wang*, 2006; *Wu et al*., 2007; *Xu et al*., 2010]. The differential surface heating between continental land and the oceans through the interactions between surface turbulent heat fluxes and latent heating associated with rainfall and deep convection produces strong pressure gradients between the land and ocean. These gradients drive the large-scale circulation that governs the monsoon climate. The precipitation associated with the monsoonal circulation is critical for the social and economic well-being of billions of people. As such, monsoons have been an active research subject for over half a century, especially since the Monsoon Experiment of 1978–1979 during the First Global Atmosphere Research Plan Global Experiment where the majority of studies focused on the Asian monsoon (AM) system [*Ding et al*., 2015].

Inhabited by over 60% of the world's population, the AM region spanning South Asia, Southeast Asia, and East Asia have economies that are crucially dependent on weather and climate fluctuations governed by the AM. The AM is one of the most dramatic and important among all climatic phenomena on Earth, with profound effects on the Earth's energy budget and hydrological cycle [*Ye et al*., 1958; *Sikka*, 1980; *Ding*, 1994; *Goswami*, 2005; *Chang et al*., 2005, 2010; *Ding and Sikka*, 2006; *Ding et al*., 2015]. In recent years, there has been a substantially increased understanding of the AM because of the availability of comprehensive and diverse data from ground-based and remote sensing observations, as well as data assimilation and modeling. The AM region is unique in its particular geography, topography, demography, and developmental history, including myriad forcings from both natural and anthropogenic sources.

Relative to many other monsoon systems, the AM is uniquely influenced by the Tibetan Plateau (TP), whose role in the AM can hardly be overstated [*Wu et al*., 2007; *Wu et al*., 2012a]. The TP, a source of elevated thermal and mechanical forcing, plays an important role in driving the monsoon circulation and moisture convergence patterns. These patterns strongly influence the timing and duration of the AM [*Li and Yanai*, 1996; *Yanai and Wu*, 2006]. Rising motion forced by the dramatic rise of the massive TP transports atmospheric moisture upward where it accumulates in the middle of the troposphere [*Xu et al*., 2008].

The AM exhibits a diverse and strong spatiotemporal variability. Over the last few decades, ample studies have been carried out on the AM variability on diurnal to multidecadal timescales, aimed at understanding the physical processes governing these variations. The causative factors of the spatiotemporal variability vary over a wide physical realm including both extraterrestrial natural forcing and internal dynamical feedbacks within the climate system. Changes in surface conditions (land cover changes or urbanization) [*Fu*, 2003] and atmospheric composition (e.g., greenhouse gases (GHGs) and aerosols) [*Ramanathan and Feng*, 2009] associated with anthropogenic factors can alter the monsoon climate.

As the world's most populated and fast-developing region, Asia is particularly vulnerable to human activities. In recent decades, the rapid industrialization and modernization of Asian countries has greatly increased the loading of aerosols in the atmosphere and has aggravated the adverse effects of aerosols on humans and the environment. The Intergovernmental Panel on Climate Change (IPCC) reports [*IPCC*, 2007, 2013] have noted that the increasing occurrence of floods and droughts in different parts of the world, in addition to causing dramatic landscape changes, may also be linked to anthropogenic activities that generate GHGs and aerosols [*Fu*, 2003]. While global change has been a primary concern for all countries around the world for a long time,

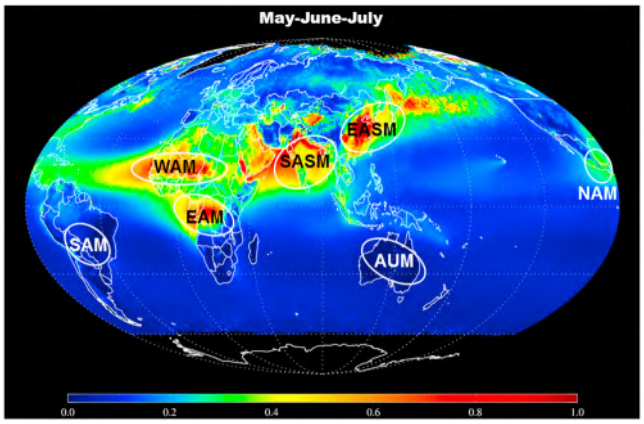

Figure 1. Global map of aerosol optical depth at 550 nm derived from MODIS (May–July, 2003–2015) using the Deep Blue algorithm over land [*Hsu et al.*, 2013] and the Dark Target ocean algorithm over oceans [*Levy et al.*, 2013] (courtesy of Jaehwa Lee of NASA/GFSC). Superimposed are the locations of the world's major monsoon systems. From left to right: SAM, South American monsoon; WAM, West African monsoon; EAM, East African monsoon; SASM, South Asian summer monsoon; EASM, East Asian summer monsoon; AUM, Australian monsoon; NAM, North American monsoon.

no place or period has witnessed changes more significant than Asia over the last few decades. Being the largest source of emissions in the world, the anthropogenic impact on climate is likely strongest given the extent, amplitude, and pace of changes taking place in Asia. Asia thus holds a key to unlocking some of the mysteries with regard to the attribution of climate changes to natural and anthropogenic causes.

The world's major monsoon systems are chiefly located in regions that experience major aerosol episodes, such as heavy pollution events in East and South Asia, and dust and biomass burning in Africa. Aerosol loading is arguably heaviest in the regions dominated by the East Asian summer monsoon (EASM) and the South Asian summer monsoon (SASM), as shown in the global map of AOD distribution and the major monsoon systems (Figure 1). Intensive human activities in the region are major contributors to aerosols (primarily sulfate, organic carbon (OC), black carbon (BC), nitrate, etc.) [*Q. Zhang et al.*, 2012]. Different types of aerosols may have completely different effects on climate. This multifaceted influence makes aerosols one of the least predictable elements in weather and climate modeling.

Extensive studies concerning the roles of aerosols in the Earth's climate did not begin until the 1990s when sulfate aerosols were found to play a key role in offsetting the global warming effect [*IPCC*, 2013], but studies concerning the effect of aerosols in weather events including interactions with the monsoon did not start until recently. Since the 2000s, particular attention has been paid to the rapid increase in air pollution and its impact on climate in Asia where intensive field campaigns were carried out, as summarized by *Lau et al.* [2008]. An increasing number of ground-based networks, balloon-borne and aircraft observations, special field campaigns, and satellite observations have helped gain a wealth of new information regarding the characteristics and climate effects of aerosols in Asia. They include, to name a few, the Indian Ocean Experiment (INDOEX) [*Ramanathan et al.*, 2001b], the Atmospheric Chemistry Experiment in Asia (ACE-Asia) [*Huebert et al.*, 2003], the Atmospheric Brown Clouds project [*Ramanathan et al.*, 2005; *Nakajima et al.*, 2007], the East Asian Study of Tropospheric Aerosols: an International Regional Experiment (EAST-AIRE) [*Li et al.*, 2007a], and the East Asian Studies of Tropospheric Aerosols and Impact on Regional Climate (EAST-AIRC), which includes the deployment of the U.S. Department of Energy's Atmospheric Radiation Measurement (ARM) Mobile Facility (AMF) deployment in China (AMF-China) [*Li et al.*, 2011a].

Aerosols can affect radiation, monsoon rainfall, and regional climate change through radiative forcing and microphysical effects [*Rosenfeld*, 2000; *Li*, 2004; *Nakajima et al.*, 2007; *Li et al.*, 2007a, 2011a, 2011b; *Huang et al.*, 2014; *Guo et al.*, 2016]. Many general circulation model (GCM) studies have investigated the impacts of aerosols on the global and regional changes in precipitation [*Menon et al.*, 2002; *Lau et al.*, 2008; *B. Wang et al.*, 2009; *Bollasina et al.*, 2011, 2013; *Cowan and Cai*, 2011; *Ganguly et al.*, 2012]. Elevated deep layers of light-absorbing aerosols can potentially affect the water cycle by significantly altering the energy balance [*Ramanathan et al.*, 2005; *Lau and Kim*, 2006; *Lau et al.*, 2006]. Despite the large number of studies, there still exist many large gaps in our knowledge and understanding of Asian aerosols and their climate effect. Aerosol processes are still poorly observed and treated in numerical models.

This paper is mainly focused on interactions between aerosols and key meteorological variables associated with the EASM and the SASM, for which a vast literature of recent studies about SASM from China and India where changes are most drastic and extensive exists. As such, the bulk of the paper is devoted to

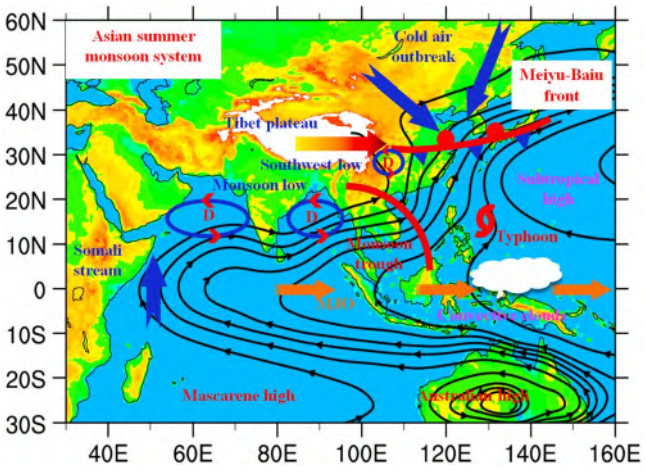

Figure 2. A schematic of the dominant major large-scale low-level moisture transport pathways and weather systems over the Asia-West Pacific region. Colored arrows show the movement of air associated with a given weather system like low-pressure systems (denoted by "D") or atmospheric phenomenon like the Madden-Julian Oscillation (MJO).

these two places, although other Asian countries and their immediate neighboring downstream regions across the Pacific Rim are also considered.

The paper is structured as follows. We first give an overview of the onset and evolution of the AM system and general trends in climate change in Asia. The mechanisms by which aerosols affect climate are described in section 3. The potential roles of aerosols on the Asian climate and its changes are reviewed in sections 4 and 5 from observational and modeling studies, respectively. Conversely, how the monsoon circulation modulates aerosols is discussed in section 6. Concluding remarks, including a synthesis of current findings and a new paradigm for furthering aerosol-monsoon studies in the future, are presented in section 7.

2. Overview of the Asian Monsoon System

The AM covers the geographic regions of South Asia, Southeast Asia, and Central and East Asia. It is the largest component of the global monsoon system, characterized by distinct wet (June-July-August) and dry (December-January-February) seasons, referred to, respectively, as the Asian summer monsoon (ASM) and the Asian winter monsoon (AWM). The prevailing low-level monsoon winds are southwesterlies during the ASM (Figure 2) and reversed during the AWM. The marked global monsoon seasonality in precipitation and winds stems from the large-scale thermal contrast arising from the different heat capacities of land and ocean in response to the seasonal changes in solar radiation reaching the Earth's surface. In the two months (April and May) leading up to the ASM, the major tropical and subtropical land masses of the Northern Hemisphere (northern Africa, the Middle East, India, and Southeast and East Asia) heat up much faster than the ocean. In turn, the surface thermal contrast is translated through surface heat fluxes, convection, and large-scale upward motions into strong tropospheric pressure gradients, which drive strong monsoon seasonal winds and heavy precipitation. The AWM is one of the most conspicuous climate systems found in the Northern Hemisphere during the boreal winter. It comprises the Siberian High, the East Asian trough, and the East Asian jet stream. The Siberian High plays an important role in largely determining the strength of the AWM. Along the eastern flank of the Siberian High, a strong northwesterly bifurcates to the south of Japan, the subtropical North Pacific, and along the east coast of East Asia. During the AWM, the land-sea thermal is reversed, with the tropical/subtropical landmasses of the Northern Hemisphere much colder than the tropical oceans to the south. The AWM region is then dominated by large-scale downward motion and suppressed precipitation.

Depending on the onset, evolution, and spatial coherence of winds and precipitation, the ASM can be broadly subdivided into two major components, i.e., the SASM and the EASM [*Lau and Li*, 1984; *Webster et al.*, 1998; *Lau et al.*, 2000]. Further regional subdivisions were also proposed that include the Southeast Asian monsoon, the South China Sea (SCS) monsoon, and the Western North Pacific monsoon [*Lau and Yang*, 1997; *Wang et al.*, 2003; *B. Wang et al.*, 2009]. Conventionally, and to a first order of approximation, the AWM can be considered the mirror image of the ASM in terms of the transition from the wet to the dry season and the reversal of the prevailing direction of the monsoon winds.

2.1. Characteristics of Asian Monsoon Onset, Evolution, and Driving Forces

The onset of the ASM begins over the eastern part of the Bay of Bengal (BOB) at the end of April [*Lau and Yang*, 1997; *Wu and Zhang*, 1998; *Wang and Ho*, 2002; *Zhang et al.*, 2002; *Wu et al.*, 2012c, 2013], followed

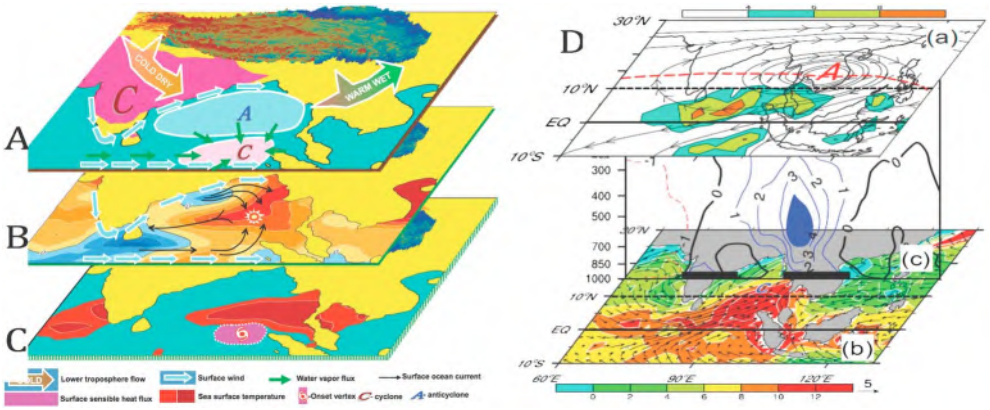

Figure 3. (left) Formation of the Bay of Bengal (BOB) warm pool and monsoon onset vortex due to the Tibetan Plateau forcing. Color shading in pink in A and C indicates surface sensible heating, and in red in C denotes the SST warm Pool. (right) Vertical coupling between upper and lower circulations during monsoon onset. The contour in the vertical cross section (c) is diabatic heating in K d^{-1}. See text for details. Copied from *G. X. Wu et al.* [2014].

by an onset over the Indo-China peninsula in early May and over the SCS in mid-May [*Lau and Yang*, 1997] (Figure 1). An exception is the early start of the rainy season in southeast China (sometimes referred to as the presummer rainy season in April and May). *Xu et al.* [2010] have suggested that it could start as early as in March due to an early reversal of surface sensible heating fluxes from the winter to summer transition over the TP. As the seasonal diabatic heating fluxes shift toward the northeast, the rainband expands. This explains the observed progression of the Mei-Yu rainband from the southwest to northeast. Having the Pacific Ocean to the east, the SCS and the Indian Ocean to the south, and the TP at its center, the AM is not only characterized by a seasonal change in wind and circulation but also by extreme weather systems [*Huang*, 2004; *R. H. Huang et al.*, 2007; *G. X. Wu et al.*, 2012b]. Frequent drought, cold air outbreaks and heat waves, extreme precipitation, tropical cyclones, and other natural disasters have seriously disrupted livelihoods and have resulted in severe economic losses.

The detailed mechanisms behind the onset of the BOB monsoon and the coupling between the upper and low tropospheric monsoon circulations are shown in Figure 3 in four major phases as proposed by *G. X. Wu et al.* [2014].

(A) During boreal spring, the cold and dry northwesterly over India induced by TP forcing generates strong surface sensible heating and cyclone circulation. The strong southwesterly along the western shores of the BOB forces a surface anticyclonic circulation over the northern BOB and a cyclonic circulation over its south. (B) The strong southwesterly along the western shores of the BOB causes an offshore current and upwelling, and a cold sea surface temperature (SST). In the eastern-central BOB, strong solar radiation and weak surface winds provide plentiful energy to the ocean. (C) A strong springtime SST warm pool and surface sensible heating are formed there, and the BOB monsoon onset vortex (MOV) is generated. (D) Due to the TP forcing in spring, the South Asia High (the blue "A" in slice A of Figure 3) is strengthened and the maximum divergence pumping is located over the southeastern BOB (stream function, (a), and divergence (shading, 10^{-6} s^{-1}) at 150 hPa in slice D of Figure 3), just over the strong SST warm pool and the MOV (the yellow spiral in slice C of Figure 3; SST in °C (shading, (b) in slice D of Figure 3); and surface wind (arrows) in m s^{-1}). This coupling leads to the BOB monsoon onset accompanied by a strong convective latent heat release of more than 4 K d^{-1} (vertical cross section at 15°N of diabatic heating in K d^{-1}, (c) in slice D of Figure 3).

2.2. Roles of the Tibetan Plateau, the Indian Ocean, and the South China Sea

Unlike the world's other major monsoon systems, the ASM is uniquely altered and driven by the TP. A theory, called the TP air-pump theory, put forth several decades ago and revised recently, proposed that the massive release of heat from the surface of the TP is a major contributor to the strength of the monsoon [*Yeh et al.*, 1957; *Luo and Yanai*, 1984; *Yanai and Wu*, 2006; *Wu et al.*, 2007; *Houze*, 2012]. Atmospheric heating over the TP can enhance East Asian (EA) subtropical frontal rainfall through two distinct Rossby wave trains and

the isentropic uplift to the east of the TP, which deforms the western Pacific subtropical high and enhances moisture convergence toward the EA subtropical front [*Wang et al*., 2008]. More recently, an alternate viewpoint based on theoretical and modeling studies has been proposed, suggesting that the orographic forcing by the Himalayan escarpment isolating extratropical influences, rather than the thermal forcing by the TP, is more important in generating the mean climate of the Indian monsoon [*Boos and Kuang*, 2010; *Boos and Kuang*, 2013]. Today, the relative importance of the TP in generating a strong Indian monsoon mean climate by insulating the thermal maximum from cold and dry extratropical air, or by providing a source of elevated heating, remains a subject of debate [*G. X. Wu et al*., 2012d; *Boos and Kuang*, 2013]. Many previous studies have shown the importance of TP thermal forcing in driving the variability of the ASM climate [*Li and Yanai*, 1996; *Hsu et al*., 1999; *Lau et al*., 2006]. From an aerosol perspective, dust and BC aerosols trapped over the Indo-Gangetic Plain (IGP) and the Himalayan foothills can alter thermal heating over the TP through dynamical feedbacks and play an important role in aerosol-monsoon interactions (see section 4 for a more detailed discussion).

The TP and surrounding regions play a crucial role in the water cycle over the ASM region. The TP "pumps" atmospheric moisture from the ocean surface upward and spreads it over the vast territory of Asia, forming a distinctive "wet pool" in the middle of the troposphere [*G. X. Wu et al*., 2012a, 2012b, 2014; *Xu et al*., 2008]. Ultimately, the bulk of the ASM moisture originates from the Southern Hemisphere, the north Indian Ocean, and the Western Pacific (see Figure 2), as a component of the strongest seasonal interhemispheric moisture transport system in the world [*Zhou and Yu*, 2005]. Moisture in the southern Indian Ocean crosses the equator near the Somalian coastal region and then flows over the Arabian Sea, the BOB, and the SCS. From there, the moisture transport moves northward into EA. A secondary moisture channel stems from the southern and western peripheries of the subtropical high over the western Pacific Ocean. These two moisture channels merge into a single channel over the SCS and the EA regions [*Simmonds et al*., 1999; *Zhang*, 2001; *Xu et al*., 2012].

Besides having strong seasonality, the ASM also possesses a distinct natural variability on intraseasonal to interannual timescales. The monsoon onset and dry and wet spells are modulated on 15–30 day timescales by so-called monsoon intraseasonal oscillations (MISO) involving quasi-periodic 20–30 day northward surges of moisture from the ocean toward land [*Krishnamurti and Bhalme*, 1976; *Lau and Chan*, 1986; *Wang*, 2006]. It is also well known that the El Niño–Southern Oscillation (ENSO) strongly affects the EASM on timescales of 2–5 years. In particular, the northward propagating MISO in the EASM system shows a significant correlation with the preceding winter extreme phase of ENSO cycles. *Yun et al*. [2008] showed that the springtime Indian Ocean SST warming induced by the ENSO through the Walker circulation leads to downward motion and suppressed convection over the Philippine Sea. This generates the forced Rossby wave train, forming the above south-to-north low-level circulation MISO anomalies associated with frequent heavy rainfall events over East Asia.

2.3. Land Surface Processes

Besides contributing to the land-sea thermal contrast, land surface processes may also play important roles in driving MISO and long-term variability. Wet soil provides an additional source of moisture for monsoon precipitation. However, this effect could be opposed by the cooler surface temperature, which tends to reduce convective instability and suppress rainfall. *Lau and Bua* [1998] found from GCM experiments that the interactions among precipitation, moisture convergence, and land surface processes play key roles in determining the fast (subseasonal and shorter scales) response of the ASM. They found that the occurrence of a preferred ASM climatic state and the abrupt transition between dry and wet states are amplified by atmospheric-land surface feedback processes involving both aspects of the regional energy and water cycles over land, dependent on the direction and magnitude of the ENSO large-scale remote forcing. However, land-atmosphere interactions do not seem to alter the basic planetary scale features of the ASM-ENSO system. As a result, while the interannual variability of the ASM may be relatively small in the absence of large-scale forcing such as ENSO, the local effect of land-atmosphere interactions on ASM could be very pronounced especially during the transition phases of the ENSO [*Yang and Lau*, 1998].

Higher land albedos during winter and spring are associated with colder land temperatures, a reduced land-sea temperature contrast, and a weaker ASM [*Hahn and Shukla*, 1976; *Meehl*, 1994; *Vernekar et al*., 1995; *Bamzai and Shukla*, 1999; *Bamzai and Marx*, 2006]. However, because Eurasian snow cover is strongly

influenced by ENSO, relationships between snow cover change and ASM rainfall derived from observations are generally not strong. *Sankar Rao et al*. [1996] found that the inverse relationship between Eurasian snow cover and the Indian monsoon became stronger in partial correlation calculations excluding ENSO effects. *Fasullo* [2004] noted robust regionally specific inverse relationships between spring-winter snow cover over the southwestern Asian/northern Indian/Himalayas and the TP with June–September all-India rainfall during neutral ENSO years. *Robock et al*. [2003] argued that Eurasian snow cover-AM relationships may be modulated by the North Atlantic Oscillation. Other studies found that Tibetan snow cover may work cooperatively with ENSO to enhance spring rainfall in southern China [*Wu and Kirtman*, 2007; *Zhao et al*., 2007]. The mechanisms underlying the snow cover-ASM rainfall are not well known and most likely involve feedback processes between atmospheric circulation and land surface hydrologic processes.

Note that studies of the aerosol impact on monsoon energy and the water cycle, and feedbacks involving land surface processes are just beginning as of this writing. Aerosols, both natural and anthropogenic, could impact energy and water cycles, first through perturbing the radiative components of the energy cycle, and then through feedback processes associated with both the energy and water cycles. Recent studies on the effects of atmospheric heating and snow darkening by light-absorbing aerosols (desert dust, BC, and OC) on the accelerated melting of snowpacks over Eurasia and the TP, leading to increased surface evaporation and drier springtime land over Eurasia, may provide a new dimension for further investigation of the snow cover-ASM rainfall relationship [*Lau et al*., 2010; *Yasunari et al*., 2015]. See section 5.2.2 for a further discussion of this topic.

3. Primary Mechanisms of the Aerosol Impact on Climate

Aerosols arise from both natural and anthropogenic sources. Natural aerosols include dust, sea salt, smoke, BC, OC from forest fires, and biogenic and biological particles, while anthropogenic aerosols (AAs) include sulfate, nitrate, organics, and soot, which is also known as BC. In particular, BC aerosols resulting from the incomplete combustion of hydrocarbons, e.g., from internal combustion engines, coal firing power plants, slash and burn agricultural practices, and smoke from cooking, are increasing rapidly in Asia as the demand for energy from a growing population and economy increases. Aerosols emitted directly are referred to as primary aerosols, which are distinct from those generated by gas-to-particle conversion, i.e., secondary aerosols [*R. Zhang et al*., 2012]. The mixture of these different aerosol species scatters and attenuates incoming solar radiation to create the appearance of semi-opaque yellowish smoke sometimes referred to as atmospheric brown clouds that prevail over urban areas and mega-metropolises of the South and East Asian regions [*Ramanathan et al*., 2007].

Note that the interaction between the AM and aerosols has a natural component because a significant fraction of aerosol particles are naturally produced. Dust aerosols transported from deserts adjacent to the AM region (e.g., deserts in Pakistan, Afghanistan and the Middle East, the Sahara, and the Taklamakan Desert) accumulate at high elevations against the southern and northern slopes of the TP during premonsoon and monsoon months. Because of the absorption of solar radiation by aerosols, the atmosphere over northern India and the southern TP is heated. This could have an impact on the thermodynamic state of the atmosphere and alter the large-scale climate through various feedback processes [*Lau et al*., 2006, 2008]. In addition, these dust particles can serve as efficient ice nuclei (IN) [*Connolly et al*., 2009; *Niemand et al*., 2012], changing cloud properties including snow precipitation and cloud radiative forcing [*Fan et al*., 2014].

3.1. Aerosol-Radiation Interactions (ARI)

IPCC [2013] refers to ARI as any change associated with aerosols' radiative effect including traditionally defined aerosol direct and semidirect effects [*Schwartz*, 1996; *Ackerman et al*., 2000]. Aerosols alter the radiation budget by scattering and/or absorption whose strength depends on aerosol optical properties that are determined by their size distribution, mixing state, and chemical composition. In many aerosol-climate models, particularly the earlier ones, only the aerosol mass mixing ratio was accounted for [*Haywood and Boucher*, 2000; *Penner et al*., 2001; *Forster et al*., 2007]. Aerosol optical properties can change depending on whether different chemical species are in the same particle (internal mixtures) or are present as separate particles (external mixtures). The mixing state of aerosols contributes not only to the magnitude but also to the sign of the radiative forcing of aerosols [*Li*, 2004; *Zhang et al*., 2015]. The shapes of aerosol particles can also impact their optical properties [*Wang et al*., 2013a].

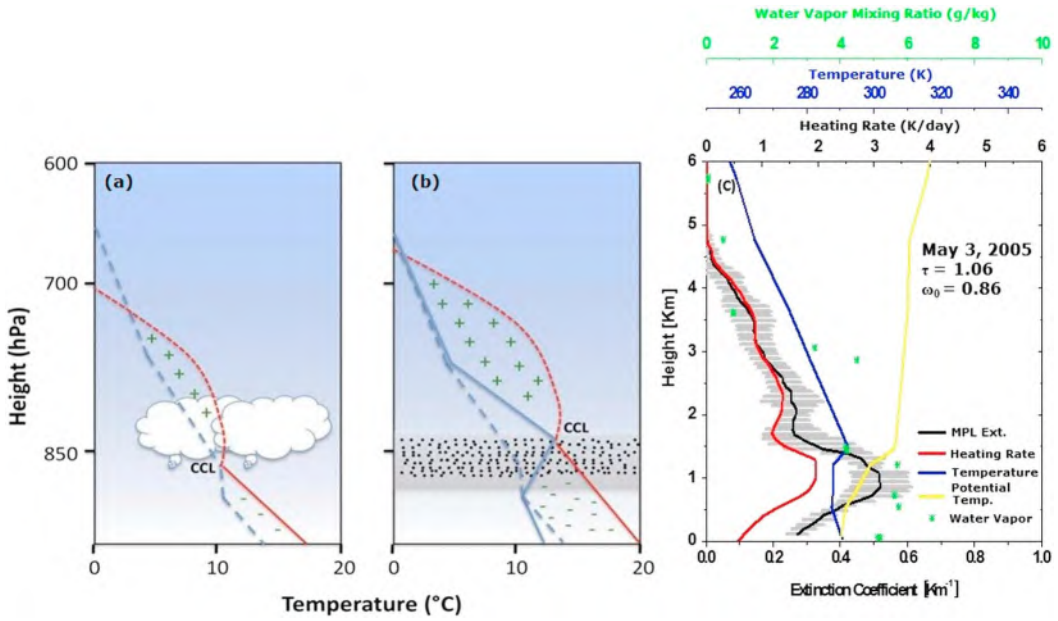

Figure 4. Schematic diagram of the atmospheric effects of absorbing aerosols on the PBL, the temperature inversion, and convection: (a) without and (b) with the presence of absorbing aerosols in the upper PBL. The dashed and solid blue lines correspond to the vertical temperature profiles in the absence and presence of the absorbing aerosol layer, respectively, and the solid and dashed red lines denote the dry and moist adiabatic conditions, respectively. The locations of the convection condensation level are shown. Areas with higher and lower levels of convective available potential energy are shown by the green plus and minus signs, respectively. Copied from *Y. Wang et al.* [2013]. (c) Vertical profiles of micropulse lidar (MPL)-retrieved aerosol extinction (MPL Ext.), heating rate, water vapor mixing ratio, ambient temperature, and potential temperature during a field campaign on 3 May 2005 in Xianghe, China. The mean aerosol optical depth at 550 nm (τ) and single scattering albedo (ω_0) are given.

In addition to the radiative effect for the total atmospheric column, absorbing aerosols have a strong influence on the atmospheric thermodynamic state due to their adiabatic heating which can be computed under clear-sky conditions if aerosol vertical extinction profiles and the single scattering albedo (SSA) are known [e.g., *J. Liu et al.*, 2012]. Most aerosol particles are found below 2 km with the bulk of them (60–80%) located below 1 km. This may be true in some places for anthropogenic aerosols; natural aerosols such as dust and smoke can rise to much higher levels. This leads to the trapping of large amounts of solar radiation in the lower planetary boundary layer (PBL) with the strongest heating near the top or in the upper part of the PBL where a temperature inversion may occur (Figures 4a and 4b). Figure 4c shows an example from measurements taken under high absorbing aerosol loading conditions during a field campaign. Note that the convective potential energy is positive above the PBL and negative inside the PBL. Both the positive and negative energies are strengthened by absorbing aerosols, leading to a more stable PBL, but more unstable free atmosphere. In general, aerosol-induced radiative heating may alter the PBL in numerous ways. First, aerosols reduce surface radiative energy and thus sensible heat fluxes that drive the evolution of the PBL. Second, absorbing aerosols warm the air in the PBL, thus altering the atmospheric thermodynamic structure. Third, aerosols and the PBL likely interact and induce a positive feedback process that exacerbates the initial radiative effect [*Yu et al.*, 2002].

Another category of ARI is the so-called aerosol semidirect effect (SDE): absorbing aerosols located interstitially in cloud droplets warm up the atmosphere, reducing the ambient relative humidity (RH) and suppressing convective overturning that leads to the burn-off of clouds, which reduces the planetary albedo [*Hansen et al.*, 1997; *Ackerman et al.*, 2000]. *Jacobson* [2002] showed that the BC effect may be enhanced due to a low-cloud positive feedback loop in which cloud loss leads to an increased opportunity for BC absorption. In addition, embedding BC into cloud droplets can reduce the cloud droplet SSA, increase the absorption of solar radiation, and expedite cloud evaporation, thus affecting the atmospheric heating profile [*Wang et al.*, 2013b].

Although the SDE was originally defined as the reduction in clouds due to increased evaporation with a resulting positive climate forcing, there are many studies showing cloud cover increases with absorbing aerosols and a negative cloud feedback, depending on the region and conditions. *Allen and Sherwood* [2010] gave two possible explanations: (a) the trapping of near-surface moisture associated with aerosol-induced enhanced lower tropospheric stability, which preferentially increases low cloud over the sea and (b) over land, heating due to aerosol absorption decreases RH, inhibiting cloud formation in the low and middle troposphere. As such, the SDE can alter the land-sea contrast in surface temperature to influence the monsoon circulation.

3.2. Aerosol-Cloud Interactions (ACIs)

ACI is defined in *IPCC* [2013] as any associated change initiated by changes in cloud microphysics by cloud condensation nuclei (CCN) or IN. CCN and IN change droplet and ice crystal formation, respectively, which incurs a chain of ensuing effects [*IPCC*, 2007].

Aerosol impacts on warm clouds are relatively less complicated compared with mixed-phase and deep convective clouds (DCC) because only the liquid phase is involved. Still, different types of aerosol indirect effects (AIE) have been proposed [*Twomey*, 1977; *Albrecht*, 1989; *Kaufman*, 1997; *IPCC*, 2007]. The well-established and accepted AIE is the first indirect effect which describes a reduction in cloud effective radius with an increase in aerosol concentration under fixed liquid water path (LWP) conditions [*Feingold et al*., 2003; *Kim et al*., 2008]. This implies an increase in the albedo of a cloud, resulting in enhanced reflection and a cooling effect [*Twomey*, 1977]. Smaller droplets mean that it takes longer to reach sizes that are large enough to precipitate. This effect, called the cloud lifetime effect, may enhance cloud cover and thus imposes an additional surface cooling [*Albrecht*, 1989].

Drizzle suppression in polluted air has been consistently observed and simulated, which is mainly due to the mechanism of a less efficient collision and coalescence process resulting from a narrower droplet size distribution. However, cloud lifetime is not significantly increased even though precipitation is suppressed because the increasing aerosol concentrations enhance evaporative cooling and create a temperature contrast with the surrounding warm air. The enhanced contrast generates an increased vorticity around cloud boundaries, which makes convective turnover faster and thus cloud lifetime shorter [*Jiang et al*., 2006; *Lee et al*., 2012]. This suggests that in addition to aerosol effects on droplet size, which is a microphysical factor, aerosol-induced changes in thermodynamics and dynamics should be considered for a comprehensive understanding of ACI and their effects on the cloud lifetime of warm clouds.

The suppression of warm rain by aerosols causes most condensates to ascend as cloud water, freeze, and release the latent heat of freezing before precipitating. Delayed precipitation leads to more persistent updrafts and to the invigoration of clouds before the precipitation-induced downdrafts take over [*Andreae et al*., 2004; *Koren et al*., 2005; *Tao et al*., 2007; *Li et al*., 2011b]. It has also been proposed that since more but smaller droplets freeze at higher altitudes and at lower temperatures, more latent heat is released higher in the atmosphere. The additional latent heat thus invigorates convection (Figure 5) [*Rosenfeld et al*., 2008; *Li et al*., 2011b]. This invigoration theory (i.e., the thermodynamic effect) had been widely used by observational studies to explain the increased cloud top height and cloud fraction by aerosols.

The invigoration of convection intensity by aerosols depends on thermodynamic and dynamical conditions [*Fan et al*., 2007, 2009; *Lee et al*., 2008; *Khain*, 2009]. Under strong wind shear conditions, convective intensity tends to be suppressed by increasing CCN due to the dominance of evaporative cooling [*Fan et al*., 2009]. However, in mesoscale convective systems comprising multiple clouds, interactions between wind shear and gust fronts can generate aerosol-induced invigoration of convection under strong wind shear conditions, while they induce suppression of convection under weak shear conditions with increasing CCN [*Lee et al*., 2008]. This indicates that in addition to the dependence of ACI on thermodynamic and dynamical conditions, ACI shows an additional dependence on whether they work in a single cloud or in multiple-cloud systems. Among the various factors affecting the interaction of aerosols with convection and precipitation, cloud base height is one of the key factors as hypothesized by *Rosenfeld et al*. [2008] and confirmed with observations using ground-based observations [*Li et al*., 2011b], satellite data [*Niu and Li*, 2012; *Peng et al*., 2016], and their combination [*Yan et al*., 2014].

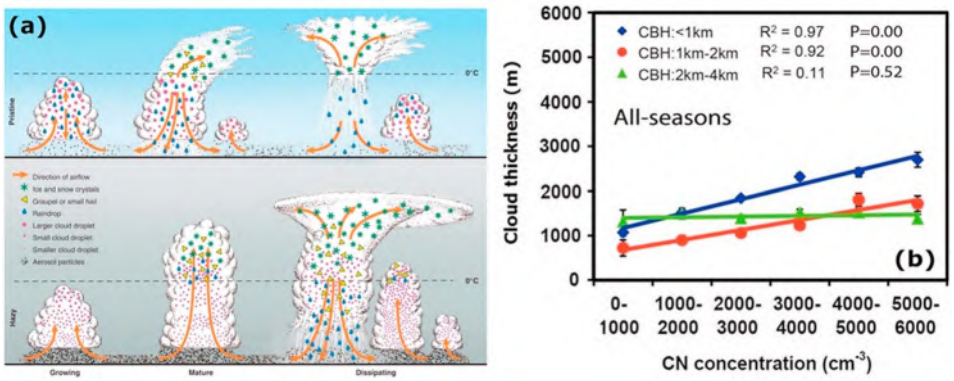

Figure 5. (a) Diagram describing the hypothesis behind the aerosol invigoration mechanism [*Rosenfeld et al*., 2008] and (b) cloud thickness (in meters) as a function of surface aerosol number concentration (cm^{-3}) for clouds with different cloud base heights (CBH). Copied from *Li et al*. [2011b]. Coefficients of determination (R^2) and significance levels (P) are shown.

Mixed-phase stratiform clouds are usually cold based. Increasing CCN often suppresses precipitation because of the suppression of warm rain and reduced riming due to smaller droplet sizes [*Fan et al*., 2012]. This has been simulated by *Fan et al*. [2012] and validated with an observed stratiform mixed-phase cloud case from the AMF-China. In contrast, for a DCC case from the AMF-China where there was a warm cloud base and weak wind shear, enhanced precipitation by CCN was simulated due to convective invigoration [*Fan et al*., 2012]. Studies have also found that increasing IN in mixed-phase clouds leads to enhanced precipitation because the increase in ice crystals leads to a stronger Wegener-Bergeron-Findeisen process, which enhances snow formation and growth [*Ovchinnikov et al*., 2011; *Fan et al*., 2014].

An important impact of aerosols on DCC is the increased cloud cover and cloud top height (CTH), which has been ubiquitously observed [e.g., *Koren et al*., 2010; *Li et al*., 2011b; *Niu and Li*, 2012]. The dominant mechanism contributing to the observed increased cloud cover and CTH is a microphysical aerosol effect, i.e., the freezing of a larger number of smaller droplets produces more numerous but much smaller ice particles in the stratiform regime of polluted clouds which leads to much reduced fall velocities of ice particles and slows the dissipation of stratiform and anvil clouds significantly [*Fan et al*., 2013].

Given the importance of CCN/IN, a brief review of its measurements in Asia is presented here. Field investigations regarding CCN activity, especially in such heavily polluted regions as Asia, are pivotal to accounting for the ACI effect in climate models. Due to the large spatial variability of aerosol types and compositions, the CCN activation efficiency varies greatly. The largest errors are associated with urban emissions [*Sotiropoulou et al*., 2007]. Several field experiments have been conducted in China with the aim of better characterizing particle physicochemical parameters influencing cloud CCN activation [e.g., *Yum et al*., 2007; *Rose et al*., 2010, 2011; *Gunthe et al*., 2011; *Liu et al*., 2011a; *Leng et al*., 2013; *F. Zhang et al*., 2014; *Zhang et al*., 2016; *Miao et al*., 2015]. These studies presented different perspectives on the influence of particle size and composition on CCN activity. For example, without predicting the CCN number concentrations (NCCN), *Gunthe et al*. [2011] parameterized the effective aerosol particle hygroscopicity and CCN activity with measured size-resolved aerosol mass spectrometer data. *Deng et al*. [2013] evaluated various schemes for CCN parameterization and recommended that the particle number size distribution (PSD) together with inferred mean size-resolved activation ratios can be used to estimate CCN number concentrations without considering the impact of particle composition. However, *B. Zhang et al*. [2014] demonstrated that the 30–40% uncertainties in NCCN are mainly associated with changes in particle composition. None of the above mentioned studies have investigated the impact of organics on estimating NCCN in northern China. *Q. Zhang et al*. [2012] noted a more significant influence of organics on CCN activity but without regarding the influences of particle oxidation or aging on CCN activity. Both factors were found to have a significant impact on CCN activation based on field measurements made at a suburban site in northern China [*Zhang et al*., 2016]. In addition, new particle formation (NPF) [*Guo et al*., 2014] was found to enhance CCN number concentrations at both a relatively clean environment and a polluted site. *Wiedensohler et al*. [2009] and *Yue et al*. [2011] also found that NPF increased CCN number

concentrations by 0.4–0.6 times in Beijing by comparing the enhancement of CCN numbers at the end of a nucleation event to that at the beginning of a nucleation event.

While such in situ CCN measurements are highly valuable in understanding nucleation processes and in developing parameterization schemes, measurements are rare and often just made from the ground. Size-resolved aerosol chemical composition and particle mixing state and aging are also hard to measure. As such, it is difficult to rely on such measurements to account for the effect on any large scale. As a result, the more readily and widely available measurements of AOD have been used as a proxy for CCN [*Andreae*, 2009] despite the very large uncertainties involved. These uncertainties can be reduced by accounting for the influences of the aerosol swelling effect and aerosol chemical composition [*Liu and Li*, 2014]. Recently, a totally new approach of obtaining CCN over large scales was proposed by *Rosenfeld et al*. [2016] who used high-resolution satellite data from the NOAA's Visible Infrared Imaging Radiometer Suite instrument. More importantly, the method derives CCN at cloud base, which matters most to cloud formation, thanks to another novel method of deriving updraft speeds at cloud base from that particular satellite sensor [*Zheng et al*., 2015].

4. Aerosols and Climate Change in Asia: An Observational Perspective

Both aerosol and meteorological variables have been extensively measured from spaceborne, ground-based, and in situ sensors. The bulk of discussion in this section is concerned with findings based primarily on ground observations, although satellite measurements are used in some studies. For large-scale studies, use of satellite data is indispensable. Among all aerosol parameters, AOD has been most widely used in many studies concerning Asian aerosols and the environment. *Ginoux et al*. [2012] discussed the global-scale attribution of anthropogenic and natural dust sources and their emission rates based on Moderate Resolution Imaging Spectroradiometer (MODIS) Deep Blue aerosol products. While satellite observations can provide global AOD and other aerosol products over a long period, all satellite products suffer from various limitations and retrieval errors that may vary considerably from one region to another depending on surface and aerosol properties [*Li et al*., 2009]. The retrieval of AOD from satellite-measured radiances is an ill-posed problem because the number of known variables is less than what is required. Over China, retrieval errors are generally large because the surface albedo is highly variable and aerosol properties are complex. There are also few in situ and ground-based measurements to constrain inversion algorithms, which is especially the case for earlier AOD products [*Li et al*., 2007c; *Mi et al*., 2007; *Xin et al*., 2007]. As such, caution must be exercised when using any satellite AOD product, as in the many studies cited in this article.

4.1. East Asia

4.1.1. Aerosol Loading, Variation Trend, and Pattern

Prior to the 1980s, there were virtually no direct ground-based aerosol measurements made in Asia. Visibility had been measured as a standard meteorological parameter for a long time using various methods. It has been used as a proxy for air quality and for deriving AOD and extinction coefficients [*Husar et al*., 2000; *Qiu and Yang*, 2000; *Kaiser and Qian*, 2002; *Che et al*., 2007, 2009a; *K. C. Wang et al*., 2009; *Lin et al*., 2014]. An investigation of clear-day visibility changes was conducted by *J. Wu et al*. [2012] using 50 years of data measured at 1400 Beijing Standard Time from 543 stations across China. Mean values and trends for big (>1 million people) and small cities (<1 million people) are shown in Figures 6a and 6b, respectively. From 1960 to 1990, both big and small cities experienced visibility declines and the rate of decline was much steeper in big cities (~30%) than in small ones (10%). Interestingly, after the 1990s, general trends were opposite with a slight recovery in big cities, but a faster deterioration in small cities. Visibility can only serve as a very rough proxy for AOD and can depict the general patterns in AOD changes in time and space. However, there are inherent limitations. First, the vertical distribution, or mixing of aerosols in the boundary layer and atmospheric mixing layer height [*Wang and Wang*, 2014], is critical in affecting AOD retrievals from visibility. Second, early measurements of visibility were done by human observers using landmarks with limited scales rather than measured in true distance. Human observation errors are the largest source of uncertainties regardless of how meticulous corrections are made.

Without direct AOD data, a somewhat better approach of deriving AOD is to make use of clear-sky radiation measurements. *Luo et al*. [2001] retrieved monthly and yearly mean AOD at 0.75 μm using a new method

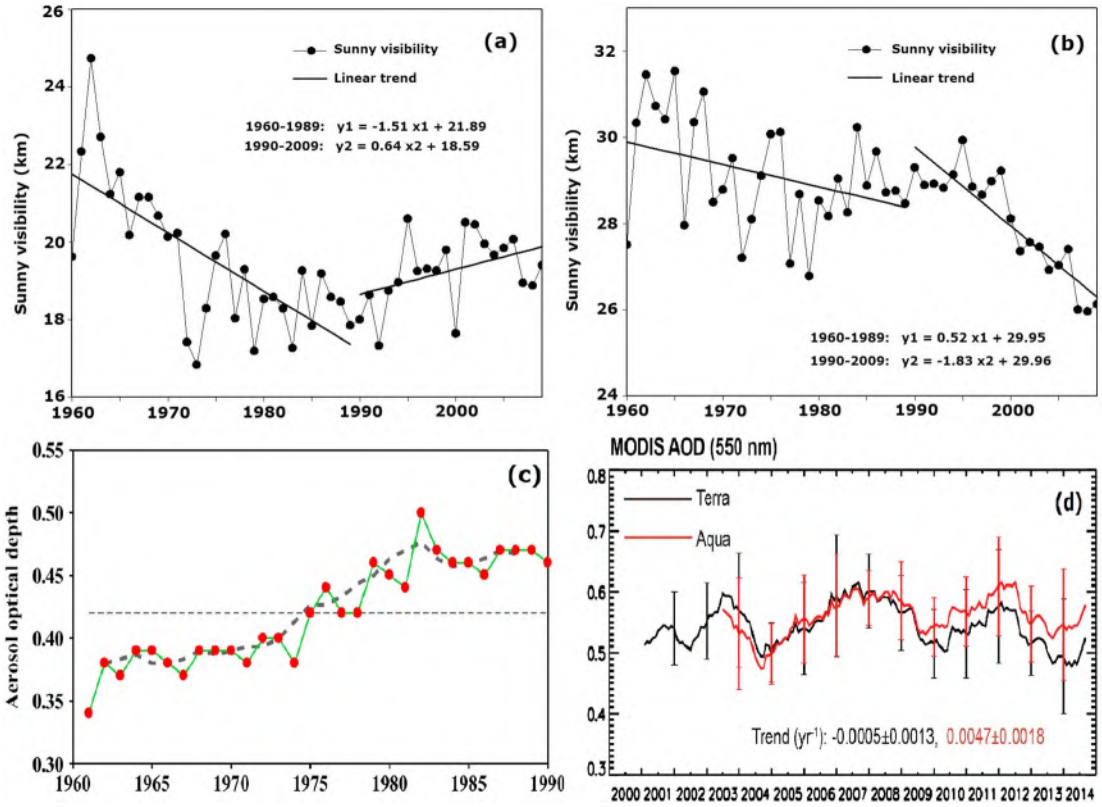

Figure 6. Long-term visibility in (a) big and (b) small cities in China (modified from *J. Wu et al.* [2012]). The regression equations are given for two separate periods (periods 1 and 2) with variables *x* and *y* denoting year and visibility. (c) The trend in AOD at 750 nm derived from surface radiation measurements made from 1960 to 1990 across China [*Luo et al.*, 2001]. The dashed line is the three-year running mean. (d) Trends in mean MODIS-retrieved AOD at 550 nm over China since 2000 (revised from *Lin et al.* [2013] over a longer period). Used with permission from Taylor & Francis Ltd. (http://www.tandfonline.com).

that incorporates daily direct solar radiation, sunshine duration, surface pressure, and vapor pressure data collected from 1961 to 1990 at 46 solar radiation ground stations located mainly in medium-sized and big cities across China. As shown in Figure 6c, the most dramatic increase in AOD happened from the 1960s to the 1980s. Both the temporal trend and spatial distribution pattern bear a close resemblance to the visibility pattern shown by *J. Wu et al.* [2012, 2014].

Since the collection of U.S. Earth Observation System satellite observations began in 2000, global AOD has been retrieved from MODIS [*Hsu et al.*, 2004; *Remer et al.*, 2013] and the Multiangle Imaging Spectroradiometer (MISR) [*Kahn et al.*, 2010]. The AOD from MODIS indicated that there was no pronounced trend for the nationwide mean AOD but a slight upward trend in retrievals from the MODIS sensor on board the afternoon satellite (Figure 6d) [*Guo et al.*, 2011; *Lin et al.*, 2013]. There is a disparity in the trends between the morning satellite (Terra) overpass and the afternoon one (Aqua) that could be a real phenomenon or an artifact because the Terra calibration has experienced a detectable drift [*Levy et al.*, 2010]. It is worth emphasizing that the nationwide trend may not mean much due to different phases of economic development over the large territory of China.

More accurate AOD data can be measured by ground-based Sun photometers. Since the 2000s, a number of Sun photometer sites have been established in Asia, which include the Aerosol Robotic Network (AERONET) [*Holben et al.*, 1998; *Xia et al.*, 2016], the Chinese Sun Hazemeter Network (CSHNET) with ~25 sites in China [*Xin et al.*, 2007], the China Atmosphere Watch Network by the China Meteorological Administration [*Zhang et al.*, 2008], and the China Aerosol Remote Sensing Network (CARSNET) [*Che et al.*, 2009b, 2015]. In addition to these aerosol observation networks, more comprehensive and systematic observation sites (often referred to as supersites) were also established to measure a suite of variables including aerosols, clouds, radiation, precipitation, and atmospheric profiles of temperature, moisture, wind, etc. Examples of these sites include those located in Beijing, Xianghe, Taihu, and Yuzhong [*Li et al.*, 2007a; *Huang et al.*, 2008; *X. Wang*

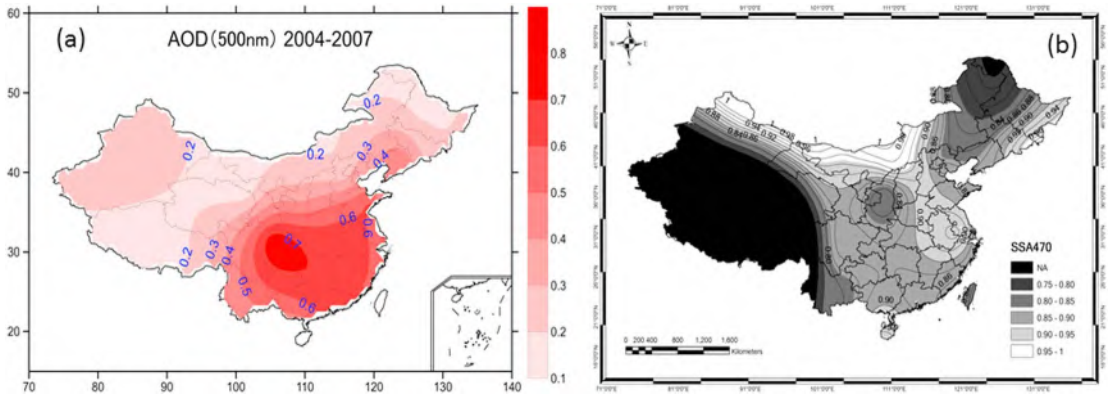

Figure 7. (a) AOD variation across China as measured by the CSHNET plotted based on data described in *Xin et al*. [2007]. (b) Aerosol SSA derived from a combination of CSHNET transmittance data and MODIS reflectance data [*Lee et al*., 2007].

et al., 2010]. Based on CSHNET and CARSNET measurements, the annual mean AOD across China is 0.43 and 0.54, respectively [*Xin et al*., 2007; *Lee et al*., 2010; *Che et al*., 2015], which is about 3 times the global mean AOD retrieved from all AERONET sites [*Holben et al*., 1998; *Dubovik et al*., 2002].

Figure 7a shows the AOD distribution across China as measured by the CSHNET from 2004 to 2007. The AOD was less than 0.2 at remote and rural stations in northwest and northeast China, 0.2–0.3 over the desert and/or semidesert regions in western and northern China, and over 0.6 in central and eastern China. AOD measurements made by the CARSNET over a longer period in northern dust-prone regions of China showed decreasing trends from 2006 to 2009 but increased by ~0.03 per year from 2009 to 2013 [*Che et al*., 2015]. In central-east and south China, biomass burning from agriculture waste significantly contributed to the AOD and in north China, dust aerosols contributed significantly to the AOD in the spring with a decreasing influence from source regions to downwind regions [*Xia et al*., 2016].

The spatiotemporal distributions of aerosol physical and chemical properties (e.g., aerosol loading, SSA, asymmetry factor, and size distribution) were measured at numerous sites having different environmental conditions, especially during the EAST-AIRE [*Li et al*., 2007a] and EAST-AIRC [*Li et al*., 2011a]. A method of combining satellite-measured reflectance at the top-of-the-atmosphere (TOA) and transmittance at the surface [*Lee et al*., 2007] was applied to CSHNET data to derive the first nationwide SSA distribution map across China (Figure 7b). Nationwide mean SSA is about 0.9, but varies considerably with the lowest values (~0.8) in the northeast and central China where coal burning is more prevalent, and the highest values (up to 1) in southeast China where nonabsorbing sulfate aerosols are more dominant presumably because of the high density of industrial activities. Lower values of SSA tend to occur in winter when heating by coal fire is prevalent [*Lee et al*., 2007]. These results are consistent with measurements by Cimel Sun photometers at 21 stations across China [*Xia et al*., 2016]. In the past decade or so, China has gradually reduced the use of raw coal for residual cooking and other applications, which may explain the recent increasing trend in SSA observed in Beijing [*Lyapustin et al*., 2011; *Logan et al*., 2013].

Kudo et al. [2012] estimated the long-term trends in AOD at 0.75 μm from both direct and diffuse irradiances measured by broadband radiometers under clear-sky conditions at 14 Japan Meteorological Agency (JMA) sites. AOD showed a decreasing trend of −0.02 per decade from the 1980s to the 2000s. *Yamaguchi and Takemura* [2011] reported that the long-term trend in annual integrated hours of smog (visibility less than 10 km with RH $<$ 75%) over Japan has tended to decrease in metropolises since the year 2000, especially in eastern and northern Japan. On the other hand, in western Japan, the integrated hours started to increase around the year 2000 and have kept steady at that level since then, especially in the Kyushu region along the East China Sea. This is mainly because of the transboundary transport of AAs from the mainland of East Asia, which has increased due to economic growth [e.g., *Takemura et al*., 2003; *Uno et al*., 2003; *Takami et al*., 2005; *Ohara et al*., 2007]. Based on aircraft and in situ measurements made by a scanning mobility particle sizer, *J. H. Kim et al*. [2014] found that aerosol hygroscopicity varied to a large extent along the western coast of Korea, depending on whether air masses come from China (higher hygroscopicity) or Korea/Japan (lower hygroscopicity).

4.1.2. Potential Impact of Aerosols on East Asian Climate Changes

The climate of China has undergone significant changes since the 1950s when a meteorological observation network was first established across the country, except for the remote western part. These changes are no doubt a combination of natural variability and anthropogenic influences and are variable across the large territory of China. The collocation of the transition in China's large-scale topography and southwesterly monsoonal flows leads to a climate-fragile and environment-fragile belt in China, which can experience drying or wetting trends depending on the increase or decrease in EASM variability [*Xu et al*., 2013]. The climate changes of China have been documented in many publications that are too numerous to list, but good summaries can be found in the IPCC reports [*IPCC*, 2001, 2007, 2013], *Ding et al*. [2007], and the *China National Assessment Report on Climate Change* [2011], among others. Given the subject of this review, emphasis will be given to those changes that have some evidence of an association with changes in atmospheric aerosols.

4.1.2.1. Surface Radiation Budget and Heat Fluxes

Based on surface solar radiation measurements made over China, direct solar radiation reaching the ground decreased by about 8.6% from 1960 to the 1990s [*Luo et al*., 2001; *Liang and Xia*, 2005; *Shi et al*., 2008; *Zhang et al*., 2013]. The total solar radiation (direct plus diffuse) showed a decreasing trend before 1990, with the most significant decrease occurring from the mid-1960s to the late 1980s [*Che et al*., 2005; *Shi et al*., 2008]. The decreasing trend in total solar radiation reversed in the early 1990s, but the absolute magnitude never reached the level of the 1960s again. This trend seems rather widespread according to a similar trend based on global radiation network data [*Wild et al*., 2009]. The total solar radiation remained approximately stable after 1995. The changes in diffuse solar radiation are different from those in total solar radiation. There was an increasing tendency in the 1960s, after which fluctuations in diffuse solar radiation continued until around 1980. Diffuse solar radiation then decreased continuously throughout the 1980s and approached a minimum value in 1990. From 1990 to the present, a gradual increasing trend has occurred. Volcanic eruptions had a large effect on diffuse solar radiation. Three clearly seen peaks occurred in the eruption years of 1966, 1982, and 1991. The abrupt increases in diffuse and total solar radiation between 1990 and 1993 is the result of the replacement of measurement instruments and methods, and the restructuring of measurement station networks [*Tang et al*., 2011; *Wang et al*., 2012a; *Wang and Dickinson*, 2013; *Wang*, 2014]. Due to a technical limitation, the pyranometers used to measure diffuse solar radiation from 1960 to 1990 suffered from a strong sensitivity drift problem, which introduced a spurious decreasing trend into the observed diffuse solar radiation and the calculated total solar radiation. However, the observed direct solar radiation did not suffer from this sensitivity drift problem, and its long-term trend is quantitatively consistent with that of sunshine duration derived from solar radiation [*Wang et al*., 2015]. As such, the time series of AOD inferred from direct solar radiation across China may echo the general trend of air quality changes across China, but more accurate direct measurements of AOD and aerosol properties are very much needed to understand aerosol radiative effects.

Coincident measurements of aerosol, cloud, and radiative variables were made during several field experiments that have taken place in China since the 2000s [*Li et al*., 2007a; *Z. Li et al*., 2010; *Xia et al*., 2007b, 2007c; *Xia*, 2010]. Using such concurrent measurements of high temporal resolution (1 Hz), *Li et al*. [2007b] were able to separate the amounts of surface solar radiation reduced by clouds and aerosols on monthly and daily timescales. At the Xianghe site located 70 km east of Beijing, the reduction in daily (24 h mean) solar total irradiance due to aerosols, or the aerosol direct radiative forcing (ADRF), amounted to 24 W m^{-2}, which is more than half of the reduction due to clouds (41 W m^{-2}) (Figure 8a). The magnitude of ADRF in China is much larger than the general conditions around the world (~5 W m^{-2}) [*Yu et al*., 2006; *Chin et al*., 2009].

Table 1 summarizes various estimates of the diurnal mean ADRF in different parts of China from simultaneous measurements of aerosol and solar radiation made by many investigators. A most outstanding feature is that aerosols cool the surface and warm the atmosphere drastically, but at the TOA, ADRF is much smaller. Across China, for example, the values at the surface, within the atmosphere, and at the TOA are -15.7 ± 9.0 W m^{-2}, 16.0 ± 9.2 W m^{-2}, and 0.3 ± 1.6 W m^{-2}, respectively [*Z. Li et al*., 2010]. Such a large shift of solar heating from the surface to the atmosphere is bound to have a significant impact on atmospheric thermodynamic conditions and further influence weather and climate. Such column-integrated estimates are, however, not sufficient to understand the effects. This would require profiles of aerosol-induced diabatic heating. The heating rate can be estimated using lidar measured or inferred aerosol extinction profiles and column mean aerosol SSA [*J. Liu et al*., 2012].

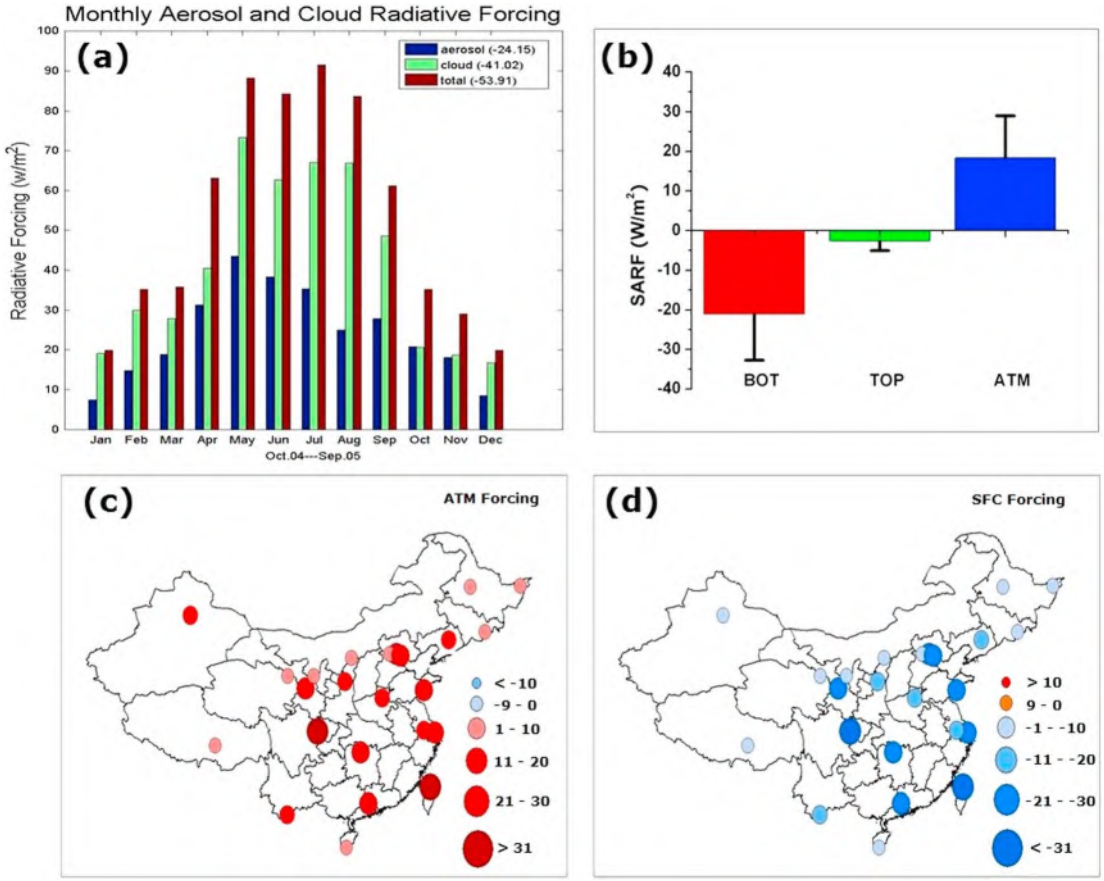

Figure 8. (a) Daily and monthly mean aerosol direct radiative forcing (ADRF) by aerosols and clouds observed at Xianghe. The numbers in the legend are −24.15, −41.02, and −53.91 W m^{-2} representing aerosol, cloud, and total radiative forcing, respectively. Copied from *Li et al.* [2007b]. (b) National mean ADRF at the top, bottom, and inside the atmosphere. (c) Aerosol-enhanced atmosphere-absorbed solar radiation. Units: W m^{-2}. (d) Aerosol-reduced surface solar radiation budget. Units: W m^{-2}. Figures 8b–8d are modified from *Z. Li et al.* [2010].

Table 1. Aerosol Direct Radiative Forcing at the Top (TOA), Bottom (SFC), and Within the Atmosphere (ATMOS) in Different Regions and Periods in China[a]

Region	References	Period	TOA(W m^{-2})	SFC(W m^{-2})	ATMOS(W m^{-2})
China, nationwide	*Li et al.* [2010]	2005	0.3	−15.7	16.0
Xianghe (39.753°N, 116.961°E)	*Li et al.* [2007b]	Jan–Dec 2005–2006		−24	
Liaozhong (40.50°N, 120.70°E)	*Xia et al.* [2007c]	Mar–May 2005		−30	
Beijing (39.98°N, 116.38°E)	*Xia et al.* [2007d]	Dec–Feb	−8.0	−20.3	
		Mar–May	−13.9	−46.1	
		Jun–Aug.	−13.5	−45.6	
		Sep–Nov 2001–2005	−10.7 ± 2.0	−30.0	
Taihu (31.70°N,120.36°E)	*Xia et al.* [2007a]	Jan–Dec 2005–2006	0	−38.4	
Nanjing (32.05°N, 118.78°E)	*B. Zhang et al.* [2014]	Jan–Dec 2011–2012	−6.9	−21.3	
Yulin (38.28°N, 109.72°E)	*Che et al.* [2009a]	Jan–Dec 2001–2003	−10	−86	76
Tongyu (44.42°N, 122.92°E)	*Wu et al.* [2015]	Jan–Dec 2010–2014	−9.4	−26.3	
Zhangye (39.08°N, 100.28°E)	*Ge et al.* [2011]	Mar–May 2008	0.52 ± 1.69	−22.4 ± 8.9	
SACOL (35.95°N, 104.10°E)	*X. Liu et al.* [2011]	Mar–May 2009	0.68	−70.02	70.70
North China Plain	*Liu et al.* [2007]	Oct 2004	−12	−50	38
Badain Jaran Desert	*Bi et al.* [2013]	Apr–June 2010	−4.8 to 0.4	−5.2 to −15.6	5.2 to 10.8
Taklamakan Desert	*Huang et al.* [2009]	July 2006	44.4	−41.9	86.3
Taklamakan Desert	*Xia and Zong* [2009]	May 2001–2005	21		
South China	*Xia et al.* [2016]	Jan–Dec 2001–2013 SZA (55°–65°)	−15.4	−42.8	27.4
Middle-east China			−23.9	−70.8	46.9
Northeast China			−13.0	−43.2	30.2
Northwest China			−5.6	−22.3	16.7

[a]SZA, solar zenith angle.

Changes in the surface radiation budget due to aerosol direct effects imply less energy available to be transformed into surface heat fluxes [*Wang et al*., 2010a, 2010b; *Wang and Dickinson*, 2013]. Based on surface observations, *Zhou et al*. [2010] illustrated that the daily mean surface sensible heat flux over northwest China has decreased since the latter half of the 1980s. Such changes in surface heat fluxes can have a wide range of impact from the local-scale boundary layer to regional-scale air quality [*J. Wang et al*., 2016] and the continental monsoon system [*Lau*, 2016]. The latter is due to the different influences of aerosol on the thermal contrast between the continent where aerosols originate and oceans where the atmosphere is much cleaner. Meanwhile, dust plumes originating from the nearby Taklamakan Desert can be transported to eastern China and Tibet, inducing radiative heating in high atmospheric layers and affecting atmospheric stability, which also affects the monsoon circulation [e.g., *J.-P. Huang et al*., 2007; *Liu et al*., 2011b].

Ohmura [2009] analyzed surface global solar irradiance at 40 sites in Japan operated by the JMA. The decadal trend shows a sharp decline (~20 W m^{-2}) after 1960 to the early 1990s and a recovery to the present, similar to that in China and Europe. A trend in global solar irradiance under all-sky conditions based on the estimated AOD and SSA is consistent with other observational studies [e.g., *Wild et al*., 2009]. These findings suggest that the brightening in Japan has been caused by changes in aerosol optical properties, especially SSA.

As a part of the ACE-Asia Project, *Nakajima et al*. [2003] studied the radiative forcings of aerosols and clouds over the East China Sea region using surface radiation measurements, satellite data, and model simulations. There are regional differences across Asia in aerosol radiative forcing caused by changes in AOD and SSA, as derived from different measurements made in the region, such as shipboard [*Markowicz et al*., 2003], ground-based [*Yoon et al*., 2005], in situ aerosol measurements used in radiative transfer model calculations [*Conant et al*., 2003], and satellite radiance measurements [*Nakajima et al*., 2003]. They generally revealed strong negative aerosol forcing at the surface and positive aerosol forcing greater than 10 W m^{-2} in the atmosphere. The monthly mean whole-sky radiative forcing of the aerosol direct effect was estimated to be 5 to 8 W m^{-2} at the TOA and 10 to 23 W m^{-2} at the surface at the Gosan (33.28°N, 127.17°E) and Amami-Oshima (28.15°N, 129.30°E) sites. This leads to an atmospheric absorption of 11.76 ± 5.82 W m^{-2}, which translates to an atmospheric heating rate of 1.5 to 3.0 K d^{-1} [*Kim et al*., 2010].

4.1.2.2. Surface Temperature

There have been many studies on the impact of GHGs on temperature changes in China, which has been reported as very likely the dominant factor in the long run [*Chen et al*., 1991a; *Wang and Ye*, 1993; *Li et al*., 2010b; *China National Assessment Report on Climate Change*, 2011]. The most prominent trend is the widespread rise in surface temperature across China, except for a small pocket of cooling in southwestern China. The warming is most significant in winter, followed by spring and fall, with the least warming in summer. Stronger warming has occurred at high latitudes than at lower latitudes, consistent with global trends [*IPCC*, 2001, 2007, 2013]. The rise in surface temperature in China has been attributed largely to the buildup of GHGs, consistent with results from global climate models such as those participating in the Coupled Model Intercomparison Project (CMIP) [e.g., *Hu et al*., 2003; *Zhou and Yu*, 2006].

The temperature trend and its spatial pattern depend on the period of analysis. From 1960 to 1990 (Figure 9 a), there was a "cooling pool" in eastern-central China [*Xu et al*., 2006]. Early CMIP simulations that only include the anthropogenic effect of GHGs cannot reproduce this feature [*Hu et al*., 2003; *Zhou and Yu*, 2006]. Given that cooling is strongest in the summer months, mainly due to a decrease in daytime maximum temperature, it is argued that the cooling is at least partially caused by the increase in aerosol loading whose rate of change was most dramatic during this period, as shown in Figure 6c. This is well corroborated by the similar spatial patterns of AOD (Figure 7a), ADRF (Figure 8d), and temperature change (Figure 9b). In the southeast quarter of China, AOD is the largest, presumably leading to significant reductions in ADRF and surface temperature. After the 1990s, however, the increase in AOD slowed down considerably (cf. Figure 6d), whereas the GHG effect has kept accumulating. As a result, the cooling trend would be dampened or even disappear as the period of analysis is extended. This seems to be the case for the temperature trend from 1958 to 2009 when the extent of the cooling region shrank in the Sichuan Basin where the AOD was the highest. Yet the largest warming occurred along the belt of the lowest AOD from north to northeast China.

Using observational climate data collected at 72 stations in eastern-central China from 1951 to 1994, *Yu et al*. [2001] found that the rates of change in annual mean daily, maximum, and minimum temperatures and the diurnal temperature range (DTR) were 0.080, −0.020, 0.18, and −0.20°C per decade, respectively. Seasonally,

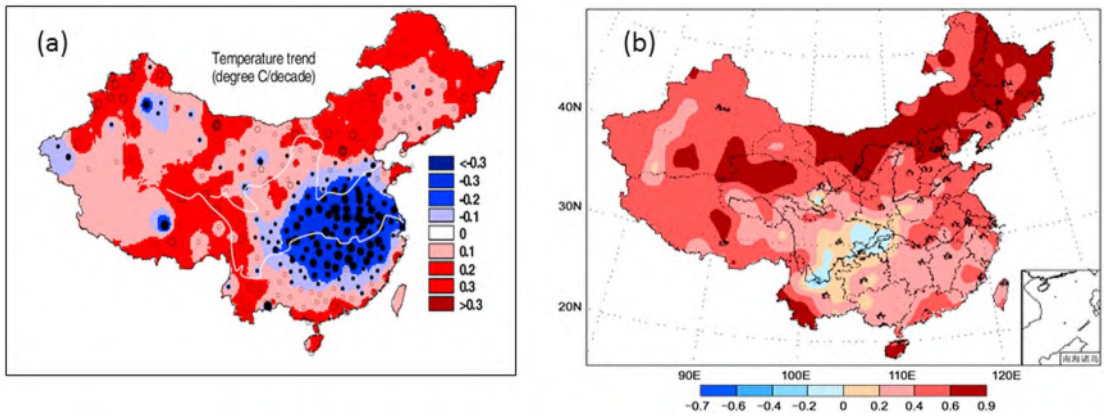

Figure 9. (a) The trend in maximum temperature (°C per decade) in the summer months (June-July-August) from 1969 to 2000 based on observations from the China Meteorological Administration. Copied from *Xu et al.* [2006]. (b) Mean temperature change (in °C) from 1958 to 2009. Copied from the *China National Assessment Report on Climate Change* [2011].

the winter mean daily temperature increased by 0.25°C per decade because of the large increase in the winter mean minimum temperature (0.38°C per decade), whereas the summer mean daily temperature decreased by −0.050°C per decade because of the large decrease in the summer mean maximum temperature (−0.13°C per decade). All seasonal mean DTRs showed decreasing trends at most stations in eastern China, which is consistent with the results of *Zhai and Ren* [1997, 1999]. *Liu et al.* [2002] also found that there was a gradual decrease in DTR of about 0.4°C from 1930 to 1970 over Taiwan Island because of a persistent increase in the nighttime minimum temperature and a nearly constant daytime maximum temperature. Using CMIP Phase-5 (CMIP5) GCM modeling results, *Liu et al.* [2016] were able to confirm that the increase in aerosol loading contributed significantly to the reduction in DTR.

The aerosol radiative effect is most significant for solar radiation during the daytime, so the decrease in maximum temperature may thus be regarded as a "smoking gun" pointing to the possible effects of aerosols on surface temperature in central-east China. As a contrast, the nighttime effect on thermal radiation is negligible. The GHG effect on temperature is cumulative over time, which may explain why the temperature trend over a longer period (1950s–2100s) shows predominant warming across almost all of China. Meanwhile, rapid and extensive urbanization across China during the last few decades may have also contributed to the widespread warming trend [*Zhou et al.*, 2004] in addition to synoptic or dynamic factors. *Gong et al.* [2014] reported a cooling episode during the Chinese New Year Festival when a dramatic increase in air pollution emissions and the aerosol burden due to fireworks during the holiday occurred. Using long-term temperature records, *Yang et al.* [2013a] made the first successful attempt in attributing temperature trends to the effects of GHGs, aerosol, and the urban heat island (UHI) by virtue of the topography in central China. They found that the maximum temperature (T_{max}) in the low-land area and the minimum temperature (T_{min}) in urban areas have exhibited decreasing and increasing trends, respectively, due presumably to the effects of aerosol cooling and UHI warming. This leads to much less of a temperature diurnal range in cities than in rural areas due to the joint effects of both aerosols and the UHI, in addition to the GHG effect [*Yang et al.*, 2013a]. This has been reinforced by CMIP5 model simulations [*Liu et al.*, 2016].

4.1.2.3. Cloud Variables

Among the various cloud bulk parameters (cloud fraction, occurrence, cloud height, etc.), cloud fraction is the most widely available parameter. Over much of China, daytime and nighttime total cloud cover has shown decreasing trends of 1–2% sky cover per decade during the second half of the twentieth century, especially over northeastern China, where magnitudes of the trend are typically 2–3% sky cover per decade [*Kaiser*, 1998, 2000; *Liang and Xia*, 2005; *Xia*, 2010]. Based on all available data from extended weather stations, *Qian et al.* [2006] also revealed that much of China has experienced significant decreases in cloud cover. This conclusion is supported by an analysis of the more reliably observed frequencies of cloud-free sky and overcast sky [*Xia*, 2012]. Total cloud cover during 1955–2005 has decreased 1.2% per decade, but low cloud cover has increased 0.12% per decade. Cloud-free days have increased 0.60% per decade, and overcast days have decreased 0.78% per decade in China from 1954 to 2001 [*Xia*, 2010].

Ground observations of long-term cloud cover are difficult to measure [e.g., *Qian et al*., 2012]. The decreasing amplitude of the diurnal cycle of surface temperature, arguably a proxy for cloud cover change, suggests an increase in cloud cover over China [*Xia*, 2013]. As hypothesized by *Warren et al*. [2007], the reported decline in total cloud cover over China may be attributed to high and middle clouds that might have been underestimated as increased haze events prevented ground-based observers from reporting high and thin clouds. The hypothesis was, however, negated by *Sun et al*. [2014] who investigated the differences between satellite and ground-based estimates of cloud cover as a function of surface visibility (a proxy for aerosol loading). They argued that if the hypothesis were true, the difference between the two types of cloud cover would increase with deteriorating visibility because satellite estimates are not subject to the contamination that ground observers experience. This turns out not to be the case. One can also argue that low cloud cover could have been overestimated by either ground or satellite observations because heavy hazy conditions may be mistaken for low cloud. Overall, the studies on the impact of aerosols on cloud cover are inconclusive at present both for China and elsewhere, but fast progress is being made as of this writing.

4.1.2.4. Precipitation

For the country as a whole, China's mean rainfall has not changed significantly over the past 100 years [*Zhai et al*., 2005; *Ding et al*., 2007; *Zhou et al*., 2009]. However, rainfall has changed drastically on regional and seasonal bases [*Hu et al*., 2003; *Gemmer et al*., 2004; *Ren et al*., 2005] and rainfall regimes have changed [*Gong et al*., 2004; *Zhai et al*., 2005; *Qian et al*., 2009]. In northern China, the number of rainy days in the 1990s is about 8 days less than in the 1950s [*Gong et al*., 2004]. In the second half of the twentieth century, rainfall has decreased in central and northeast China, but has increased in the south, especially in the mid-to-lower reaches of the Yangtze River, and northwest China. This trend has been known as the "north drought and south flood" or "north drying and south wetting" (NDSW).

The trend is most striking during the summer monsoon season which is responsible for over 50–70% of rainfall in most parts of China [*Zhai et al*., 2005]. This trend happens because the EASM circulation has weakened dramatically since the late 1970s [*Yu et al*., 2004; *Zhou et al*., 2009], which is very likely due to the phase change of the Pacific Decadal Oscillation [*Li et al*., 2010a] and further amplified by the increased emission of AAs [*Rosenfeld et al*., 2007; *Yang et al*., 2013a, 2013b; *Song et al*., 2014]. It is worth noting that the NDSW pattern may also be caused by other factors such as changes in atmospheric circulation. *Yu et al*. [2004], for example, found a strong cooling downstream of the TP which may drag or stop the northward movement of the subtropical high system and weaken the summer circulation that brings in moisture and precipitation to northern China.

Precipitation intensity in Taiwan was also found to have increased, but the number of rainy hours has decreased, resulting in a relatively constant rainfall amount but a more polarized rainfall trend [*Liu et al*., 2002]. They suggested that the decrease in rainy hours was probably related to the increase in the number of cloud droplets due to the increasing number of anthropogenic CCN that prevents light rain, as suggested by the Twomey theory. However, it does not help explain the increase in heavy rain. A possible explanation is that cloud particle size increases with increasing aerosol loading over moist regions with a high water vapor content and strong convection, such as the Gulf of Mexico, China [*Yuan et al*., 2008; *Tang et al*., 2013], and India [*Panicker et al*., 2010]. Heavy rain has been found to increase with increasing aerosol loading through aerosol indirect effects on DCCs [e.g., *Rosenfeld et al*., 2008; *Qian et al*., 2009; *Li et al*., 2011b; *Fan et al*., 2013], due to invigoration of convection and/or enhanced ice microphysical processes.

Based on 50 year long-term observational data, *Qian et al*. [2009] revealed that both the frequency (Figure 10 a) and amount of light rain (Figure 10b) have decreased in eastern China from 1956 to 2005. This is different from the trend in total rainfall observed in eastern China. Their analyses imply that the significantly increased aerosol concentrations produced by air pollution are at least partly responsible for the decrease in light rain events.

Yang et al. [2013b] analyzed precipitation and visibility data in Xi'an and found that the impact of aerosols on rainfall frequency is much more significant than on rainfall amount. *Rosenfeld et al*. [2007] proposed a ratio of rainfall at the Hua Mountain site to that at the Huayin foothill site as a measure of the relative impacts of aerosol versus large-scale dynamics. Due to the elevating effect of the mountain, the ratio is more sensitive to the aerosol effect than to the dynamic effect. They found that rainfall amount at both locations, as well as their ratio, has decreased from 1970 to 2005 as aerosol loading increased.

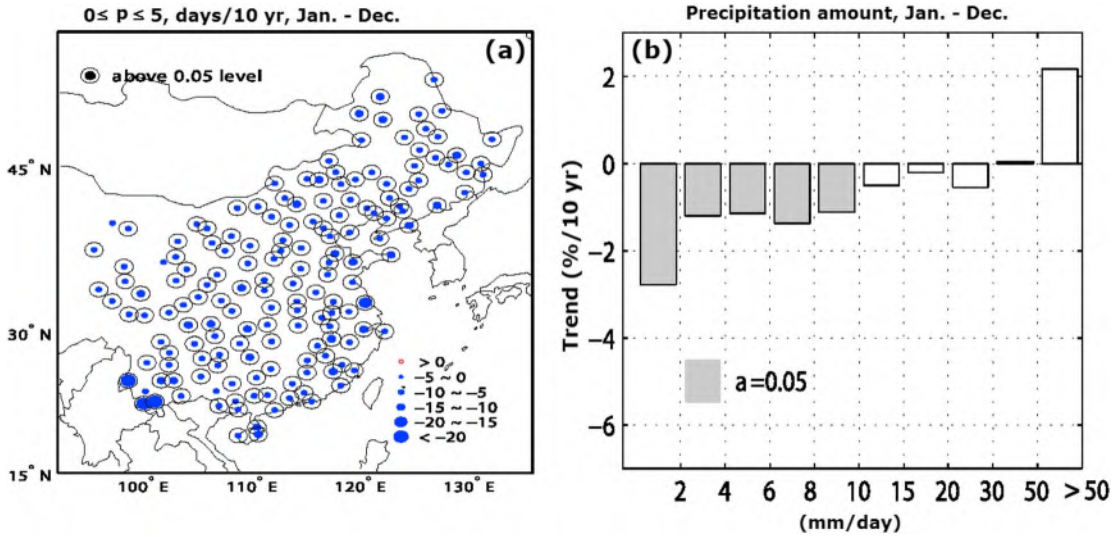

Figure 10. (a) Spatial distribution of trends in annual mean precipitation from 1956 to 2005 for light rain events less than 5 mm d^{-1}. Station trend indicators with circles around them are significant at the 95% confidence level. (b) Linear trends in the frequency of annual precipitation amount as a function of precipitation bins, averaged over East China from 1956 to 2005 (in % per decade). Modified from *Qian et al*. [2009].

Satellite retrievals of the vertical evolution of cloud drop effective radius with height have shown a similar impact of air pollution on clouds over China [*Rosenfeld et al*., 2014] where an increase in AOD of 1.0 can lead to an increase in the threshold of cloud thickness to initiate raining by 5 km [*Zhu et al*., 2015]. A combination of ground-based PM_{10} and Tropical Rain Measurement Mission (TRMM) precipitation radar observations in China indicated that there was an 8.5% increase in the 30 dBZ radar echo top height associated with convective rain under polluted conditions and a 6.5% (2.5%) decrease for stratiform (shallow-cloud) rain relative to those under clean conditions (J. P. Guo et al., Aerosol-induced changes in the vertical structure of precipitation: A TRMM precipitation radar perspective, *Journal of Geophysical Research*: *Atmospheres*, under revision, 2016). *Chen et al*. [2016] found systematic differences in the radar reflectivity of CLOUDSAT between clouds under dirty and clean environments that reverse the sign from cloud base to cloud top.

An analysis of air pollution and meteorological data collected in eastern China revealed a strong weekly cycle in aerosol-meteorology interactions [*Gong et al*., 2007]. They found that in response to the weekly cycle in the amount of AAs, the frequency of precipitation, particularly light rain events, tended to be suppressed around midweek days through indirect aerosol effects. *X. Yang et al*. [2016] gained a deeper insight in the impact of aerosols on the weekly cycle of rainfall whose effect depends critically on aerosol type. Using a combination of satellite and ground-based measurements, *Jiang et al*. [2016] examined the influences of aerosol on precipitation via altering surface fluxes, atmospheric stability, and aerosol invigoration. They found evidence of these mechanisms, as well as the dependence on rainfall regimes.

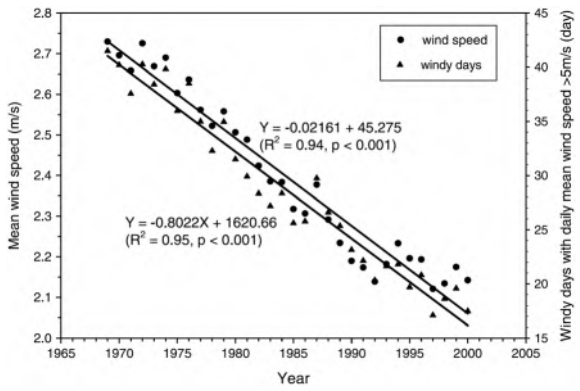

Figure 11. Long-term trends in surface mean wind speed and the mean number of windy days at 305 weather stations across China. Copied from *Xu et al*. [2006].

4.1.2.5. Wind and Thunderstorms

From 1969 to 2000, surface wind speeds measured across China have steadily decreased by 28% and the number of gusty days has decreased by 58 days [*Xu et al*., 2006] (Figure 11).

Both changes have taken place in summer and winter. *Xu et al*. [2006]

proposed that global warming and aerosols are most likely the two primary contributors to the decrease in wind speed and gusty wind events.

Jacobson and Kaufman [2006] investigated wind speed changes over China using satellite data and proposed that aerosol particles, through their radiative effects and their enhancement of clouds, may reduce near-surface wind speeds by up to 8% locally. They argued that this reduction might explain a portion of observed "disappearing winds" in China. They hypothesized that an increase in air stability due to aerosol interactions with radiation or any other mechanism reduces vertical mixing which, in turn, reduces the vertical flux of horizontal momentum. This argument is consistent with the finding of a positive correlation between the trends in increasing aerosol loading and atmospheric thermodynamic stability in China [*Zhao et al*., 2006]. Since winds are generally higher aloft than at the surface, reduced vertical mixing reduces the transfer of fast winds aloft to the surface, slowing surface winds relative to those aloft. *Y. Wang et al*. [2013] furthered the hypothesis by arguing that absorbing aerosols warm the upper PBL, leading to a temperature inversion and a more stable lower PBL and a more unstable atmosphere in the upper PBL. The elevated temperature in the upper PBL contributes to an unstable free atmosphere by enlarging convectively available potential energy.

These hypotheses were put to test using long-term wind speed and thunderstorm data from two stations, one at the top of Hua Mountain and the other in the lowlands of Xi'an City in central China [*Yang et al*., 2013a, 2013b], where solar absorption by aerosols is maximal due to both high AOD and low SSA (Figure 7). Despite the short distance between the two stations (~200 km), the trends in wind speed are opposite: increasing at Hua Mountain and decreasing at Xi'an City (Figure 12a). This is consistent with the hypothesis concerning different effects of aerosol absorption on atmospheric stability in the valley and over the mountain range. Because there is little aerosol radiative effect at night, the two parameters acquired at 2 A.M. (local time) showed no relationship, but did show a negative relationship at 2 P.M., as is seen in Figure 12b. The impact of air pollution on afternoon thunderstorms is also seen clearly from the long-term trend of the ratio of the number of thunderstorms occurring in the afternoon to those occurring at other times of the day. As shown in Figure 12c, the ratio has steadily decreased at Xi'an in the last half a century, but little trend is observed at Hua Mountain. In fact, the absolute number of thunderstorms in every decade has reduced by about half from the 1990s to the 2000s (Figure 12d). A stabilized PBL resulting from increasing aerosol loading is thus a likely cause for the systematic decline in thunderstorm activities.

If the above findings suggest the effects of absorbing aerosols, one may not see the same phenomenon over regions such as southeastern China where SSA is highest (solar absorption is minimal) in China (cf. Figure 7b) [*Lee et al*., 2007]. Using thunderstorm data from both surface and TRMM satellite retrievals as well as ground visibility data in southeast China, *Yang and Li* [2014] found an opposite trend. Low visibility corresponded to a high number of daily flashes, or to more days with thunderstorms, and the height of thunderstorms increased with decreasing visibility. As far as the aerosol-thunderstorm relationship is concerned, it is possible that aerosol loading can change the microphysics of clouds and hence the convection intensity (lightning activity). A similar positive relationship between AOD and thunderstorms was noted by *Y. Wang et al*. [2011] using data from the Pearl River Delta (PRD) region of southern China. Using ground PM_{10} and lightning data from the PRD, *Guo et al*. [2016] found that heavy precipitation and lightning occurred more frequently, and later in the day, under polluted conditions than under clean conditions. Due to the reduction in solar radiation by aerosols, convection becomes difficult until the late day when surface temperatures are hot enough to trigger convection. The aerosol-induced invigoration effect then leads to stronger convection and thunderstorms. This observation-based inference is reinforced by a modeling study simulating this effect [*Lee et al*., 2016]. Likewise, distinctly different weekly cycles in thunderstorm activities were found between central (Xi'an) and southeast China. At both locations, visibility is at its lowest on Fridays when thunderstorms occur less often in central China and most often in southeast China [*X. Yang et al*., 2016].

4.1.2.6. Fog and Atmospheric Circulation

Accompanied by the sharp decline in wind speed is a significant increase in fog occurrence in China (Figures 13a and 13b). The long-term trend and trends in the occurrence frequency of light wind and cold-air outbreaks are also shown (Figures 13c and 13d). Note that fog was measured by human observers who may not have been able to differentiate between haze and fog. These changes are likely caused by multiple factors including the effects of global warming and aerosols. Global-scale warming may reduce the thermal contrast between high and midlatitudes, weaken the troughs and ridges of midlatitude waves,

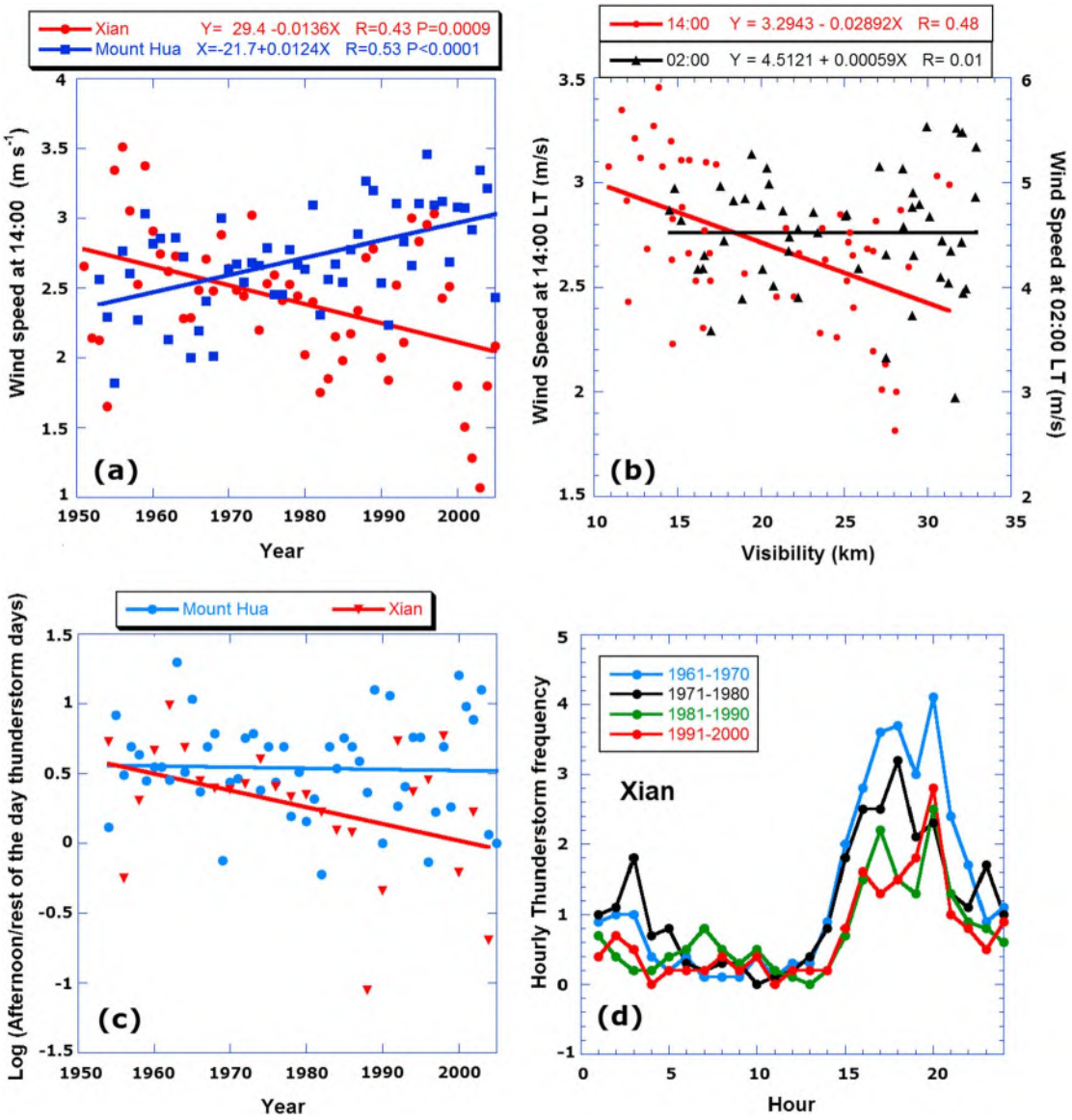

Figure 12. (a) Long-term trends in wind speed at Xi'an and Hua Mountain at 1400 LT. (b) Correlation between wind speed and visibility at 0200 and 1400 LT. (c) Diurnal variations in thunderstorms from 1950s to 2000s. (d) Long-term trends in the number of thunderstorm events in the afternoon over that for the rest of day at the two stations. Modified from *Yang et al*. [2013a].

and diminish the strength of the Siberian high and the EA winter monsoon. This leads to fewer invasions of dry and cold air from the northwest (cold fronts) and lower wind speeds, creating a favorable background for the development of fog.

Using the National Center for Atmospheric Research (NCAR) community climate model (CCM), the National Centers for Environmental Prediction (NCEP)/NCAR reanalysis, and MODIS AOD data, *Niu et al*. [2010] demonstrated that an increase in aerosols also contributes significantly to changes in fog. The observed increase in aerosol loading and absorption over China reduces the total amount of radiation reaching the surface but heats the lower atmosphere. This generates a low-level cyclonic circulation anomaly over eastern-central China. The anomalous circulation weakens the northwesterly wind over eastern-central China but enhances the northerly wind over southern China. As such, fog forms more easily over eastern-central China than over southern China. The effects of global warming and aerosols may work in harmony to explain the changes in fog frequency over eastern-central and southern China in the recent past three decades, although the two effects are often thought to offset each other in the context of global warming in general.

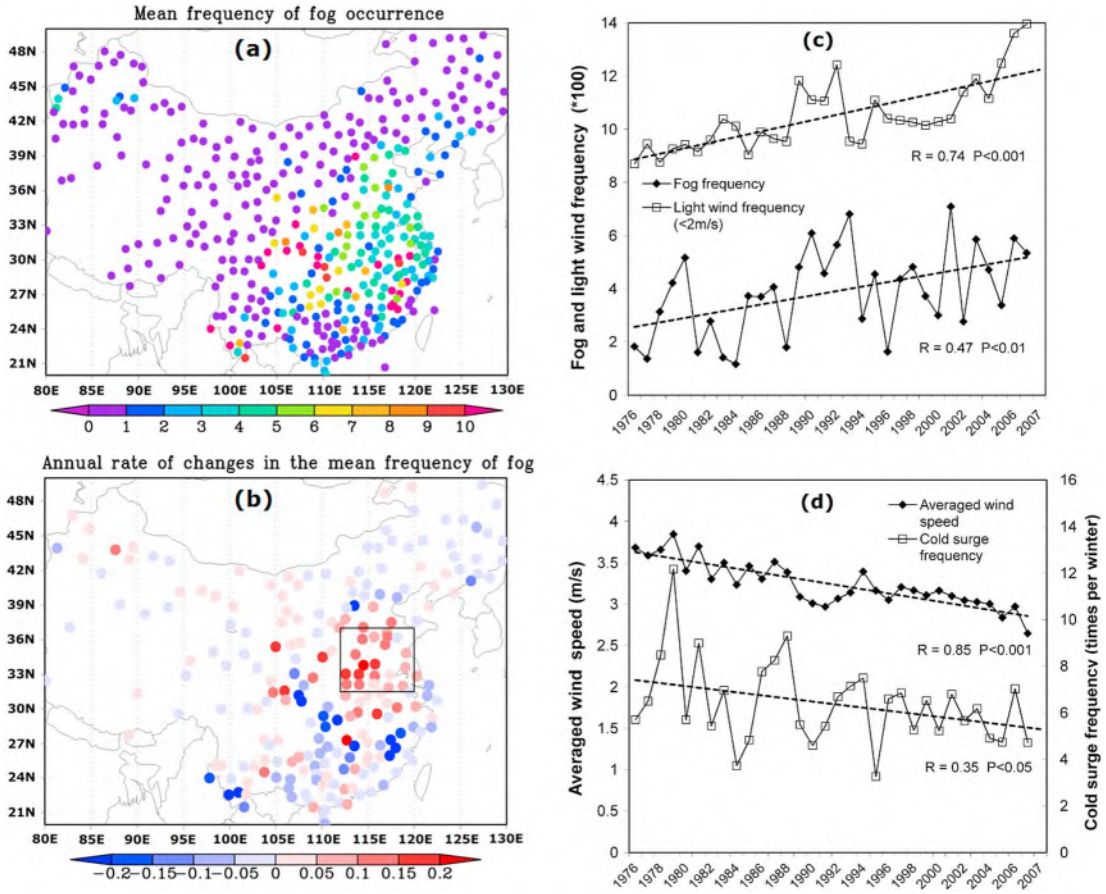

Figure 13. (a) Changes in the frequency of fog occurrence (in %) and (b) the rate of change (in % per year) from 1976 to 2007. (c) Trends in light wind (in %), fog (in %), and (d) cold-air outbreaks. Modified from *Niu et al.* [2010].

4.2. South Asia

The SASM system and the adjacent north Indian Ocean (NIO) have witnessed some of the largest trends in surface and atmospheric radiation budgets, temperatures, and regional circulation during the last half of the twentieth century. Like many other parts of the world, surface solar dimming in India has been reported. The annual mean solar radiation absorbed by the surface over the NIO and over India (observations for other South Asian regions are not available) has decreased by about 5% to 15% depending on the location [*Ramanathan et al.*, 2001b]. This has been accompanied by a concomitant reduction in evapotranspiration over India. Such changes are likely to be related to the ever-changing aerosols in India.

4.2.1. Aerosol Loading, Variation Trends, and Patterns

South Asia, especially India, is home to a variety of aerosols produced both naturally and anthropogenically over the land region. Surrounded by oceans on three sides, abundant marine aerosols such as sea salt and sulfates are found over the Indian subcontinent. Up until the 1990s, much of the aerosol properties over South Asia remained largely unknown.

In 1985, spectral AODs were first measured by a multiwavelength radiometer developed by the Indian Space Research Organization (ISRO) at Trivandrum, a south Indian coastal station [*Moorthy et al.*, 1989]. Around the same time, the aerosol vertical distribution was first measured by a ground-based lidar at Trivandrum and Pune, an urban semiarid station [*Parameswaran et al.*, 1989; *Devara et al.*, 2002]. *Dey and Di Girolamo* [2010] presented a 9 year seasonal climatology of size- and shape-segregated AOD and Ångström exponent (AE) over the Indian subcontinent using the MISR Level 2 aerosol product. The mean seasonal climatological values of AOD at 558 nm and AE based on the retrieved spectral AOD values are shown in Figure 14.

The AOD peaks during the premonsoon and monsoon seasons because of the enhanced emission and transport of natural aerosols, mainly desert dust, sea salt, and wildfires. The broad regional differences in AOD

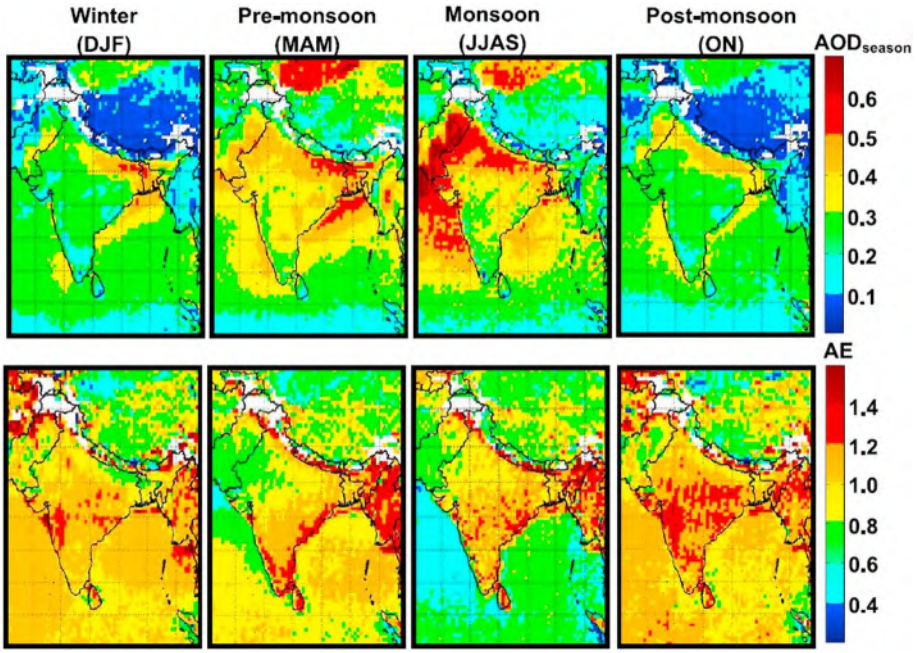

Figure 14. Spatial distributions of climatological mean aerosol optical depth (AOD) at 558 nm and the Angstrom Exponent (AE) from MISR observations made during the period of March 2000 to November 2008. DJF: December-January-February; MAM: March-April-May; JJAS: June-July-August-September; ON: October–November. Copied from *Dey and Di Girolamo* [2010].

depend in part on the emission sources, but the variation within a particular region depends significantly on meteorology and topography. For example, wintertime AOD in the IGP is higher than in any other region because of higher emissions of AAs and the trapping of aerosols within the stable boundary layer. The high aerosol loading over the Indian subcontinent, a fraction of which is absorbing BC, has several climate implications as suggested by recent studies [*Menon et al*., 2002; *Lau et al*., 2006; *Ramanathan and Carmichael*, 2008; *Ramanathan and Feng*, 2009; *Bollasina et al*., 2011; *Manoharan et al*., 2014]. Based on MISR data for the period 2000–2010, *Dey and Di Girolamo* [2011] showed that many aerosol hot spots over India have statistically significant linear trends in AOD (0.1–0.4 increase in seasonal AOD per decade), which are associated with urban centers and densely populated rural areas.

In India, the seasonal median value of AE is lowest in the monsoon season, presumably because of the presence of a large amount of mineral dust transported from the deserts of the Middle East and West Asia, and sea salt from the Arabian Sea. During the premonsoon season, fine aerosol particles with AE $>$ 1.0 (BC and sulfate) are mostly found over northeastern India, the BOB, and the coastal regions of India, but coarse particles with AE $<$ 1.0, indicating desert dust and sea salt, are found over northwestern India, Pakistan, and the eastern Arabian Sea. During the postmonsoon winter season, aerosols over India consist mainly of fine particles with AE $>$ 1.0, suggesting local and industrial pollution sources.

A regional synthesis of long-term (going back to over 25 years at some stations) direct measurements of AOD from a network of aerosol observatories under the Aerosol Radiative Forcing over India project of ISRO (ARFINET) has revealed a statistically significant increasing trend with a significant seasonal variability, as shown in Figure 15b [*Moorthy et al*., 2013a; *Babu et al*., 2013]. The trends in the spectral variation of AOD reveal the significance of anthropogenic activities on the increasing trend in AOD. Figure 15a reveals an increasing trend in the AE, indicating a continued increase in the submicron aerosol abundance. Seasonally, the rate of increase is consistently high during the dry months (December to March) over the entire region, whereas the trends are inconsistent and weak during the summer monsoon period (June to September) [*Babu et al*., 2013]. The insignificant trend in AOD observed over the IGP, a regional hot spot of aerosols, during the premonsoon and summer monsoon seasons is mainly attributed to the competing effects of dust transport and wet removal of aerosols by the monsoon rain [*Babu et al*., 2013]. During the

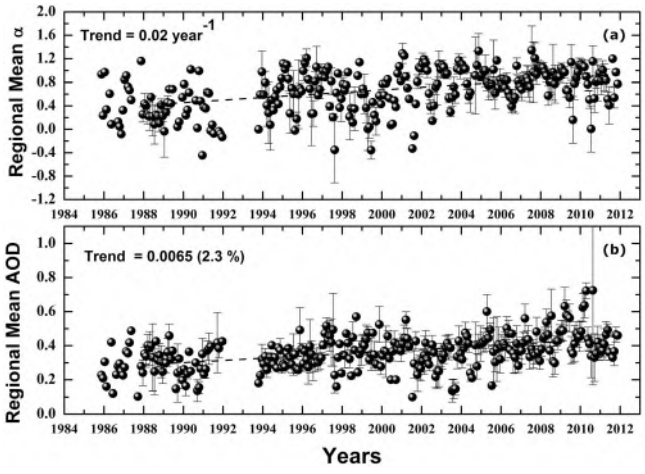

Figure 15. Long-term trends (year^{-1}) in the regional mean values of (a) the Angstrom exponent (α) and (b) AOD at 500 nm over India from the network of aerosol observatories. Copied from *Moorthy et al.* [2013a].

INDOEX field campaign, *Jayaraman et al*. [2001] found that AE ranged from 1.3 to 1.7 in the high optical depth region over the Arabian Sea and ranged from 0.5 to 0.7 over the pristine region.

From March to May 2006, a major multiplatform, multiinstrumental field experiment called the Integrated Campaign for Aerosols gases and Radiation Budget (ICARB) was conducted over a region covering the Indian subcontinent, the Arabian Sea, and the BOB [*Moorthy et al*., 2008]. The second phase of ICARB was conducted from December 2008 to January 2009 with a major focus over the BOB [*Babu et al*., 2012]. The strong convection that prevails during premonsoon and summer monsoon seasons over the Indian region favors lifting up of aerosols to higher elevations in the atmosphere, even up to upper tropospheric altitudes. Aircraft experiments as part of ICARB showed that during the premonsoon season, most of the Indian region is characterized by elevated aerosol layers [*Satheesh et al*., 2008]. This premonsoon elevated aerosol system over India is significantly contributed by BC aerosols (as high as ~12 μg m^{-3}) at free tropospheric altitudes, as is evident from the high-altitude balloon experiment conducted in central India (17.48°N, 78.40°E) during March 2010 [*Babu et al*., 2011]. *Satheesh et al*. [2008] reported a threefold increase in aerosol extinction coefficient at higher atmospheric layers (>2 km) compared to that near the surface, and a substantial fraction (as much as 50 to 70%) of AOD was found to be contributed by aerosols above (reflecting) clouds.

In another study employing aircraft, *Jai Devi et al*. [2011] reported the spatial and vertical distributions of aerosol radiative properties over the Indian continental tropical convergence zone during the premonsoon and monsoon seasons of 2008. During the premonsoon season, aerosol layers were found at altitudes of 6 km over the IGP and Himalayan foothills. During the monsoon season, aerosols were mostly confined to the lower troposphere. However, levels of absorbing aerosols rebuilt much faster than scattering aerosols after the rains ended.

By combining long-term AOD measurements from the ARFINET and the vertical distribution of aerosol extinction coefficient from the Cloud-Aerosol Lidar and Infrared Pathfinder Satellite Observation (CALIPSO) platform, *Prijith et al*. [2016] also reported the meridional structure of the vertical distribution of the aerosol extinction coefficient and the premonsoon enhancement of free tropospheric aerosol loading with an increasing trend toward northern latitudes. *Babu et al*. [2016] reported the significant absorptive nature of these elevated layers of aerosols during the premonsoon season compared to the winter and the high aerosol absorption at free tropospheric altitudes. Heavy aerosol loading over the central and northern latitudes of the Indian subcontinent, with a large (~4 km) vertical spread and significant absorbing aerosol fraction prior to the onset of Indian summer monsoon, might have a significant impact on the dynamics of Indian monsoon circulation and associated rainfall [*Lau et al*., 2006, 2008].

Values of SSA over various locations in India reported by several investigators were either from aerosol models coupled with measurements of BC mass fraction in aerosols or retrieved from sky radiance measurements made by a Sun/sky radiometer. Both methods have significant uncertainties. Accurate estimates of SSA from simultaneous measurements of scattering and absorption coefficients are very limited. Over the IGP, SSA typically ranges from 0.75 to 0.9 [*Ganguly et al*., 2005], indicating very strongly absorbing aerosols. *Satheesh and Ramanathan* [2000] found that anthropogenic sources contributed to ~60% or more to the observed optical depths in their study. *Jayaraman et al*. [2001] reported large north-south gradients in aerosol properties across the Intertropical Convergence Zone (ITCZ) during a ship campaign as part of the INDOEX. The mean SSA was approximately 0.9. Based on extensive observations of aerosol scattering

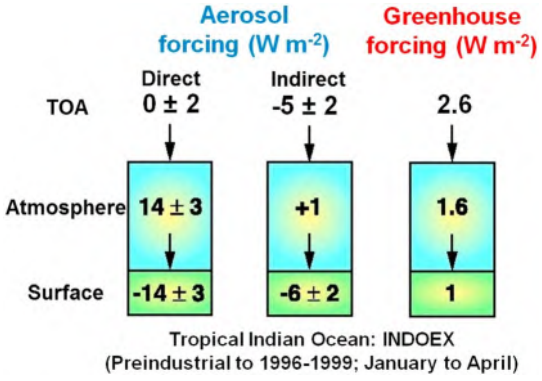

Figure 16. Estimates of aerosol direct, indirect, and GHG radiative forcing at the TOA, within the atmosphere, and at the surface, respectively, relative to the preindustrial era during INDOEX. Copied from *Ramanathan et al.* [2001a].

and absorption coefficients over the Arabian Sea and the BOB during the premonsoon season of 2006, *Moorthy et al.* [2009] reported low SSA at 550 nm (~0.9–0.94) over the BOB compared to that over the Arabian Sea (~0.94–0.98). *Babu et al.* [2012] reported still lower SSA (0.88 ± 0.02) over the BOB during winter. *Dumka et al.* [2014] studied the premonsoon SSA around the industrial city of Kanpur (26.51°N, 80.23°E) during the international TIGERZ intensive operational period from April to June 2008 [*Giles et al.*, 2011]. During an aircraft campaign over the east coast of India, *Satheesh et al.* [2008] showed that SSA ranged from 0.85 to 0.95 at the surface and dropped down to <0.80 at an altitude of ~2 km. This indicates substantially higher absorption in atmospheric layers aloft ($\geq$2 km). Based on aircraft measurements of aerosol scattering and absorption coefficients over central India, northwest India, the IGP, and the foothills of the Himalayas, conducted as a part of the Regional Aerosol Warming Experiment (RAWEX) under the ISRO Geosphere Biosphere Program, *Babu et al.* [2016] reported significant spatiotemporal variability in the altitude distribution of SSA over different regions of India. The columnar values of SSA estimated from altitude-resolved measurements decreased during spring (premonsoon) compared to winter over most of the regions except over northwest India where the mineral dust transport is significant during spring.

4.2.2. Potential Impact of Aerosols on South Asian Climate Change

4.2.2.1. Aerosol Direct Radiative Forcing

Intensive observational studies of AAs were conducted during the INDOEX [*Ramanathan et al.*, 2001a, 2001b]. Over 200 scientists from around the world have documented various aspects about aerosols over this region in two special issues of the Journal of Geophysical Research: Indian Ocean Experiment, Part I, 2001 and Indian Ocean Experiment, Part II, 2002. Key findings from these studies include the following.

1. BC is a major contributing factor to aerosol radiative forcing. Atmospheric solar absorption due to BC can reach as high as 15 W m^{-2}.
2. The surface dimming by manmade aerosols, mainly sulfate, BC, and OC, contributes as much as 70 W m^{-2} per unit AOD [*Satheesh and Ramanathan*, 2000].
3. The present-day optical depth of manmade aerosols (about 0.3 or more) is sufficient to explain the anomalously large dimming observed at the surface over India.
4. Aerosols introduce a significant seasonal asymmetry in the solar forcing of the surface (both land and oceans) and the atmosphere, with a maximum ADRF during the dry season (November to March) and a minimum ADRF during late August.

During the INDOEX field campaign, the ADRF of the atmospheric column over the Indian Ocean in the vicinity of the urban aerosol outflow from the IGP has been estimated to be on the order of +14 W m^{-2} [*Ramanathan et al.*, 2001b]. This is almost completely compensated by the cooling (negative ADRF) at the surface (Figure 16). Most importantly, the magnitude of the atmospheric heating and cooling at the surface due to GHG radiative forcing over the region is negligibly small compared to the ADRF. Clearly, ADRF is an important first-order climate forcing on regional monsoon scales [*Pielke et al.*, 2009].

There have been several efforts in India to estimate ADRF under clear-sky conditions [*Satheesh and Ramanathan*, 2000; *Babu et al.*, 2002; *Pandithurai et al.*, 2004; *Ganguly et al.*, 2005; *Pant et al.*, 2006; *Ramachandran et al.*, 2006; and so on]. A compilation of the ADRF estimates over different regions and periods by various investigators is provided in Table 2.

High values of surface forcing (reaching a maximum value of -35 W m^{-2} for Jaipur) were obtained for various stations in northern India during the premonsoon season of 2009 [*Gautam et al.*, 2011]. Based on data from a

Table 2. Radiative Forcing in Different Regions/Periods in India at the Top (TOA), Bottom (SFC), and Within the Atmosphere (ATMOS), Relative to Global Estimates

Region	References	Period	TOA($W\,m^{-2}$)	SFC($W\,m^{-2}$)	ATMOS($W\,m^{-2}$)
Bangalore (12.97°N, 77.59°E)	*Babu et al.* [2002]	Nov 2001	+5	−23	+28
Pune (18.54°N, 73.85°E)	*Pandithurai et al.* [2004]	Nov–Apr 2000–2002	0	−33	+33
Kanpur	*Tripathi et al.* [2005]	Dec 2004	+9 ± 3	−62 ± 23	
Central India	*Ganguly et al.* [2005]	Feb 2004	+0.7 to −11	−15 to −40	
Nainital (29.2°N, 79.3°E)	*Pant et al.* [2006]	Dec 2004	+0.7	−4.2	+4.9
Hisar (29.1°N, 75.7°E)	*Ramachandran et al.* [2006]	Dec 2004	−3	−21	+18
Kharagpur (22.13°N, 87.3°E)	*Niranjan et al.* [2007]	Dec 2004	−4.53	−54	+50
Hyderabad (17°N, 78°E)	*Badarinath and Latha* [2006]	Jan–May 2003	+9	−33	+42
Trivandrum (8.5°N, 77.00°E)	*Babu et al.* [2007]	Dec–Mar 2000–2003	+4.1 to +1.8	−48.9 to −44.8	+52.9 to +46.6
		Apr–May 2000–2003	+0.3 to −1.4	−37.4 to −34.2	+37.6 to +32.8
		June–Sep 2000–2003	−1.4 to −2.6	−26.9 to −24.4	+25.5 to +21.8
		Oct–Nov 2000–2003	−1.5 to −2.8	−30.2 to −27.8	+28.7 to +25.0
Ahmedabad (23.05°N, 72.55°E)	*Ganguly and Jayaraman* [2006]	June–Sep 2002–2005	+14	-41	55
		Oct–Nov 2002–2005	−22	−63	41
		Dec–Mar 2002–2005	−26	−54	28
		Apr–May 2002–2005	+8	−41	49
Visakhapatnam (17.7°N, 83.8°E)	*Sreekanth et al.* [2007]	Nov–Feb 2006	+8.4	−35.8	+44.2
		Mar–May 2006	+3.9	−16.8	+20.8
		June–Aug 2006	+2.4	−9.9	+12.3
		Sep–Oct 2006	+0.7	−2.8	+3.5
Dibrugarh (27.3°N, 94.6°E)	*Pathak et al.* [2010]	Dec 2008 to Feb 2009	−1.0	−34.2	+33.2
		Mar–May 2009	−1.4	−37.1	+35.7
		June–Sep 2008	−1.5	−33.7	+32.2
		Oct−Nov 2008	0.1	−12.5	+12.6
Chennai (12.81°N, 80.03°E)	*Aruna et al.* [2016]	Jan–Feb 2013	+5.4	−35.3	+40.7
		Mar–May 2013	+5.8	-32.5	+38.3
		June–Sep 2013	−6	−38.4	+32.4
		Oct–Dec 2013	−4.3	−32.3	+28
Gadanki (13.5°N, 79.2°E)	*Gadhavi and Jayaraman* [2010]	Apr–Nov 2008	−4 to 0	−10 to −20	9 to 25
Delhi	*Singh et al.* [2010]	Annual 2006	−1.4 to +21	−46 to 110	+46 to +115
Pune (18.54°N, 73.85°E)	*Kumar and Devara* [2012]	Oct–Nov 2004–2009	−6.3	−37	30.8
		Dec–Feb 2004–2009	−6	−36.5	30
		Mar–May 2004–2009	−6.8	−40	32.4
Arabian Sea	*Moorthy et al.* [2005]	Mar–Apr 2003	−11.6 to −12.3	−25.7 to −28.3	+13.4 to +16.7
Bay of Bengal	*Satheesh* [2002]	Mar 2001	−4	−27	+23
Indian Ocean	*Satheesh* [2002]	Feb–Mar 2001	−10	−29	+19
Coastal India	*Ramachandran* [2005]	Dec–Feb 1996–2000	−10	−29	+19
Arabian Sea			−9	−22	+13
Tropical Indian Ocean			−4	−5	+1
Northern Bay of Bengal	*Moorthy et al.* [2009]	Mar 2006	−20	−45	+25
	Babu et al. [2012]	Jan 2009	~ −8	~ −17	~ + 10

network of 35 aerosol observatories over the entire India region, *Moorthy et al.* [2013a] reported that the regionally and annually averaged surface-reaching solar radiation was estimated to have decreased by $57\,W\,m^{-2}$ per unit AOD. In such a scenario, the aerosol-induced warming of the lower atmosphere is estimated to be $1.1\,K\,d^{-1}$. Using surface observations from a wide network of Indian stations, *Padmakumari et al.* [2013] showed a significant decreasing trend in surface evaporation for the period of 1971–2010, which has implications for the regional hydrologic cycle.

4.2.2.2. Aerosol Effects on Cloud Parameters

Nair et al. [2012] used aircraft measurements of microphysical parameters in cumulus clouds taken during Phase I of the Cloud Aerosol Interaction and Precipitation Enhancement Experiment (CAIPEEX) over India to study the aerosol influence on cloud parameters such as cloud effective radius, cloud liquid water content, and the cloud droplet number concentration. Cumulus clouds were significantly diluted due to entrainment mixing. A linear relationship between the cloud droplet number concentration and adiabatic fraction (a measure of mixing between the cloud and its environment) was found. Using the same CAIPEEX data, *Konwar et al.* [2012] found that greater CCN concentrations gave rise to clouds with smaller droplets and larger number concentrations. They also found that cloud drop effective radius increased with distance above

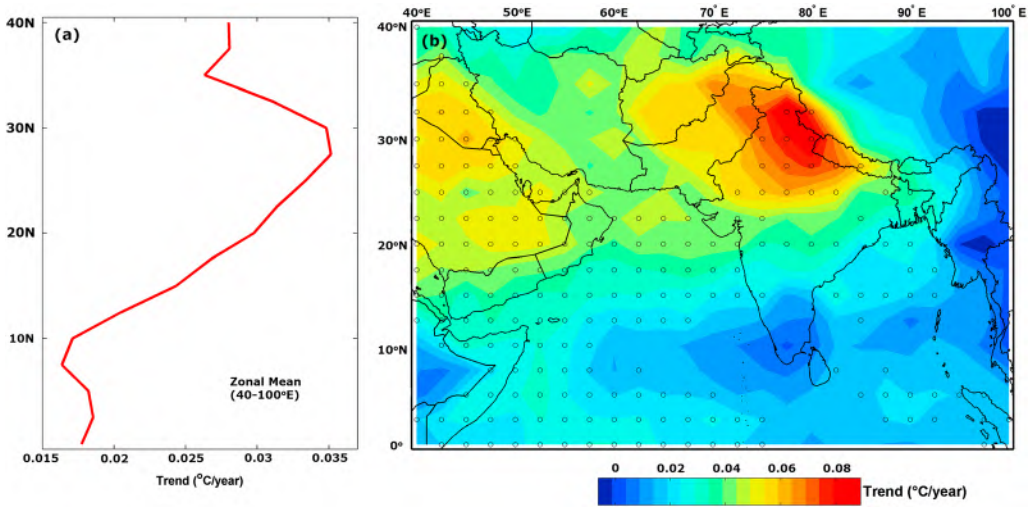

Figure 17. (a) Zonal mean (40°E–100°E) latitudinal profile of the midtropospheric temperature trend for the premonsoon season (March–May) from 1979 to 2007 and (b) the spatial distribution of the midtropospheric temperature trend over the Indian monsoon region in May. The midtroposphere corresponds to the 4–7 km atmospheric layer as recorded by the Microwave Sounding Unit. Open circles represent linear trends at the 95% confidence level. Modified from *Gautam et al.* [2009].

the cloud base. Drizzle was detected from warm clouds with water contents $> 0.01\,g\,kg^{-1}$ and cloud droplet effective radii at the cloud top exceeding 12 μm. The cloud droplet spectral width (σ) was small in premonsoon clouds developed from dry boundary layers. This was attributed to numerous aerosol particles and the absence/suppression of collision-coalescence during the premonsoon period. For polluted and dry premonsoon clouds, σ was constant with height. In contrast to premonsoon clouds, σ in monsoon clouds increased with height irrespective of whether they were polluted or clean. The mean radius of polluted monsoon clouds was half that of clean monsoon clouds. *Prabha et al.* [2012] also analyzed the effect of aerosols on reducing premonsoon cloud droplet spectral widths. Based on nearly year-long observations of CCN concentration and aerosol optical properties from a high-altitude Himalayan site (Nainital, 29.4°N, 79.5°W), *Gogoi et al.* [2015] reported enhanced CCN concentrations during periods of high aerosol absorption than during periods of high aerosol scattering. The spectral changes in absorption coefficient show a significant contribution of biomass burning aerosols to CCN activity over the Himalayan region.

4.2.2.3. Aerosol Impact on Temperature

Based on a 29 year (1979–2007) record of microwave satellite measurements, *Gautam et al.* [2009] reported widespread warming over the Himalayan-Gangetic region and consequent strengthening of the land-sea thermal gradient (Figure 17). Subsequently, they found an enhanced premonsoon warming of 2.7°C in the meridional temperature gradients where dust aerosol loading exerts an influence even at higher altitudes. Based on the high-altitude balloon-borne measurements from central India, *Babu et al.* [2011] reported aerosol-induced free troposphere warming associated with the presence of a significant amount of BC aerosols (~12 $\mu g\,m^{-3}$) from 4 to 5 km. The enhanced warming is associated with the presence of AAs, which heats the middle troposphere of the IGP and the Himalayan foothills, promoting a positive dynamical feedback to warming through the elevated heat pump (EHP) effect (*Lau et al.* [2006], see discussion in section 5.2). *Manoj et al.* [2011] explored a physical mechanism by which the radiative effects of AAs facilitate the transition from break to active spells of Indian monsoon intraseasonal oscillations by inducing a meridional gradient in lower atmosphere temperature.

4.2.2.4. Aerosol Impact on Monsoon Rainfall and the Hydrological Cycle

Aircraft measurements in India have shown that heavier air pollution manifests as a greater concentration of CCN, which nucleates greater number concentrations of smaller drops in convective clouds. This causes the height for the initiation of warm rain to be elevated to greater heights above the cloud base, with extreme pollution delaying the initiation of rain to heights greater than 6 km [*Prabha et al.*, 2011; *Freud and Rosenfeld*, 2012; *Konwar et al.*, 2012].

Recent studies have shown that while the trend in total monsoonal precipitation has remained relatively stable, the nature of the precipitation has changed dramatically in terms of frequency and intensity. *Goswami et al*. [2006] found significant rising trends in the frequency and the magnitude of extreme rain events, and a significant decreasing trend in the frequency of low-to-moderate events over central India during the latter half of the twentieth century. *Krishnan et al*. [2013] showed that the intensity of the boreal summer monsoon overturning circulation and the associated southwesterly monsoon flow has significantly weakened over the past 50 years. The role of aerosols in modulating monsoon rainfall over India has recently gained increased scientific attention due to heavy and increasing aerosol loading over the region. Using MODIS and complementary data sets, *Manoj et al*. [2012] showed that AIE could catalyze the asymmetric spatial distribution of Indian monsoon rainfall in one of the worst drought conditions in 2009, depending on the regional moisture conditions.

The role of the observed increasing trend in Arabian dust activity on the interannual to decadal timescale variations in the Indian summer monsoon rainfall has revealed dynamical and positive feedback due to dust-induced diabatic heating over the region [*Solmon et al*., 2015]. This is in line with the meridional and zonal gradients in the aerosol-induced atmospheric heating rate in the lower free troposphere estimated based on extensive ship-borne and satellite measurements made over the region [*Nair et al*., 2013a]. The study confirmed that aerosol-induced gradients (meridional and zonal) in surface cooling and atmospheric warming are mostly anthropogenic in origin [*Nair et al*., 2013a]. The distinctly different gradients in warming at lower and middle parts of the troposphere due to BC and dust over the Indian region could influence the thermal structure of the atmosphere and regional circulation patterns [*Nair et al*., 2013a]. The elevated layer of absorbing aerosols over northern India during the spring raises concerns about aerosol-induced snow darkening and enhanced snow melting over the Himalayan glaciers. *Nair et al*. [2013b] reported that the magnitude of snow albedo radiative forcing is much higher than the direct radiative forcing of aerosols, and both these effects trap more energy in the Earth-atmosphere system, which enhances the regional warming and glacier melting over the Himalayas. However, there exist large uncertainties in the simulation of aerosol fields over the South Asian region [*Nair et al*., 2012; *Moorthy et al*., 2013b; *Kumar et al*., 2014], which demands further investigations on aerosol life cycle, aging, and transport pathways.

The strong low-level southwesterly winds over the Arabian Sea associated with the monsoon not only transport moisture from the oceans but also serve as a source and conduit of natural aerosols of marine (sea salt) and continental (dust) origins that depend on both wind speed and direction. These natural aerosols dominate the aerosol mass loading over the Arabian Sea and could influence the monsoon precipitation over central Indian on short timescales [*Vinoj et al*., 2014]. The high positive correlation between precipitation over central India and AOD over the Arabian Sea in both observations and model simulations evident in their study (Figure 18) points to the clear signature of ADRF and the induced downstream influence of absorbing aerosols on Indian summer monsoon rainfall.

4.3. Asia-Pacific Rim

Located in the downwind region of the Asian continent, the North Pacific experiences a significant amount of aerosol transport during the dry phase (November to April) of the AM. Meanwhile, there are prevalent wintertime storms in the same region regulated by the monsoonal flow from the Siberian High to the Aleutian Low originating from Asia. Over the northwest Pacific, the near-surface meridional temperature gradient is high and heat and moisture sources from the warm ocean surface are abundant. These two preconditions sustain high tropospheric baroclinic instability which facilitates the development of the storm track characterized by a belt of local maximal precipitation across the North Pacific [*Zhang et al*., 2007]. Through interactions with maritime clouds and precipitation systems in winter, Asian pollution outflows exert potentially great impacts on regional and global climate and therefore have raised considerable concerns. However, there are limited long-term aerosol and cloud measurements available over the open North Pacific Ocean. Satellite measurements serve as the major observational tool used to assess aerosol effects over the Asia-Pacific Rim, as shown in Figure 19.

Satellite measurements have provided strong evidence of the trans-Pacific transport of the Asian pollution outflow in wintertime. The MODIS AOD winter season climatology has a noticeable zonal gradient over the North Pacific, indicating the prevailing transport of aerosols by Asian monsoonal outflows [*Li et al*., 2008]. The plume with high AOD takes 2–3 days to reach the coastline of North America based on MODIS Level 2

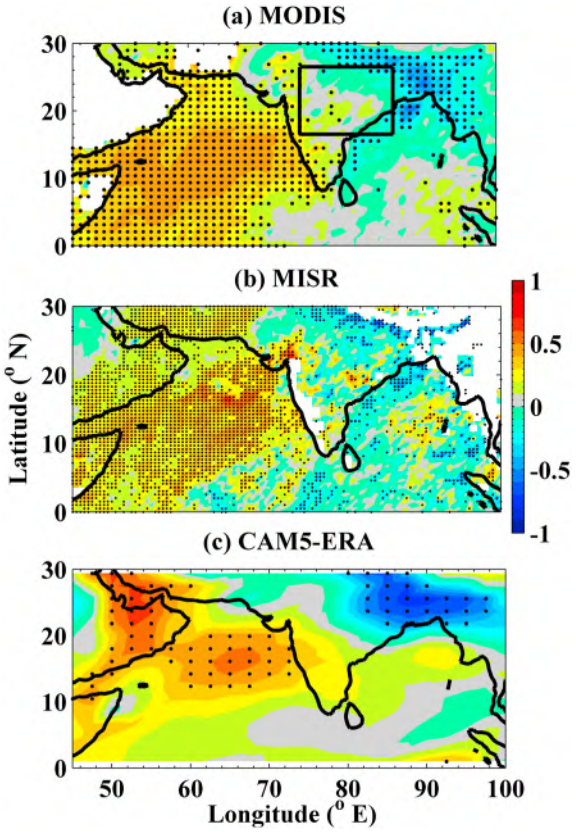

Figure 18. Correlation coefficient between precipitation over central India (outlined by the square box) and AOD over the Indian region. (a) MODIS Terra AOD at 550 nm, (b) MISR AOD at 558 nm, and (c) Community Atmosphere Model Version 5 simulated AOD at 550 nm. Data are from June, July, and August 2000–2009. The black dots represent the statistical significance at the 95% confidence level. Copied from *Vinoj et al.* [2014].

daily data. Using the MODIS AOD climatology, *Yu et al.* [2008] estimated that about 18 Tg yr^{-1} of pollution aerosols are exported from East Asia to the northwestern Pacific Ocean, of which about 25% reaches the west coast of North America.

The wintertime North Pacific is highly vulnerable to the aerosol effect because of favorable dynamical and microphysical conditions arising from interactions between the storm track and Asian pollution outflow. By analyzing cloudiness using data from the International Satellite Cloud Climatology Project (ISCCP), which contains a long-term record (1984–2005) with a global coverage, *Zhang et al.* [2007] reported a trend of increasing DCC over the North Pacific Ocean in winter (Figure 19) and suggested that the intensified Pacific storm track is climatically significant and represents possibly the first detected climate signal of ACI associated with anthropogenic pollution. Similarly, on the basis of long-term satellite measurements from the Global Precipitation Climatology Project, *Li et al.* [2008] reported a significant trend in wintertime precipitation (~1.5 mm yr^{-1}) over the North Pacific from 1984 to 2005. The Pacific storm intensity in terms of eddy meridional heat transport also exhibits an interdecadal trend since the 1980s based on NCAR Reanalysis data [*Wang et al.*, 2014a]. Hierarchical modeling studies revealed that the strengthened Asian pollution outflows in the recent decades contributed to such a change in storminess [*Wang et al.*, 2014a, 2014b].

5. Model Simulations and Theories of Aerosol and Monsoon Interactions

Modeling the effects of aerosols on climate requires an inventory of emissions from both natural and anthropogenic sources. Rapid changes in both surface and atmospheric environments of Asia pose a special challenge in the development of an emission inventory even though many efforts have been made. It is even more challenging to do a historical inventory. *Lamarque et al.* [2010] attempted to quantify historical anthropogenic and biomass emissions of climate-relevant species for the period 1850–2000. *Granier et al.* [2011] illustrated the diversity between different published inventories for different regions of the world and provided yearly global emissions for the period 1980–2010. These inventories have been used in World Climate Research Project (WCRP) CMIP simulations conducted in support of the most recent IPCC assessment. Several other studies provide specific information on recent trends. *Klimont et al.* [2013], for example, showed that the SO_2 emissions in China from the energy sector declined over the period 2000–2011, and that as a result, the total emissions in this country stabilized during this decade. *R. Wang et al.* [2014] found that the annual emissions of BC during the period 1960–2007 increased globally, but that the amount of BC emitted per unit of energy production had decreased in all the regions of the world, especially in China and India. The spatial resolution adopted for emission inventories also affects model results. Evaluating modeled surface BC concentrations against observations in Asia, *H. J. Wang et al.* [2013] noted that the bias between the two

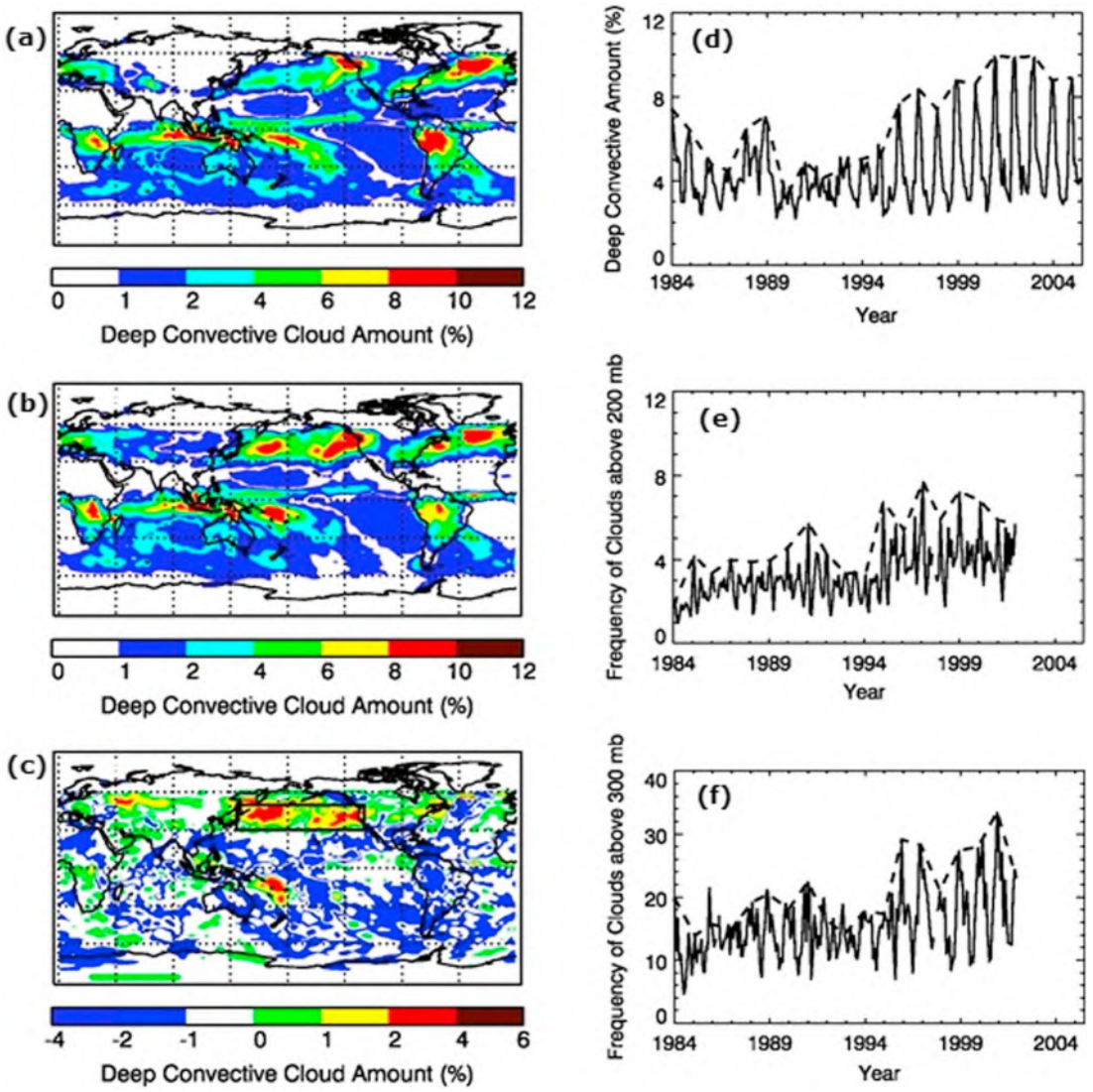

Figure 19. Global measurements of ISCCP-derived deep convective clouds (DCC) decadal mean amounts for the period of (a) 1984–1994, (b) 1994–2005, and (c) Figure 19b minus Figure 19a. The black rectangle in Figure 19c outlines the North Pacific region (30°N–50°N, 140°E–230°W). The time series of (d) ISCCP-derived DCC amounts, (e) the frequency of clouds above 200 mb, and (f) the frequency of clouds above 300 mb from high-resolution infrared sounder-averaged data over the black rectangle in Figure 19c from 1984 to 2005. The dotted line corresponds to the maximum wintertime (December–February) values. Copied from *Zhang et al.* [2007]. Copyright 2007 National Academy of Sciences.

quantities was considerably reduced in Asia when a simulation performed with a high-resolution model replaced a lower resolution model calculation. Using the aforementioned or other types of inventories, climate modelers have investigated the impact of anthropogenic and natural forcing on regional and global climate. Only the major findings concerning the impact on the EASM and SASM are reviewed here.

5.1. East Asia

5.1.1. Monsoon Circulation

In the latest CMIP5 study, model simulations were conducted under various historical external forcing conditions, which are useful for investigating the influences of different external forcings on the EASM. *Song et al.* [2014] used 17 CMIP5 models to investigate the response of the EASM to external forcing from GHG and anthropogenic aerosol emissions during the second half of the twentieth century (Figure 20). The first empirical orthogonal function (EOF1) of a multivariate empirical orthogonal function analysis shows a strong dipole sea level pressure (SLP) pattern over the western tropical Pacific and the East Asian land region. The principal component analysis of the leading mode (PC1) shows a decreasing trend indicating increasing SLP centered over the Philippines and decreasing SLP over China from 1965 until the 1980s when

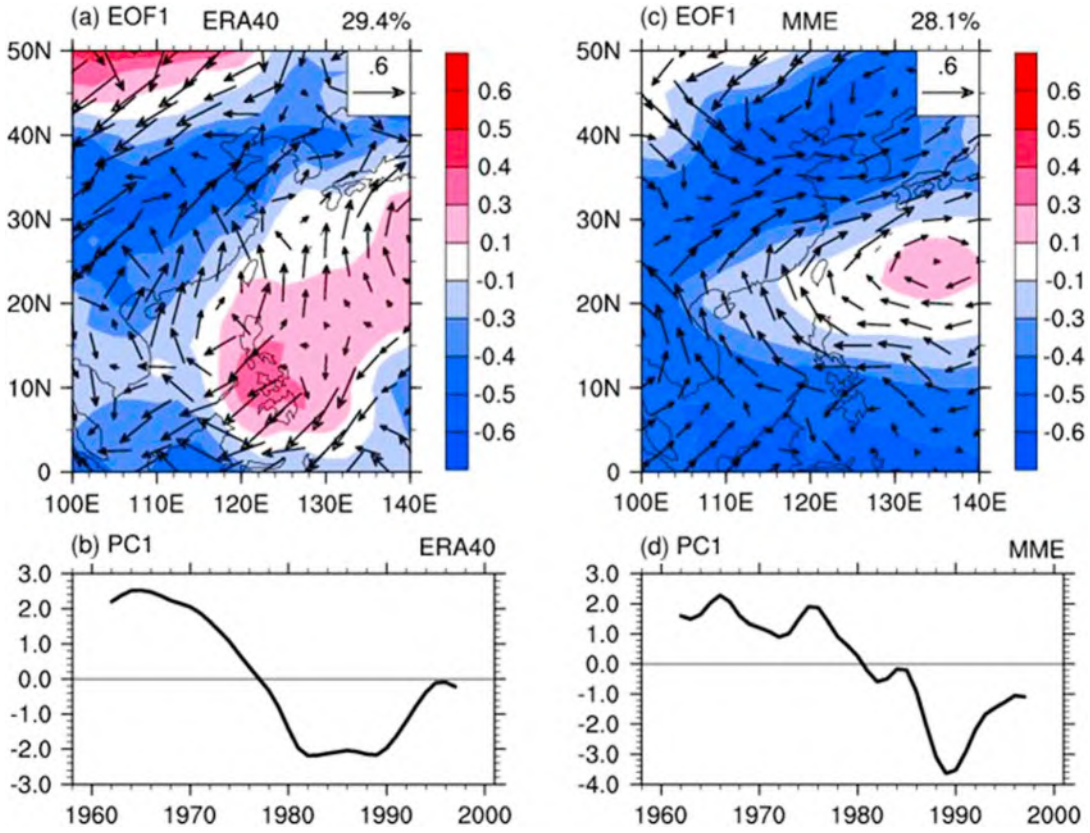

Figure 20. The leading multivariate empirical orthogonal function patterns (a and c) and corresponding PC1 (b and d) of the sea level pressure (shaded, hPa $(44\ \text{years})^{-1}$) and the 850 hPa wind field (vectors, m s^{-1} $(44\ \text{years})^{-1}$) from the European Centre for Medium-Range Weather Forecasts 40 year Reanalysis (ERA-40, Figures 20a and 20b) and the multimodel ensemble (MME, Figures 20c and 20d). The percentage values above Figures 20a and 20c are the explained variances. The MME is constructed using 35 realizations from 17 CMIP5 models. Copied from *Song et al.* [2014].

the SLP stabilizes and then begins to recover in the 1990s. This feature is well reproduced in the all-forcing runs but with a smaller magnitude and differences in the exact location of the dipole centers. These results suggest that the response of the EASM to anthropogenic forcing may include a component of decadal-scale variation. A comparison of separate forcing runs shows that aerosol forcing plays a primary role in the weakening of the EASM in the all-forcing run.

5.1.2. Surface Air Temperature

It has been suggested that the observed surface cooling over eastern China is partly due to aerosols [*Qian et al.*, 2003]. Other studies have connected surface cooling to the EASM precipitation change [*T. Wang et al.*, 2013; *Ye et al.*, 2013; *Guo et al.*, 2013], suggesting that aerosols induce surface cooling and weaken the land-sea thermal contrast, thereby weakening the monsoon circulation and related precipitation changes. However, *He et al.* [2013] conducted different external forcing experiments with an atmospheric GCM and found that GHGs, and to a lesser extent, the direct effects of aerosols, are mainly responsible for the surface cooling trend. In short, the roles of various factors in the long-term changes in surface air temperature (SAT) are uncertain.

It is plausible that the surface cooling over the EA continent is associated with aerosols. Since the aerosol-induced cooling is offset by the GHG-induced warming, a weak cooling trend exists over eastern China. The weakening trend in EASM circulation is driven by the decreased land-sea thermal contrast, which is evident in the linear trends in SAT over central China (Figure 21a). Observations show that central China has undergone a significant cooling trend (-0.70 K $(44\ \text{years})^{-1}$) during 1958–2001. The cooling trend over central China diminishes the land-sea thermal contrast. The warming trend over central China is evident in the GHG-forcing run due to the smaller heat capacity over land, while the cooling trend is more significant in the aerosol-forcing run due to the preferential cooling over East Asia (Figure 21b). Hence, it is likely that ADRF plays a primary role in the central China cooling and contributes to the weakening of the land-sea

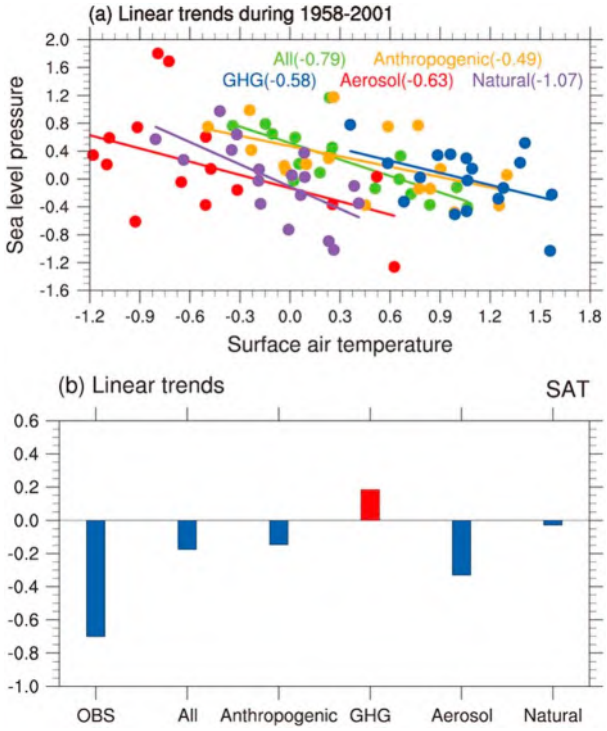

Figure 21. (a) Scatterplot of the linear trends in SAT (K (44 years)$^{-1}$) averaged over eastern China (28°N–38°N, 105°E–122°E) and sea level pressure (hPa (44 years)$^{-1}$) averaged over northern China (32°N–42°N, 105°E–122°E) in June-July-August of 1958–2001. The dots indicate 17 models in different forcing runs identified by different colors. The lines indicate the best linear fit lines between SAT and sea level pressure. The fitting coefficients are given in parentheses. (b) Linear trends in SAT averaged over eastern China (28°N–38°N, 105°E–122°E) from observations, the all-forcing run, the anthropogenic-forcing run, the GHG-forcing run, the aerosol-forcing run, and the natural-forcing run of the MME. The SAT averaged over the EASM region (0°–50°N, 90°E–160°E) has been subtracted. The MME is constructed using 35 realizations from 17 CMIP5 models. Copied from *Song et al.* [2014].

thermal contrast. However, the decreasing trend in EASM under external forcing is weaker than observations. This discrepancy indicates that the internal variability mode of the Pacific Decadal Oscillation may also play an important role in the monsoon [*J. P. Li et al.*, 2010; *Zhou et al.*, 2013; *Lei et al.*, 2014], while ADRF plays a secondary or complimentary role.

5.1.3. Precipitation

The EASM witnessed a significant decadal weakening during the second half of the twentieth century [*Wang*, 2001; *Zhou et al.*, 2009] but has somewhat recovered since the 1990s [*Zhu et al.*, 2011; *H. Liu et al.*, 2012]. The mechanism for the decadal variation in the EASM is an active research topic, and aerosols are regarded as one possible important factor [*T. Wang et al.*, 2013].

Menon et al. [2002] used global climate model simulations of the direct radiative effect of aerosols to investigate possible aerosol contributions to the tendency toward increased summer floods in south China, increased droughts in north China, and moderate cooling in China and India while most of the world has been warming. In simulating June-July-August (JJA) precipitation changes for two experiments (Experiment A where SSA = 0.85 and Experiment B with SSA = 1), they found precipitation and temperature changes in the model that were comparable to those observed if aerosols included large amounts of absorbing BC (Figure 22). Absorbing aerosols heat the air, alter regional atmospheric stability and vertical motions, and affect the large-scale circulation and hydrologic cycle with significant regional climate effects. However, the assumed SSA value for China used in their model appears to be systematically too low, i.e., too much solar absorption. *Lee et al.* [2007] found that the mean SSA is about 0.9. With this value of SSA, *Menon et al.* [2002] would not be able to simulate the same trends seen in a few meteorological variables including rainfall [*Zhang et al.*, 2009; *H. Zhang et al.*, 2012].

Since *Menon et al.* [2002], there have been a number of studies with diverse results regarding the impacts of aerosols on the EASM. *Mahmood and Li* [2011] found that the impact of BC is less important for the 1990s precipitation change. *Zhou et al.* [2013] suggested that the rapidly growing SO_2 emissions and its uneven distribution contributed to the late 1990s precipitation change over eastern China. *L. Wu et al.* [2013] further stressed that the location of the monsoon precipitation and its location relative to the location of aerosols are important when considering aerosol effects on the EASM. The influence of aerosols on precipitation characteristics has also been investigated by *Qian et al.* [2009]. Based on observations and model simulations, they found that the decrease in light rainfall events in China during 1956–2005 is partly due to the increase in AAs because aerosols increase the cloud droplet number concentration and reduce droplet sizes. A high-resolution Weather and Research Forecasting (WRF) model coupled with Chemistry (WRF-Chem) modeling study revealed that anthropogenic pollution contributed to a ~40% reduction of precipitation over Mount

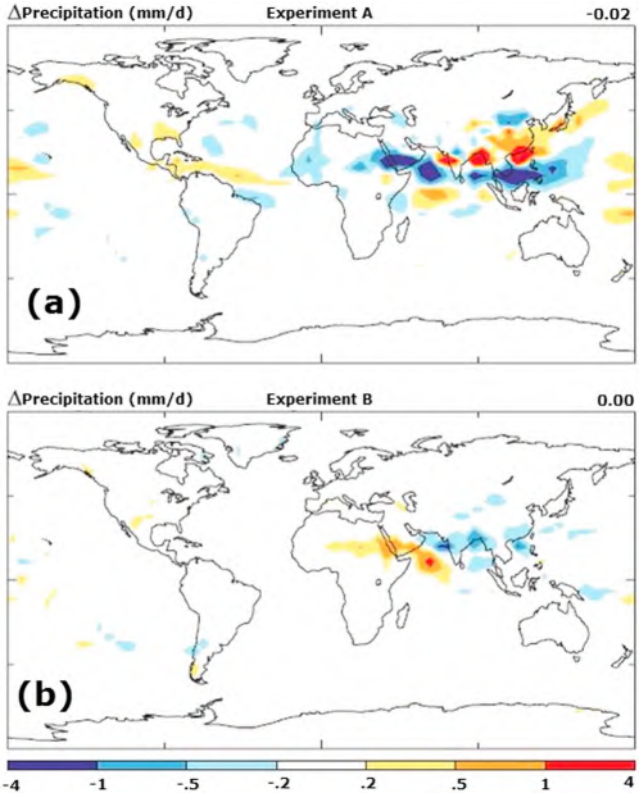

Figure 22. Simulated June-July-August precipitation changes from (a) the experiment with SSA = 0.85 and (b) the experiment with SSA = 1.0. The Goddard Institute for Space Studies SI2000 12 layer climate model was used. Both experiments were run for 120 years. The numbers in the upper right corner are the global mean changes. Modified from *Menon et al.* [2002].

Hua during a one-month summer time period [*Y. Yang et al.*, 2016]. The weakened mountain-valley circulation due to warming aloft and cooling near the surface induced by AAs is one of the major mechanisms contributing to the suppressed precipitation.

There have been an increasing number of recent studies regarding possible responses of the EASM to ADRF [*Lau and Kim*, 2015]. However, because of different observation periods, different model experimental designs, and uncertainties in model physics, especially with regard to AIE, results have been as confusing as they are informative. Most studies have focused on the causes for the observed NDSW pattern [*Lau and Weng*, 2001; *Wang and Zhou*, 2005].

Other GCM experiments have shown reduced rainfall in northern China due to surface cooling by the increased loading of sulfate aerosols and increased rainfall in the southern part of China in July due to induced strengthening of the local Hadley circulation [*Gu et al.*, 2006]. They found that heating of the air column by BC and dust particles in the middle to high latitudes tends to move the simulated precipitation inland. However, the inclusion of BC in their simulations did not produce the observed NDSW precipitation pattern. Furthermore, the solar dimming effect (SDM) of sulfate aerosols can reduce atmospheric baroclinicity and cause a deceleration of the East Asia jet stream and consequent rainfall reduction over East Asia in late spring and early summer [*Kim et al.*, 2007]. In one study, the combined effect of BC and sulfate aerosols was found to be largely dominated by sulfates in producing a weakened East Asia monsoon for both summer and winter seasons [*Liu et al.*, 2009]. Through semidirect and indirect effects, BC aerosols have been shown to cause a reduction in clouds and rainfall over southern China and an increase in rainfall over northern China through increases in moisture transport by the western Pacific subtropical high [*Zhang et al.*, 2009]. However, this pattern is opposite to the NDSW pattern.

Some recent studies based on CMIP5 multimodel ensemble simulations indicated that the decrease in the land-ocean thermal contrast and precipitation over land in monsoon regions was dominated by aerosol forcing during the historical boreal summer period, contributing to a more localized distribution of anthropogenic aerosols over land relative to the well-mixed GHGs [*X. Li et al.*, 2015; *Zhang and Li*, 2016]. Recent work by *Q. Wang et al.* [2016] showed that increases in global AAs in 2000 relative to 1850 weakened the EASM circulation and precipitation. However, the weakening of the circulation due to changes in EA and non-EA aerosol emissions was comparable, and the effect of nonlocal aerosols was larger in individual regions. The important effect of aerosols in simulations of historical climate change suggests that there will be a substantial effect on future climate change due to the decreased emissions of aerosols and their precursors. *Wang et al.* [2016a] showed that reducing the amount of aerosols could significantly change local thermodynamic and dynamic processes, and the hydrological cycle, thus strengthening the EASM circulation and precipitation. An additional warming of the Earth due to the decline in AAs in the 21st century from present-day levels would aggravate the precipitation extremes over EA caused by GHG-induced warming [*Wang et al.*, 2016b]. The

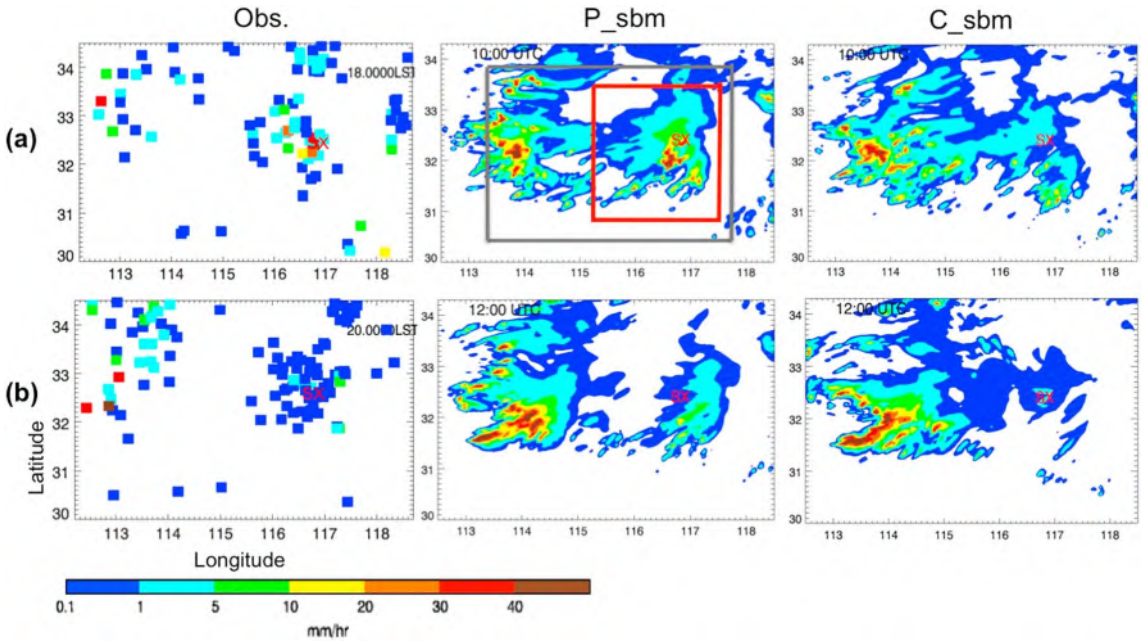

Figure 23. Spatial distribution of hourly rain rates (mm h^{-1}) from (left column) observations and model simulations for (middle column) polluted cases (P_sbm) and (right column) clean cases (C_sbm) at (a) 10:00 UTC and (b) 12:00 UTC for a mesoscale convective system occurring in Southeast China on 17 July 2008. The model used was the Weather Research and Forecasting (WRF) Model [*Skamarock et al.,* 2005] coupled with an explicit bin microphysics parameterization based on work by *Khain et al.* [2004]. The red box shows the study region, and the gray one denotes the large region for the statistical results shown in the paper. SX stands for Shouxian where an intensive field experiment was conducted using the ARM Mobile Facility [*Li et al.,* 2011a]. Copied from *Fan et al.* [2012].

increased rate of precipitation extremes with global mean surface warming in the 21st century caused by aerosol forcing was significantly larger than that caused by GHG forcing [*Lin et al.*, 2016].

The studies cited above represent a small sample of studies attempting to attribute the impact of aerosols on aspects of the East Asia long-term rainfall change. However, because of multiple factors controlling long-term variations in the EASM, including flow variability downstream of the TP, the southwest monsoon flow of South Asia, the displacement of the western Pacific subtropical high, and the strong remote forcing from SST anomalies associated with climate variability and change [*Lau et al.*, 2000], studies of the aerosol impact on variations in the EASM have so far yielded diverse and largely inconclusive results.

The diversity in results is understandable given the large uncertainties in accounting for the complex effects of aerosols in any global model. For more regional and local features with short-time duration, the impacts of aerosols on the EASM are better illustrated using high-resolution atmospheric models with more realistic microphysics [*Fan et al.*, 2012]. Model simulations were conducted using the high-resolution WRF model with spectral bin microphysics (SBM) for two different cloud regimes encountered during an intensive field experiment [*Li et al.*, 2011a]. Changes in CCN significantly change the timing of storms, the spatial and temporal distributions of precipitation, the frequency distribution of precipitation, and the cloud base and cloud top heights for DCC, but not for stratiform clouds (Figure 23).

A recent study by *Fan et al.* [2015] shows that AAs in the Sichuan Basin may have contributed significantly to the flooding in mountainous regions downstream. They proposed a mechanism called "aerosol-enhanced conditional instability" whereby under polluted conditions over the Sichuan Basin, strongly absorbing aerosols cool the surface and heat the atmosphere aloft, which stabilizes the atmosphere and suppresses convection over the basin. This allows greater amounts of moist static energy to build up over the basin during daytime and to be transported to the mountainous area by the prevailing winds. The lifting by topography triggers convection and causes extremely heavy precipitation over the mountains at night.

5.2. South Asia

Similar to the EASM, global and high-resolution regional climate models have been used to simulate the effects of direct (radiative), indirect (microphysics), and dynamical feedbacks on SASM precipitation and climate.

The strong land-ocean asymmetry in the solar heating due to aerosols over South Asia can significantly affect atmospheric circulation and meteorological variables, which have stimulated intense inquiries over the past decade into the fundamental causes for the observed meteorological trends [e.g., *Ramanathan et al*., 2005; *Lau et al*., 2006; *Bollasina et al*., 2011; *Ganguly et al*., 2012]. While these studies seem to be inconsistent with each other on the surface, a deeper enquiry into various model studies reveals certain common features.

1. The observed dimming, the cooling of winter surface temperatures, and decrease in summer monsoon precipitation cannot be explained by the buildup of GHGs alone. They also cannot be explained by natural variability.
2. All the model studies conclude that aerosols have perturbed the monsoon circulation and precipitation patterns, but none has been able to explain all of the observed features.
3. Because of the trends in SSTs and the changes in SST gradients, any explanation of the weakening of the monsoon precipitation must account for the changes in SSTs since it is one of the major drivers of monsoon circulation.
4. The decrease in the monsoon (JJA) rainfall over the IGP is likely due to SDM by manmade aerosols, both by local aerosols emitted by South Asia as well as by aerosols emitted globally. The dimming by local aerosols decreases the land (South Asian)-ocean (NIO) contrast in surface solar heating and decreases the north-south gradient in SST of the NIO and thus weakens the fundamental drivers of the monsoon circulation. The dimming by global aerosols, on the other hand, weakens the interhemispheric solar heating gradient of the ocean since aerosols are more concentrated in the polluted Northern Hemisphere. This preferential cooling of the Northern Hemisphere leads to a southward shift of the ITCZ and weakens the northern monsoon circulation. Overall, studies to date conclude that the influence of local aerosols is a major factor for the observed decrease in the monsoon rainfall over north India (the IGP).

There have been two classes of model studies so far. One is the self-consistent climate-aerosol model that simulates aerosol forcing using simulated transport and simulated aerosol spatial distributions [e.g., *Lau et al*., 2006; *Meehl et al*., 2008; *Ganguly et al*., 2012; *Bollasina et al*., 2013]. The other class consists of studies in which aerosol forcing is estimated from satellite and ground-based observations [e.g., *Ramanathan et al*., 2005], and as a result, the aerosol forcing is independent of the simulated meteorology. The problem with self-consistent climate-aerosol studies is that the simulated forcing underestimates the direct aerosol forcing by BC and likely other aerosols too. For example, a comprehensive assessment of models by *Bond et al*. [2013] finds that models underestimate BC optical depths by factors of 2 to 4 over Asia and thus severely underestimate the atmospheric heating as well as dimming. The problem with the prescribed aerosol forcing is that while it preserves the observed dimming and atmospheric solar heating by aerosols, it ignores the feedback between aerosol forcing and circulation. Independent of such vast differences between the two classes of studies, they converge on the dominant factor determining the observed trends in monsoon precipitation: it is likely not the GHG buildup but the buildup of air pollution-related aerosols. Details about the various studies are described below.

Ramanathan et al. [2005] and *Chung and Ramanathan* [2006] showed that through the attenuation of solar radiation reaching the surface by aerosols, i.e., SDM, the high aerosol regions of the northern portion of the Indian subcontinent and the Arabian Sea are cooled relative to the oceans to the south, leading to a reduction of the meridional thermal gradient and a slowing down of the local meridional circulation. The slower circulation reduces surface evaporation and provides a positive feedback, further weakening the monsoon. In a somewhat different vein, *Lau et al*. [2006] and *Lau and Kim* [2006] emphasized the importance of temporal (early versus late monsoon) and regional (northern versus southern South Asia) distributions of both natural and AAs not only as a forcing agent but also as an integral part of a dynamical feedback mechanism involving clouds, rainfall, and winds that can alter the evolution of the entire SASM system. They proposed the EHP hypothesis which posits that atmospheric heating by deep layers of dust and BC accumulated over the IGP and the Himalayan foothills can induce an atmospheric moisture convergence feedback, leading to increased precipitation in northern India and the foothill regions during the early monsoon (May–June) season. Specifically, shortwave (SW) absorption by the accumulation of BC and dust over the northern and southern slopes of the Himalayas over the longitudes of the Indian subcontinent during pre-monsoon and early monsoon periods (May–June) heats the lower and middle troposphere around the TP. The heated air rises via dry convection, creating a positive temperature anomaly in the mid-to-upper troposphere over the Himalayan foothills and the southern TP relative to the region to the south. The rising hot air

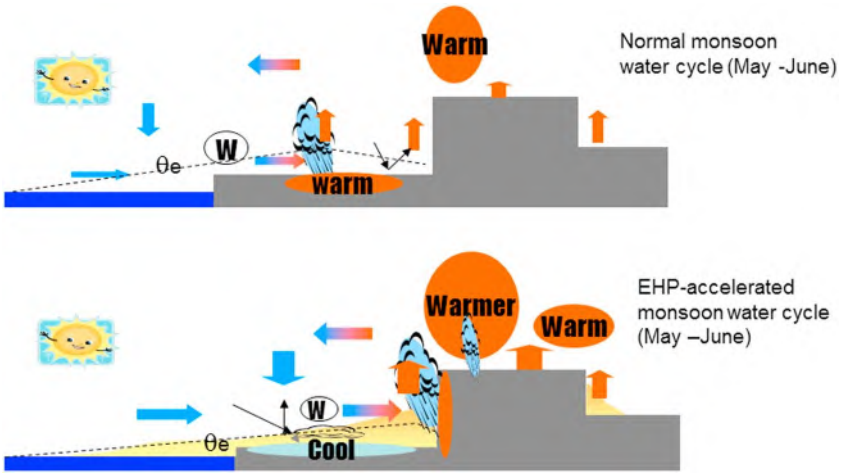

Figure 24. Diagram illustrating the elevated heat pump (EHP) hypothesis. Schematic showing the monsoon water cycle (top) with no aerosol forcing and (bottom) with the aerosol-induced EHP effect. Low-level monsoon westerlies are denoted by W. The dashed line indicates magnitude of the low-level equivalent potential temperature θe. Deep convection is indicated over regions of maximum θe. Arrows denote air circulation. Copied from *Lau et al.* [2008]. ©American Meteorological Society. Used with permission.

forced by the increased heating in the upper troposphere draws in more warm and moist air over the Indian subcontinent, setting the stage for the onset of the South Asia summer monsoon (Figure 24). A subsequent modeling study by the same authors [*Lau and Kim*, 2007] found that while the EHP could strengthen the Indian monsoon during the early part of the rainy season (May–June), the SDM effect, possibly coupled with a cloud-land surface feedback, may lead to a subsequent weakening of the Indian monsoon in July–August. The above studies suggest the possible contributions of aerosols to the observed variability in rainfall but did not address the contributions from other factors. Therefore, these hypotheses are plausible but not without ambiguity, even though aspects of the observed signals are consistent with those from numerical simulations. Moreover, the same sets of observations could have been subjected to different interpretations and conclusions [*Lau and Kim*, 2007].

A different hypothesis has been proposed by *Nigam and Bollasina* [2011] who argued that increased aerosol loading is linked to suppressed precipitation, due to the semidirect effect. *Bollasina et al.* [2008] found that the EHP mechanism may be related to the expansive zonal averaging used. The western and eastern sectors may have hydro-climate signals that are opposite in sign, leading to the spurious collocation of aerosol loading.

Other modeling studies have provided support for the EHP mechanism, showing that aerosols may increase the premonsoon (March–May) rainfall while decreasing the total monsoon precipitation in JJA, consistent with an earlier onset of the monsoon [*Meehl et al.*, 2008; *Collier and Zhang*, 2009; *Bollasina et al.*, 2013]. The monsoon response to ADRF depends on the way aerosols are treated in models and also on the model fidelity to simulate the observed mean monsoon climate [*Manoj et al.*, 2011]. Using the Geophysical Fluid Dynamics Laboratory (GFDL) GCM, *Randles and Ramaswamy* [2008] examined the atmospheric-only response of the South and East Asian monsoon climate to a range of aerosol absorption and extinction optical depth increases, by including only the direct and semidirect aerosol effects. Precipitation changes were found to be less sensitive to changes in aerosol absorption optical depth at lower aerosol loadings. However, at higher absorption optical depths, low-level convergence and increases in vertical velocity overcome the stabilizing effects of AAs and enhance the monsoonal circulation and precipitation in northwestern India. By contrast, an increase in only scattering aerosols weakens the monsoonal circulation and inhibits precipitation in this region. *Bollasina et al.* [2011] used a more recent GFDL fully coupled model (CM3) to investigate the multidecadal SASM response to natural and anthropogenic forcing. The study emphasized the global impacts of aerosols and suggested that the observed precipitation decrease (Figure 25) was mostly attributed to anthropogenic increases in global aerosol emissions through interactions with the global-scale coupled ocean-land-atmosphere system. Their results suggest that the reduction in precipitation over South Asia is the outcome

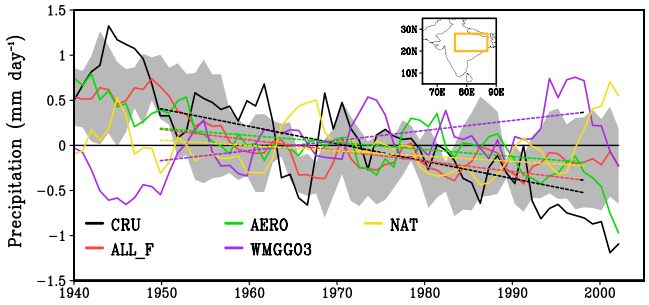

Figure 25. Five-year running mean June–September average precipitation anomalies over central north India (76°E–87°E, 20°N–28°N). Anomalies are calculated as deviations from the 1940 to 2005 climatology. The black line is based on the Climatic Research Unit (CRU) Time Series Version 3.0 observational data set. The red, green, blue, and yellow lines represent ensemble mean all forcing (ALL_F), aerosol only, greenhouse gases and ozone-only (WMGGO3), and natural forcing-only (NAT) CM3 historical integrations. The gray shading represents the standard deviation of the five--member all-forcing ensemble. The least squares linear trends during 1950–1999 are plotted as dashed lines with the different colors representing the different runs shown. Copied from *Bollasina et al.* [2011]. ©American Meteorological Society. Used with permission.

of a slowdown of the tropical meridional overturning circulation, which compensates for the aerosol-induced energy imbalance between the Northern and Southern Hemispheres.

In another modeling study, *Hazra et al.* [2013] revealed the importance of aerosols on the intraseasonal oscillations of the Indian monsoon through complex interactions between direct radiative forcing, cloud microphysics, and large-scale dynamics. Figure 26 is a schematic of the processes and feedbacks involved during monsoon breaks. BFA and BNFA mean that the breaks are followed by an active rainfall condition and not followed by an active rainfall condition, respectively. The BFA cases have higher aerosol concentrations, induce a stronger north-south temperature gradient, and have stronger moisture convergence and smaller cloud droplets lifted by convergence, which results in larger latent heat release at upper levels. This invigorates clouds and produces heavy rain. The hypothesis is that enhancement of precipitation can occur if "mixed-phase precipitation" is generated even in a dirty environment. Using the same GFDL model as in *Bollasina et al.* [2011], *Levy et al.* [2013] found that under the Representative Concentration Pathways 4.5 scenario, the largest

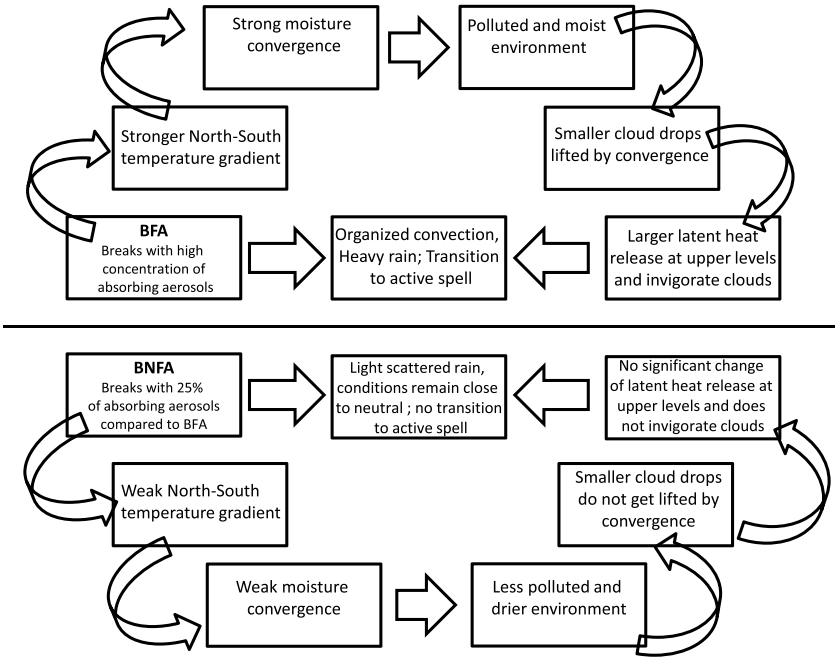

Figure 26. Schematic diagram of the possible hypotheses that may lead to either enhancement (moist environment) or suppression (drier environment) of precipitation under dirty background conditions during Indian summer monsoon breaks. BFA and BNFA stand for Indian summer monsoon breaks that are followed by an active condition and Indian summer monsoon breaks that are not followed by an active condition, respectively. Redrawn with modifications from *Hazra et al.* [2013]. ©American Meteorological Society. Used with permission.

precipitation increase occurs in and downwind of the Asian continent over the Pacific where there is a decrease in aerosol loading.

At present, the question of the relative roles of local aerosols or remote forcing from nonlocal aerosols through altering the large-scale ocean-atmosphere circulation is still a matter of debate. *Ganguly et al*. [2012], however, showed that Asian aerosols have made a major contribution to the drying trend of the SASM. *Lau et al*. [2006] maintained that changes in regional rainfall over South Asia by the EHP effect are crucially dependent on the local spatial and temporal distribution of aerosols over northern India. *Cowan and Cai* [2011] found that the reduction in monsoon precipitation over the twentieth century was attributed mainly to non-Asian aerosols. *Bollasina et al*. [2014] attributed the observed negative trend in SASM rainfall to nonlocal AAs. They argued that aerosols, mainly concentrated in the Northern Hemisphere, induced an anomalous cross-equatorial northward transport to compensate for the interhemispheric TOA energy imbalance.

5.2.1. ADRF on the SST Trend

Globally, aerosols probably exert the second largest anthropogenic radiative forcing on climate after GHGs [*Mitchell et al*., 1995; *IPCC*, 2007, 2013]. The inclusion of ADRF in climate system models can improve the simulation of global mean temperature over the last few decades [*Mitchell et al*., 1995].

It is plausible that the global-averaged near-surface temperature hiatus during the 1950s and 1960s, and the coincident decrease in precipitation have been influenced by anthropogenic ADRF [*Tett et al*., 2002; *Stott et al*., 2006; *Wilcox et al*., 2013]. The recent global warming hiatus has also been linked to other factors such as the pronounced cooling of the tropical eastern Pacific, mostly likely due to the interdecadal scale natural variability of the ocean [*Kosaka and Xie*, 2013]. Increasing the amount of aerosols in the atmosphere may cause reductions in heat content in both hemispheres [*Cai et al*., 2006]. The Northern Hemisphere is cooled via a reduction in surface heat flux. The Southern Hemisphere is cooled via hemispheric heat transport. Increasing aerosols strengthens the global conveyor which increases the warming rate in the subtropics and takes heat out of the off-equatorial region, generating the cooling trend [*Cai et al*., 2007]. The emission of AAs can influence ocean circulation [*Cowan and Cai*, 2013; *Cowan et al*., 2013] and is associated with the fast warming of the southern midlatitude oceans [*Cai et al*., 2010]. There are significant correlations between observed decadal surface temperature changes and simulated surface temperature changes from recent sulfate aerosol forcing in an equilibrium framework. Sulfate ACI might be a contributor to the spatial patterns of recent temperature forcing but not to the global mean "hiatus" itself [*Gettelman et al*., 2015]. In addition, ADRF has been suggested as a driver of the Atlantic multidecadal oscillation [*Booth et al*., 2012]. It also acts to modify the Pacific Decadal Oscillation and contributes to the width of the tropical belt [*Allen et al*., 2014]. For the Indian Ocean, the potential roles of AAs in the temperature trends of the subthermocline [*Cai et al*., 2007; *Cowan et al*., 2013], as well as the decadal variability of sea level and thermocline depth [*Trenary and Han*, 2013], have been pointed out.

An analysis based on one climate model has shown that the observed Indian Ocean warming is largely attributed to external forcing (more than 90%), especially anthropogenic forcing [*Dong et al*., 2014]. The competing effects of GHGs and AAs in the Indian Ocean warming and their mechanisms during the twentieth century have been further examined by *Dong and Zhou* [2014] using 17 CMIP5 models. The Indian Ocean warming trend during 1870–2005 from observations (0.40 K/100 yr) is well reproduced by the all-forcing run (0.41 K/100 yr), which is mainly caused by GHG forcing (0.66 K/100 yr) and weakened by the emission of AAs (−0.34 K/100 yr), especially through the indirect effect of AAs (Figure 27).

Both the basin-wide warming effect of GHGs and the cooling effect of AAs, mainly through indirect aerosol effects, are achieved through atmospheric processes. The positive contributions of surface latent heat flux from the atmosphere and surface longwave (LW) radiation due to GHG forcing dominate the basin-wide warming, while the reductions in surface SW radiation, surface LW radiation, and latent heat flux from the atmosphere associated with AAs induce the basin-wide cooling.

5.2.2. Impact of Light-Absorbing Aerosols in Snow/Glaciers on the Asian Monsoon

Light-absorbing aerosols (LAA, e.g., BC, brown carbon, and dust) influence atmospheric circulation and monsoon climate in multiple ways. In addition to their effects associated with atmospheric heating by absorption of solar radiation and interactions with clouds, LAA in snow or in glaciers (dirty snow/ice) can reduce the surface reflectance (i.e., surface darkening), which likely reduces snow albedo and accelerates snowpack melt [e.g., *Warren and Wiscombe*, 1980; *Hansen and Nazarenko*, 2004; *Y. Wang et al*., 2011; *Qian et al*., 2014]. Climate modeling studies suggest that this mechanism has a greater warming and snow melting efficacy than any

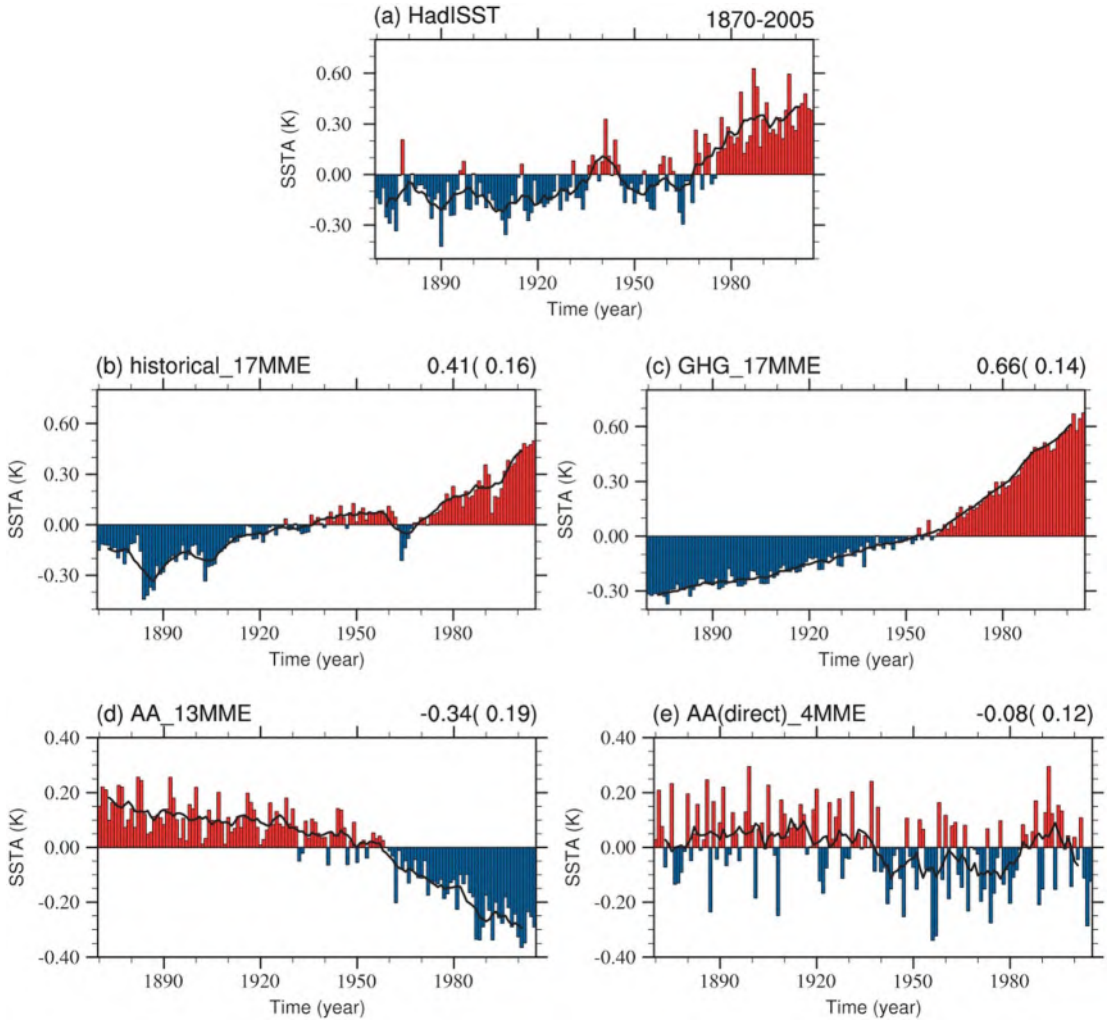

Figure 27. Time series of Indian Ocean (40°S–15°N, 40°E–100°E) annual mean (bars) and 8 years running average (lines) SST anomalies (SSTA) from (a) observations, (b) all-forcing runs of the 17 models' MME, (c) GHG-only forcing runs of the 17 models' MME, (d) AA-only forcing of 13 models' MME which include both direct and indirect effects, and (e) AA-only forcing of four models' MME which only include direct effects. SSTA is relative to the mean of the period 1870–2005. Units are in K. The numbers on the top right of Figures 27b–27e represent the trend values (in K (century)$^{-1}$) and standard deviations of intermodel variations, respectively. Copied from *Dong and Zhou* [2014]. ©American Meteorological Society. Used with permission.

other anthropogenic agent [*Hansen et al*., 2005; *Qian et al*., 2011; *Y. Wang et al*., 2011] because of its effectiveness in removing snow cover. LAA in snow and ice has been identified as one of the major forcings affecting climate change [*IPCC*, 2007, 2013].

The TP has long been identified as critical in regulating the Asian hydrologic cycle and monsoon climate [e.g., *Yanai et al*., 1992; *Wu and Zhang*, 1998]. The glaciers on the Himalayas and on the TP act as a water storage tower for many Asian countries. Long-term trends and/or seasonal shifts in water supply provided by the Himalayas/TP may significantly affect agriculture, hydropower, and even national security for the countries in the region. In addition, the TP exerts significant mechanical and thermal forcings that influence the SASM and EASM systems [*Manabe and Terpstra*, 1974; *Yeh et al*., 1979]. Anomalous snow cover can influence the energy and water exchange between land surfaces and the lower troposphere by modulating radiation and water and heat fluxes [*Cohen and Rind*, 1991], which, in turn, could affect monsoon rainfall in China and India in the subsequent summer [e.g., *Wu and Qian*, 2003].

Qian et al. [2011] conducted a series of numerical experiments with the Community Atmosphere Model to assess the relative impacts of anthropogenic carbon dioxide (CO_2) and carbonaceous particles (e.g., BC and OC) in the atmosphere and in snow on the snowpack over the TP, and subsequent impacts on the Asian monsoon climate and hydrologic cycle. They found that BC in snow increases the SAT by around 1.0°C and

reduces spring snowpack over the TP more efficiently than the increase of CO_2 and carbonaceous particles in the atmosphere. As a result, runoff shows an earlier melting trend, i.e., increasing during late winter and early spring but decreasing during late spring and early summer. Simulations made by *Qian et al*. [2011] also show that during boreal spring, aerosols are transported by a southwesterly flow, allowing some LAA to reach higher altitudes and to settle on the snowpack/glaciers on the TP. While LAA in the atmosphere directly absorbs sunlight and warms the air, the darkened snow surface polluted by LAA absorbs more sunlight and warms the snow surface. Both effects enhance the upward motion of air and spur deep convection along the TP during the premonsoon season, resulting in a possible earlier onset of the SASM and an increase in moisture, cloudiness, and convective precipitation over northern India. In East Asia, LAA in snow and ice has a more significant impact on monsoon circulation in July than do CO_2 and LAA in the atmosphere. The role of the TP as a heat pump is likely strengthened by aerosol atmospheric heating effects such as the EHP, and snow darkening by LLA in snow from spring through summer as the land-sea thermal contrast increases to strengthen the EASM, probably due to the increase in both sensible heat flux associated with the warm skin temperature and latent heat flux associated with increased soil moisture. As a result, summer precipitation increases in both southern China and northern China but decreases in central China (i.e., the Yangtze River basin), which has a near-zonal anomaly pattern consistent with the dominant mode of precipitation variability in East Asia.

The radiative forcing and climate response due to BC in snow and/or ice were also investigated by *Z. Wang et al.* [2011]. The results show that the global annual mean surface radiative forcing due to BC in snow/ice is $+0.042\,W\,m^{-2}$, with maximum forcing found over the TP, and regional mean forcing exceeding $+2.8\,W\,m^{-2}$. The global annual mean surface temperature increased 0.071°C due to BC in snow/ice. Positive surface radiative forcing was clearly shown in winter and spring and increased the surface temperature of snow/ice in the Northern Hemisphere. Surface temperatures of snow-covered areas of Eurasia in winter (spring) increased by 0.83°C (0.6°C). Snowmelt rates also increased greatly, leading to earlier snowmelt and peak runoff times. With the rise of surface temperatures in the Arctic, more water vapor could be released into the atmosphere, allowing easier cloud formation, which could lead to higher thermal emittance in the Arctic. However, the total cloud forcing could decrease due to increasing cloud cover, which would offset some of the positive feedback mechanism of the clouds.

Using data from the Indian Institute of Tropical Meteorology's Cloud Aerosol Interactions and Precipitation Enhancement Experiment and WRF simulations, *Dipu et al*. [2013] showed that the direct radiative effect of dust aerosols leads to an increase in the ice mixing ratio and ice water content in regions of dry to wet transition, thus inducing changes in the regional hydrologic cycle.

6. Impact of the Asian Monsoon on Aerosols

So far, preceding discussions have been focused on the impact of aerosols on monsoon climate. On the contrary, monsoon systems can also exert their influences on aerosol variations [*Chen et al*., 2008; *He et al*., 2008; *Zhao et al*., 2010; *Zhang et al*., 2010a, 2010b; *Zhu et al*., 2012]. Aerosols are transported by monsoon winds from source regions to downstream regions, depending on the size of the aerosol species. Dry deposition by gravitational settling and wet deposition by rainfall (wash-out) are major sinks of aerosols. In the heavily populated monsoon region, it is common knowledge that even with wash-out by heavy monsoon rain which occurs intermittently, aerosols can build up to high concentrations within hours or days because of the continuous high rate of local emissions, as well as the transport and the trapping of aerosols by local topography. Observational data showed that the annual variability of atmospheric aerosol concentrations is significantly correlated with the annual variability of dry days at 120 sites in China from 2000 to 2011 [*Wang et al*., 2012b]. Natural aerosols such as desert dust are mobilized and emitted from the desert surface by changing surface winds and transported over long distance from deserts to monsoon regions [*Chin et al*., 2007]. Typical aerosol residence times in the atmosphere are days to weeks, depending on the particle size and atmospheric conditions. Aerosols lofted into the upper troposphere and stratosphere by volcanic eruptions or jet stream dynamics can remain aloft for months to years before settling to the ground and have been known to contribute to cooling of the global climate [*IPCC*, 2007].

Overall, transportation and scavenging are as important as emission in determining aerosol concentration. Monsoon circulations play an important role in driving the variations in aerosols. *Chen et al*. [2008]

systematically analyzed the relationship between atmospheric pollution processes and synoptic pressure patterns in northern China and pointed out that the air quality in northern China had a prominent correlation with pressure systems. *R. H. Zhang et al.* [2014] investigated the effect of meteorological conditions on the daily evolution of visibility in January 2013 when a severe fog-haze event of strong intensity, long duration, and extensive coverage occurred in eastern China. They found that the daily evolution of this fog-haze event was affected significantly by the meteorological dynamic factors of surface wind velocity and vertical shear of horizontal winds, and by the thermodynamic factors of stratification instability in middle and lower troposphere and the inversion and dew point deficit in the near surface. The variance explained by the meteorological factors to that of the daily fog-haze evolution exceeds more than two thirds. The onset of the EASM has important roles in China's regional air quality. In addition to transportation factors, the change in chemical reactions during the monsoon season caused by the weak photochemical activity of pollutants is also an important factor [*He et al.*, 2008; *Zhao et al.*, 2010]. The monsoon affects aerosols on multiple timescales, from synoptic, seasonal, and interannual to decadal scales.

6.1. Seasonal Variations

Both observations and numerical simulations suggest that the seasonal variation of aerosol concentrations over eastern China has a strong negative correlation with the EASM. Every summer, accompanied by the ASM onset, most parts of eastern China are controlled by warm and humid air from the ocean to the southwest. Approaching the summer, the southwest summer monsoon usually shifts northward. However, the influences of the summer monsoon vary year by year due to differences in the monsoon onset date and the strength of the summer monsoon. Likewise, the winter monsoon also has strong interannual variations. In weak monsoon years, the northwesterly winter monsoon can barely reach the Yangtze River Basin and even farther north, while the strong winter monsoon may affect the tropics and the Southern Hemisphere [*Chen et al.*, 1991b].

Ground measurements have suggested that the ASM has a strong influence on the seasonal variations of aerosols. *Qin et al.* [1997] analyzed chemical compositional data measured at 11 stations in Hong Kong for their seasonal and spatial variations and found low concentrations of atmospheric aerosols in summer and high concentrations for the rest of the year due to the seasonal variation of the EASM. *Chen and Yang* [2008] analyzed the spatiotemporal patterns of aerosols over the Taiwan Strait and its adjacent areas using MODIS aerosol data. The lowest AOD in the summer over the study area was attributed to the influence of heavy rainfall brought on by the EASM. With aircraft campaigns and in situ measurements made by a scanning mobility particle sizer, aerosol properties have been measured over the last 10 years in Korea. *Y. Kim et al.* [2014] showed that there is a strong seasonal variation in aerosol concentration due to monsoons that brings maritime air to the Korean Peninsula during the summertime, causing a dip in aerosol concentration.

Zhang et al. [2010a] explored the effects of different regimes and intensities of the EASM on the seasonal and interannual variability in EA aerosols using a global three-dimensional atmospheric chemistry transport model (GEOS-Chem). The effects of the summer monsoon have a greater impact on aerosol concentration than that due to the seasonal variation in aerosol emissions. This may explain the finding that the aerosol concentration (not AOD) is high in winter and low in summer in East Asia. The transport of aerosols associated with the monsoon wind field overwhelms the wet deposition due to monsoon precipitation.

The seasonal variation of the SASM also significantly modulates aerosol variations. Model simulations showed that about 50–70% of the springtime OC above 700 hPa over eastern China originated from biomass burning in South Asia, transported by the strong southwesterlies of the South ASM (SASM) [*Zhang et al.*, 2010b]. By employing the WRF-Chem, *Shahid et al.* [2015] indicated that the lowest $PM_{2.5}$ concentration in July in Pakistan may be attributed to the largest summer rainfall associated with the SASM, and that winds over South Asia are the major meteorological factor that determines the transboundary aerosol transport to northeastern Pakistan.

Like the summer monsoon, the winter monsoon also has a significant impact on local aerosol concentrations. *Hao et al.* [2007] found there is always higher AOD over the SCS in winter with a strong winter monsoon, which is conducive to the transport of aerosols from land. However, there is usually lower AOD in summer, as the prevailing southerly wind brings clean maritime air onshore. Under the influence of the monsoon circulation, winter aerosol concentrations over Hong Kong are always higher than those in Guangzhou and vice-versa in summer [*Louie et al.*, 2005; *Ho et al.*, 2011].

Accompanying the movement of the EASM is enhanced atmospheric humidity in eastern China during the summer. By means of model simulations, *Li et al*. [2012, 2014] found that the summer tropospheric water vapor in East Asia is high compared to Europe and the United States, thus favoring the growth of hygroscopic aerosols (such as sulfates) and increasing the optical thickness and the corresponding direct radiative forcing. This illustrates that the aerosol radiative effect in East Asia is not only related to the aerosol concentration but also closely related to the regional water vapor distribution.

6.2. Interannual and Decadal Variations

Increasing anthropogenic emissions in China have been blamed for the frequent occurrence of severe haze episodes, but the interdecadal variability in monsoons can have a significant influence on the interannual variability in aerosol concentration and the spatial distribution of aerosols in China [*Zhang et al*., 2010a; *X. Liu et al*., 2011; *Yan et al*., 2011; *Zhu et al*., 2012]. Weakening of the winter monsoon as characterized by the increasing number of calm or light-wind days and the decreasing number of cold-air outbreaks in the EA is likely a major cause for the increasing occurrence of fog/haze in eastern-central China in recent decades [*Niu et al*., 2010]. It was reported that the severe fog-haze event over eastern China that occurred in January 2013 was accompanied by a weak EA winter monsoon [*R. H. Zhang et al*., 2014; *Mu and Zhang*, 2014]. Based on meteorological visibility data, two recent studies investigated the interannual variability in haze over China and its relationship with the EA winter monsoon [*Chen and Wang*, 2015; *Q. Li et al*., 2015]. Their results show that the wintertime fog-haze days across central and eastern China have a close relationship with the EA winter monsoon on interannual timescales [*Q. Li et al*., 2015]. The occurrence of severe haze events generally correlates with weakened northerly winds and the development of inversion anomalies in the lower troposphere, a weakened EA trough in the midtroposphere, and a northward EA jet in the high troposphere [*Chen and Wang*, 2015].

Zhang et al. [2010a] found a negative correlation between the interannual variability of aerosol concentration and the EASM in eastern China. Here weak EASMs refer to the rainband mainly located in the middle and lower Yangtze River valley, and strong monsoons refer to the rainband located in northern and southern China [*Li and Zeng*, 2002]. During the 1998 weak summer monsoon year, the aerosol concentration was significantly higher than that during the 2002 strong summer monsoon year. *X. Liu et al*. [2011] found that the Indian summer monsoon can affect the summer spatial distribution of AOD in East Asia. In strong monsoon years, the anomalies of AOD in the East Asian region present the pattern of "southern negative and northern positive" anomalies of AOD, while the contrary occurs in a weak monsoon year, as shown by both a data analysis [*X. Liu et al*., 2011] and numerical experiments [*Yan et al*., 2011; *Zhu et al*., 2012]. Through quantitative analysis, they found that a weak EASM is accompanied with high summer surface layer $PM_{2.5}$ concentrations in northern China. Regionally, the weakening of the EASM induces an increase in $PM_{2.5}$ concentration in the middle and lower reaches of the Yellow River by ~10 $\mu g\,m^{-3}$ with a relative change of ~29.6%. However, the absolute value of the differences is generally small, less than 1 $\mu g\,m^{-3}$ (<1%) in southern China. Relative to the strong monsoon years, $PM_{2.5}$ concentrations in the weak monsoon year is higher by 20.3% based on aerosol concentrations averaged over northern China.

There is a similar phenomenon in the Indian monsoon domain as that over the EASM. The NIO undergoes a major transition from AAs during the northeastern winter monsoon season to mineral dust and sea salt during the southwest summer monsoon. The former is dominated by low-level transport from south and southeast Asia, while the latter results from lower to middle tropospheric transport from the African continent and the Arabian Peninsula [*Li and Ramanathan*, 2002; *Nair et al*., 2003]. *Corrigan et al*. [2006] found that BC and other AAs over the Indian Ocean vary with the cyclic nature of the Indian monsoon. In summer, the wet monsoon brings clean air into the region from the Southern Hemisphere. Conversely, the dry monsoon brings polluted air from the Indian subcontinent and Southeast Asia in winter.

Based on simulations with the GEOS-Chem, *Zhu et al*. [2012] noted that the years of high aerosol concentration in eastern China in recent decades are partly caused by the weakening of the EASM on an interannual timescale. Even if anthropogenic emissions did not increase in the past 60 years, aerosol concentrations in eastern China in weak EASM years are about 20% higher than that in strong EASM years due to the interdecadal weakening of the EASM (Figure 28). *Zhu et al*. [2012] showed that the observed decadal-scale weakening of the EASM contributed to an increase in aerosols in China and found that aerosol concentrations in weak monsoon years of 1980–2010 were higher than those in the strong monsoon years of 1948–1979 by about 20%, based on differences in the EASM index (EASMI) and the assumption of no changes in anthropogenic emissions over

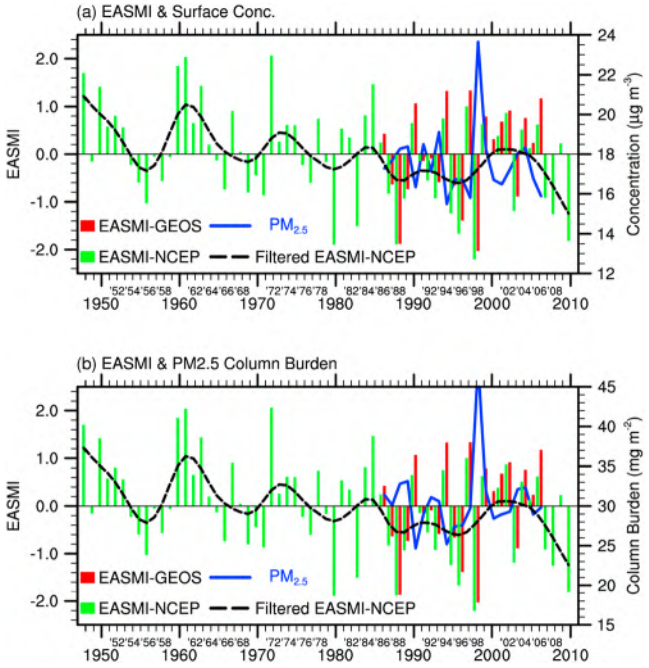

Figure 28. (a) The normalized time series of the EASM index (EASMI, bars, left *y* axis, [*Li and Zeng*, 2002; *J. P. Li et al.,* 2010]) and simulated JJA surface layer $PM_{2.5}$ concentrations (blue line, right *y* axis, $\mu g\ m^{-3}$) averaged over eastern China (110°–125°E, 20°–45°N) for the years of 1986–2006. The EASMI-GEOS for the years 1986–2006 (red bars) are calculated using GEOS-4 assimilated meteorological data, while the EASMI-NCEP for the years 1948–2010 (green bars) are calculated using the NCEP/NCAR reanalysis data. The thick dashed line is the 9 year Gaussian-type filtered value of the EASMI-NCEP, which represents the decadal variation in EASM. (b) The same as Figure 28a but for tropospheric column burdens of $PM_{2.5}$ (right *y* axis, $mg\ m^{-2}$). Copied from *Zhu et al.* [2012].

1948–2010. These studies provide a new perspective to the understanding of high aerosol concentration in China. The remote forcing from two types of ENSO may exert important influences on aerosols in East Asia, e.g., the El Niño Modoki event in 1994/1995 had a considerable impact on aerosol concentrations over southern China [*Feng et al.*, 2016].

Wang et al. [2015] proposed that the rapid decline of the Arctic sea ice extent as a result of global warming weakens the synoptic disturbances south of 40°N in eastern China, which could be the ultimate cause for the intensification of haze pollution in eastern China. They showed a significant relationship between the preceding autumn Arctic sea ice extent and total numbers of winter haze days in eastern China in both the interdecadal and interannual variability. They found that the sea ice variability can explain about 67% of the total interannual to interdecadal variance of winter haze days.

6.3. Vertical and Horizontal Transport

The Asian monsoon also plays a role in the vertical and horizontal transport of air pollutants, as high as the upper troposphere/lower stratosphere (UTLS) above the ASM anticyclone. Recent satellite observations and numerical simulations suggested that the ASM provides an important pathway for the transport of lower tropospheric water vapor and pollutants into the global stratosphere [*Bian et al.*, 2011; *Randel et al.*, 2010]. A number of studies suggested that the deep convection and anticyclone in the upper troposphere associated with the ASM have significant impacts on the stratosphere-troposphere exchange [*Gettelman et al.*, 2004; *Li et al.*, 2005; *Fu et al.*, 2006; *Park et al.*, 2008; *Randel et al.*, 2010; *Yin et al.*, 2012; *Chen and Yin*, 2014].

Using a cloud-resolving model coupled with a spectral bin microphysical scheme, *Yin et al.* [2012] investigated the effects of deep convection on the concentration and size distribution of aerosol particles within the upper troposphere. Their results showed that aerosols originating from the boundary layer can be more efficiently transported upward, compared to those from the midtroposphere, due to significantly increased vertical velocities through the reinforced homogeneous freezing of droplets. The concentration of aerosol particles within the upper troposphere increased by a factor of 7.71, 5.36, and 5.16, respectively, when enhanced aerosol layers existed at 0–2.2 km, 2.2–5.4 km, and 5.4–8.0 km, with Aitken mode and a portion of accumulation mode (0.1-0.2 μm) particles being the most susceptible to upward transport.

Another process that is of great interest is the lofting of pollutants out of the boundary layer into the free troposphere, where they have a greater potential for horizontal transport over long distances. The warm conveyor belt, often associated with midlatitude wave cyclones, has been identified as a major meteorological mechanism for such long-range transport phenomena [e.g., *Jacob et al.*, 2003; *Liu et al.*, 2003; *Liang et al.*, 2004; *Dickerson et al.*, 2007; *C. Li et al.*, 2010]. Since the EASM is located in the inflow area of the warm conveyor belt, polluted air can be transported far away [*Stohl*, 2001; *Eckhardt et al.*, 2004], extending the influence

of Asian pollution to much larger areas [e.g.,*Yu et al*., 2008; *van Donkelaar et al*., 2008; *Hara et al*., 2009; *C. Li et al*., 2010; *Hsu et al*., 2012; *He et al*., 2012]. Some investigations [*Biscaye et al*., 2000; *Wilkening et al*., 2000; *van Curen and Cahill*, 2002; *Yu et al*., 2012] indicated that Asian dust can travel over a long distance across the North Pacific to reach North America in 1–2 weeks. On the other hand, a recent study shows that strong biomass burning in South Asia plays a very important role in influencing air quality in China [*Zhang et al*., 2010b]. The study suggests that the high biomass burning emissions of OC in South Asia and Southeast Asia in spring contribute to 5–50% of the surface layer OC mass in southern China, and up to 40–80% and 40–60% of OC at 500 hPa over eastern China and the United States, respectively. Thus, in addition to focusing on the influence of emissions from East Asia, other factors and sources can also affect air quality in China and beyond and should be paid more attention. To help understand any interactions and roles of the vertical transport of aerosols by monsoon circulation and vice-versa, as well as for a general understanding of ARI and ACI, information about the aerosol vertical distribution is essential. While the vast majority of ground and space observations only provide column-integrated aerosol quantities, height-resolved aerosol data have been acquired from space (e.g., CALIPSO) and ground-based lidar networks. An Asia-wide lidar network known as the Asian Dust and aerosol lidar observation Network (AD-Net) has been in operation since 2001 with three original stations in Beijing, Nagasaki, and Tsukuba that have expanded to 20 stations covering a large area along the pathway of Asian dust as a part of the Global Atmosphere Watch program of the World Meteorological Organization. The network provides continuous observations using polarization-sensitive two-wavelength lidars and Raman lidars (http://www-lidar.nies.go.jp/AD-Net/).

Data from the AD-Net have been used in various studies of Asian dust and regional air pollution, including the validation/assimilation of chemical transport models [e.g., *Shimizu et al*., 2004; *Hara et al*., 2009, 2011; *Sugimoto et al*., 2015]. *Hara et al*. [2011] found that the Asian summer-winter monsoon system plays a major role in determining the seasonal variation in aerosol vertical distributions, but no significant trend in the interannual variations in aerosol concentrations was found.

7. Concluding Remarks and Recommendations for Future Studies

With the densest population and fastest economic growth in the world, Asia is experiencing an unprecedented rate of changes in many ways. Of utmost concern to scientists, the public, stakeholders, and governments are those environmental changes that may affect the monsoon climate of the region. The increasing frequency of episodes of severe air pollution (smog in particular) not only affects people's daily lives and health but also further influences the monsoon climate, which has been changing drastically over the past few decades. Better understanding of connections between aerosols and the monsoon climate of Asia is paramount in the formulation and implementation of sound policies for sustainable development and the well-being of more than half of the world's population.

The Asian monsoon region is unique due to its particular geography, especially the TP, and its role as the largest source of diverse natural and anthropogenic aerosols. Because aerosol radiative forcing of the monsoon is substantial, and aerosols are fundamental building blocks of rainfall and clouds, aerosol-monsoon interactions are expected to occur not only on climate change timescales (>50 years) but also on monsoon intrinsic (intraseasonal, seasonal-interannual, and interdecadal), as well as much shorter, timescales. A high-level summary of the current findings and a paradigm change needed for future research and development follows.

7.1. Aerosol Forcing on the Monsoon (Sections 3 and 4)

The most fundamental influence of aerosols on the monsoon may lie in the widespread solar dimming over both South and East Asia. The monthly mean decrease in solar radiation averaged over India is on the order of 10 to 25 W m^{-2} and that over China ranges from 15 to 45 W m^{-2}. This is accompanied by an increase in atmospheric solar heating in the range of 10 to 20 W m^{-2}. The observed dimming is due to a combination of three major factors: (1) reflective aerosols such as sulfates, nitrates, and organics; (2) BC aerosols that by absorbing sunlight in the atmosphere shields the surface from solar radiation; and (3) the increase in cloud depths and areal fractions through aerosol-cloud microphysical interactions. A recent comprehensive intercomparison of over 15 IPCC Fifth Assessment Report (AR5) models [*Bond et al*., 2013] suggests that IPCC AR5 and most other aerosol chemical transport models underestimate the atmospheric absorption of solar radiation by BC by a factor of 2 to 4 over China and India. A major source of uncertainties that influences model estimates of

atmospheric aerosol concentrations lies in the lack of detailed information on the emission rate of primary particles (e.g., BC and OC) and of gas-phase precursors (e.g., SO_2, NO_x, and volatile organic compounds) for secondary particles. Specifically, the historical evolution of these emissions during the twentieth century is poorly quantified. Many efforts have been devoted to developing inventories of emissions in the recent decade(s), but it is extremely difficult to date it back to a few decades or earlier.

Solar dimming, the systematic reduction of solar radiation reaching the ground, has been reported worldwide, but its magnitude is generally bigger in Asia than elsewhere. These surface dimming and atmospheric heating values are about 10% to 20% of the latent heating of the atmosphere and surface evaporation. The observationally inferred values are accompanied by measurements of a decrease in pan evaporation of comparable magnitudes over South and East Asia. The main implication is that the hydrological cycle of the entire Asian continent has been perturbed significantly during the twentieth century. The diminishing pan evaporation by itself suggests that the Asian monsoon has weakened in terms of the water cycle. Many studies have confirmed that the summer and winter monsoons have weakened. On the other hand, the degree to which the weakening is caused by aerosols is subject to large uncertainties due to various factors that play important roles in the Asian monsoon system. Most IPCC models are unable to simulate the magnitude of the observed solar dimming, which undermines their ability to simulate the impact of aerosols on the monsoon climate in terms of primary features such as the weakening of the monsoon circulation, the decreased rainfall in South Asia, and the north-south rainfall shift over East Asia.

7.2. SASM Versus EASM (Section 5)

For the SASM, aerosols can alter the monsoon circulation and rainfall by the following plausible mechanisms. 1. Decreases in land-ocean contrast due to aerosol-induced solar dimming, because there are more aerosols over the continent than over the ocean, weaken the monsoon. Additionally, a decrease in the north-south gradient of the SST of the Indian Ocean due to stronger aerosol-induced dimming over the Arabian Sea and the BOB compared with the rest of the north Indian Ocean and south Indian Ocean can lead to a suppression of monsoon rainfall over central and northern India. 2. The increase in atmospheric stability due to the semidirect effect (heating above and cooling below) by absorbing aerosols can suppress monsoon rainfall. 3. The TP/Himalayan foothills region facilitates the buildup of dust and BC during the premonsoon season, through the EHP or similar mechanisms, induces heating of the upper atmosphere, and advances the onset of the rainy season in northern India and the Himalayan foothills in May–June. Subsequently, in July and August, rainfall over the Indian subcontinent is suppressed due to the reduced meridional surface thermal gradient possibly arising from aerosol dimming and the negative feedback from increased clouds in the early monsoon, weakening the monsoon through a spin-down of the local meridional circulation. 4. While the above three mechanisms represent regional patterns of aerosol forcing and responses, the thermal contrast has a hemispherical-scale asymmetry with more dimming in the Northern Hemisphere compared with the Southern Hemisphere. 5. Aerosol indirect effects can also modulate monsoon clouds and convection, but their impacts on the overall SASM are still not clear because virtually none of the state-of-the-art global climate models can simulate ACI in a realistic way.

For the EASM, the fundamental mechanisms of aerosol forcing are similar to the SASM. However, the responses are even more complex, due to the much longer duration of the monsoon and much farther northward excursion of the monsoon rain belt, i.e., the Mei-yu rain belt, to higher latitudes ($>$40°N), as well as additional influences from the North Pacific Subtropical High, and extratropical weather systems [*Lau and Kim*, 2015]. Studies on aerosol-monsoon interactions have so far yielded mixed results, suggesting influences from both aerosol direct and indirect effects, as well as atmospheric feedback. There is more compelling and direct evidence of aerosol radiative effects on surface temperature, especially on the most significant cooling trend experienced in eastern-central China from the 1960s to the 1990s when air quality in China had deteriorated most dramatically. Because aerosols tend to cool the surface and warm the atmosphere, and thus stabilize the atmosphere, the increasing aerosol trend may have contributed to the significant decline in wind speed in China as well. The general trends of decreasing light rain and increasing heavy rain are consistent with aerosol microphysical and invigoration effects. The observed opposite trends of thunderstorms activities, i.e., increasing in moist southern China and decreasing in semidry northern/central China, seem to be correlated with the different dominant aerosol types in the two regions. In general, soot aerosols from both natural

and anthropogenic sources tend to suppress thunderstorms, while sulfate aerosols mainly from man-made sources do the opposite, provided that suitable dynamic conditions are present. Natural dust aerosols over monsoon regions, because of their high solar absorption, can stabilize the atmosphere through the semidirect effect. On the other hand, dust aerosols can serve as giant IN and facilitate deep convection. Despite such plausible pieces of evidence of connections between aerosol and climate changes, their relationships remain elusive.

In addition to the impacts by local emissions of aerosols, the EASM appears to be also affected by teleconnections emanating from the EHP effects over South Asia. Natural decadal variability of the North Pacific SST seems to play an important role in the NDSW pattern in recent decades, as well as in the long-term temperature trend. At this time, possible contributions of aerosols to decadal climate changes are still fraught with large uncertainties. This is due to the highly chaotic nature of the dynamics of the EASM and a plethora of other possible first-order climate forcings ranging from downstream influences from the TP, variability of moisture transport from the SASM, and the western Pacific subtropical high, as well as land use and change, regional SST anomalies, remote forcing from the ENSO, decadal-scale oscillations, and GHG warming.

7.3. A New Paradigm

There is no question that the vast research efforts made in the last decade have substantially advanced our knowledge of the diverse effects of aerosols along both direct and feedback pathways. However, there are still many inconsistencies and large uncertainties that pose a major challenge in assessing the impact of any particular mechanism played by aerosols, let alone quantifying it. This is a result of various factors, their interactions, and feedback processes involving both physical and dynamical processes that all come into play and eventually contribute to changes in the monsoon variables depicting cloud development, precipitation formation, and circulation changes.

The ongoing debate over climate change due to GHGs and the recent slowdown of global warming could possibly be better explained if key aerosol effects and trends were accurately incorporated into climate models. The buildup of GHGs should have led to warming and increased precipitation overall. While both the SASM and the EASM have witnessed warming trends during the twentieth century, the observed precipitation trends contradict the projection of the greenhouse effects by models. The South Asia region has witnessed a decrease in precipitation of about 7% during the twentieth century, while the overall change over all of East Asia is near zero. Instead, the EASM has witnessed an increase in rainfall over southern China followed by a decrease in the north, i.e., the NDSW pattern. Thus far, none of the models that include just the buildup of GHGs have simulated the observed patterns. There are even disagreements on the sign of the change in precipitation and the pattern. Models that include the effects of aerosols have been able to simulate some aspects of the precipitation changes but with large uncertainties. To date, none of the models (there are hundreds of model studies of the problem) have satisfactorily accounted for the combination of the most dramatic changes: weakening of the monsoon circulation, decrease in South Asian rainfall, and increase in southern China's rainfall accompanied by drying of the north. A fundamental reason is that none of the numerical models can reliably tackle the multiscale nature (from microphysical, cloud-resolving, synoptic scales, to interannual, decadal, and beyond) of aerosol-monsoon interactions where deep convection and large-scale feedbacks play key roles.

Up until now, studies have devoted much attention to aerosols as an external (anthropogenic) forcing to the monsoon, but less so on the role aerosols as an internal (natural) source contributing to internal monsoon dynamics and feedback processes. As evident in this review, dynamical feedback processes likely play a critical role in determining the evolving quasi-equilibrium state of the monsoon climate system in the real world, subject to both forcing from anthropogenic sources and from natural variability.

Given the abundance of both natural and anthropogenic aerosols in monsoon regions, their fundamental contributions to the distribution of heat sources and sinks, and the formation of clouds and precipitation, a deeper understanding of the roles of aerosol-monsoon interactions on climate change needs to be built on a new framework that treats natural aerosols with the same status as temperature, moisture, clouds, and precipitation. Aerosols must be considered as an integral part of a natural aerosol-monsoon climate system (inner oval area in Figure 29), governed by fundamental thermodynamic, dynamic, and diabatic heating controls, which affects monsoon climate changes. These controls together with related natural processes and

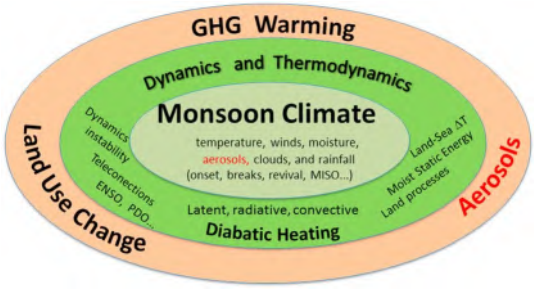

Figure 29. Schematic showing key components of an aerosol-monsoon climate system: Intrinsic observables of the natural system (inner oval area), fundamental governing processes (middle oval ring), and anthropogenic forcing (outer oval ring). Copied from *Lau* [2016]. Used with permission from Springer.

remote forcing from teleconnections (middle oval ring in Figure 29) are likely to be altered by humans through increased GHGs and anthropogenic aerosol emissions, as well as land use and change practices (outer oval ring in Figure 29). We believe that this is the right approach to tackle the complex aerosol-monsoon climate change issues. Further work should focus on how fundamental processes governing the natural aerosol-monsoon climate system have been and will be altered by GHGs, anthropogenic aerosols, and land use and change, jointly and separately. Under such a framework, observations and modeling strategies can be developed synergistically to better understand the impacts of humans on monsoon climate variability and change, and to inform sound policy for adaptation and mitigation.

Better observations and improved modeling are paramount to unraveling aerosol and global warming effects on monsoon climate change. However, uncertainties in observations and in model physics for monsoon processes, especially ACI, are still very large and undermine the exploration of the underlying truth by observations or modeling alone. As demonstrated in many studies cited in this review, aerosol effects depend on both meteorological conditions and a variety of aerosol properties whose differences may lead to totally different influences on climate variables. They include, among others, aerosol optical properties (loading and absorption in particular), hygroscopic properties, and CCN/IN, and their horizontal and vertical distributions. While satellites can monitor the spatial and temporal variations of aerosols to some extent, such observations are limited in both accuracy and in quantity. Most remote sensing techniques still suffer from very large uncertainties due to numerous assumptions made regarding aerosol and surface properties, and to cloud screening, while routine observations are usually limited to certain specific observation quantities.

Field experiments may overcome some of these limitations by increasing the number of observed quantities and observation accuracy. Many international and national projects/programs have taken place in Asia, aimed at gaining a better understanding of the Asian monsoon system, climate, hydrology, aerosols, and their interactions, as summarized in Figure 30. The experiments cover both the Asian summer and winter monsoons, and include elements that are valuable for studying aerosol-monsoon interactions. To take advantage of these experimental data and to better coordinate future studies on the Asian monsoon and aerosols, the WCRP endorsed the Asian Monsoon Year (AMY) program in 2007. This program has fostered the use of existing observational data sets through the development of an Asian regional reanalysis data set called

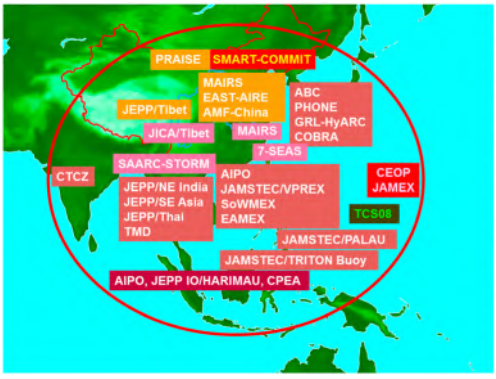

Hydroclimatology, Weather	CEOP, PRAISE, SCHeREX, XSoWMEX/TiMRE, IITM/rain, CTCZ, STORM, MAHASRI/JEPP
Tibetan Plateau	ITP/TORP JICA/Tibet
Aerosol-Climate Interactions	ABC, ACE-Asia, EAST-AIRE, ARM/AMF-China, SACOL, 7-SEAS, IITM/CAIPEX, JAMEX, SACOL, SMART-COMMIT, ARCS-ASia
Atmosphere-Ocean Interactions	AIPO, CTCZ, JEPP/IO, PALAU2008, TCS08
Monsoon Prediction	AAMP, APEC, CEOP, ...
Land-Atmosphere interactions	MAIRS

Figure 30. A summary of major research projects conducted in Asia associated with monsoon and aerosol studies, classified grossly by their primary scientific themes. Modified from *Matsumoto et al.* [2010].

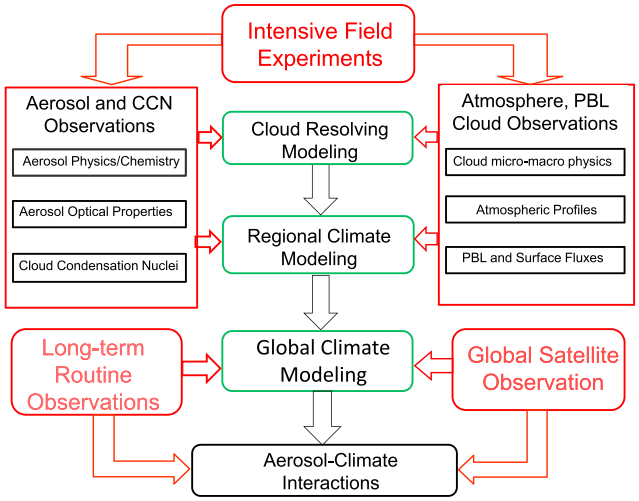

Figure 31. A schematic of an integrated approach for the synergetic use of different types of observations and a hierarchy of models to tackle with the complex issues of aerosol and climate interactions especially under the monsoon climate regime.

the AMY Reanalysis covering the years 2008–2010 at a 20 km resolution. This data set, developed at the Meteorological Research Institute (MRI) of the JMA, will be released to the AMY community first in 2016 and then to all the research community in 2018. Coordinated international programs such as the WCRP/AMY but with more emphasis on aerosol-monsoon interactions need to be implemented and sustained for the foreseeable future.

Armed with a diverse array of observation data and modeling tools, and a new paradigm of the aerosol-monsoon climate system (see Figure 29), the scientific community is now well poised to tackle the complex problem of aerosol-monsoon interactions. We strongly recommend a synergetic effort in exploiting the wide variety of observation data and modeling tools in a systematic manner as illustrated in Figure 31. The essence of the approach is to make full use of data by building on their strengths while minimizing their limitations. For example, rich, high-accuracy field measurements are most needed for understanding fundamental processes underlying aerosol effects on deep convection, monsoon variability, and their interactions through model simulations using high-resolution cloud-resolving models (CRMs) and regional climate models (RCMs). One approach to minimize model uncertainties is through model sensitivity tests, model intercomparisons, and validation against observations. Using observational constraints, we should select only models with demonstrated skills in simulating various fundamental processes governing aerosol-cloud-radiation-precipitation interactions with a focus on key aerosol hot spots in climatically sensitive regions. Increasing model resolutions will improve regional aerosol-monsoon simulations, especially in regions with complex topography, but inadequate model physics is still the major impediment. Just as field campaign data are appropriate for validating CRMs/RCMs, long-term ground-based and global satellite data are more useful for validating GCMs, as well as for understanding long-term trends and global patterns. Meanwhile, model simulation results from creditable CRMs/RCMs can also help improve a GCM by improving parameterization schemes. Because aerosols (natural and anthropogenic) are likely to play a pivotal role in weather and climate, it is essential to span aerosol-monsoon interaction studies on monsoon intrinsic scales, from diurnal, seasonal to interannual timescales, and beyond, using a hierarchy of models, with constraints from observations.

One must be mindful of some intrinsic limitations in both observation and modeling. They include, among others, the lack of reliable long-term observations and model physics uncertainties. Because natural variability in individual coupled free-running climate models can hardly match natural variability in observations, multimodel ensemble means are used to get at the forced response to GHG and anthropogenic aerosol forcing. This presents an intrinsic problem. Even if we had perfect observations, there is always the difficulty in comparing observations of a single realization of the real world system in the presence of natural variability versus a forced response in multimodel realizations of imperfect representations of the real world. Many realizations of the real world are needed to get a real forced response.

As a final remark, while observational analyses and model simulations have provided compelling information regarding the interactions between aerosols and the Asian monsoon, many unknowns and large uncertainties remain. Due to the complexity of the processes involved, it is an extremely challenging task to untangle aerosol effects from natural dynamic and physical processes, as they are inherently connected. To conduct research under the new vision and framework espoused here, the joint efforts of the aerosol and monsoon climate dynamic communities is essential. These joint efforts should involve international collaboration in obtaining new and sustained existing measurements of key variables of meteorology and aerosol properties,

as well as the better use of observations to constrain climate models so that uncertainties in model historical simulations and future projections can be significantly reduced.

Notation List

7-SEAS	Seven South East Asian Studies
AA	anthropogenic aerosols
AAMP	Asian-Australian Monsoon Panel
ABC	Atmospheric Brown Cloud
ACE-Asia	Asian-Pacific Regional Aerosol Characterization Experiment
ACI	aerosol-cloud interactions
AD-Net	Asian Dust and aerosol lidar observation Network
ADRF	aerosol direct radiative forcing
AE	Ångström exponent
AERONET	Aerosol Robotic Network
AIE	aerosol indirect effects
AIPO	Ocean-Atmosphere Interaction over the Joining Area of Asia and Indian-Pacific Ocean and its impact on the short-term climate variation in China
AM	Asian monsoon
AMF	Atmospheric Radiation Measurement Mobile Facility
AMF-China	Atmospheric Radiation Measurement Mobile Facility field campaign in China
AMY	Asian Monsoon Year
AOD	aerosol optical depth
APEC	Asia-Pacific Economic Cooperation
AR5	Fifth Assessment Report
ARCS-Asia	Aerosol and Regional Climate Studies-Asia
ARFINET	Aerosol Radiative Forcing over India project
ARI	aerosol-radiation interactions
ARM	Atmospheric Radiation Measurement
ASM	Asian summer monsoon
AUM	Australian monsoon
AWM	Asian winter monsoon
BC	black carbon
BOB	Bay of Bengal
CAIPEEX	Cloud Aerosol Interaction and Precipitation Enhancement Experiment
CALIPSO	Cloud-Aerosol Lidar and Infrared Pathfinder Satellite Observation
CARSNET	China Aerosol Remote Sensing Network
CCM	community climate model
CCN	cloud condensation nuclei
CEOP	Coordinated Energy and Water Cycle Observation Project
CM3	GFDL fully coupled model
CMIP	Coupled Model Intercomparison Project
CMIP5	Coupled Model Intercomparison Program Phase 5
CRM	cloud-resolving model
CSHNET	Chinese Sun Hazemeter Network
CTH	cloud top height
DCC	deep convective clouds
DTR	diurnal temperature range
EA	East Asian
EASM	East Asian summer monsoon
EASMI	EASM index
EAST-AIRE	East Asian Studies of Tropospheric Aerosols: an International Regional Climate
EAST-AIRC	East Asian Studies of Tropospheric Aerosols and Impact on Regional Climate

EHP	elevated heat pump
ENSO	El Niño–Southern Oscillation
EOF1	first empirical orthogonal function
ERA-40	European Centre for Medium-Range Weather Forecasts 40 year Reanalysis
GCM	general circulation model
GEOS-Chem	Goddard Earth Observing System global three-dimensional model of tropospheric chemistry
GFDL	Geophysical Fluid Dynamics Laboratory
GHGs	greenhouse gases
ICARB	Integrated Campaign for Aerosols gases and Radiation Budget
IGP	Indo-Gangetic Plain
IITM/CAIPEX	Indian Institute of Tropical Meteorology/Cloud Aerosol Interaction and Precipitation Enhancement Experiment
IITM/Rain	Indian Institute of Tropical Meteorology/Rain program
IN	ice nuclei
INDOEX	Indian Ocean Experiment
IPCC	Intergovernmental Panel on Climate Change
ISCCP	International Satellite Cloud Climatology Project
ISRO	Indian Space Research Organization
ITCZ	Intertropical Convergence Zone
ITP/TORP	Institute of Tibetan Plateau Research/Tibetan Observation and Research Platform
JAMEX	Joint Aerosol-Monsoon Experiment
JEPP/IO	Japan EOS Promotion Program
JICA/Tibet	Japan International Cooperation Agency/Tibet
JJA	June-July-August
JMA	Japan Meteorological Agency
LLA	light-absorbing aerosol
LT	local time
LW	longwave
LWP	liquid water path
MAHASRI/JEPP	Monsoon Asian Hydro-Atmosphere Scientific Research and Prediction Initiative
MAIRS	Monsoon Asia Integrated Regional Studies
MISO	monsoon intraseasonal oscillation
MISR	Multiangle Imaging Spectroradiometer
MME	multimodel ensemble
MODIS	Moderate Resolution Imaging Spectroradiometer
MOV	monsoon onset vortex
MRI	Meteorological Research Institute
NAM	North American monsoon
NCAR	National Center for Atmospheric Research
NCCN	CCN number concentration
NDSW	North Dry South Wet
NIO	north Indian Ocean
NOAA	National Oceanic and Atmospheric Administration
NPF	new particle formation
OC	organic carbon
PALAU2008	Pacific Area Long-Term Atmospheric Observation for Understanding of Climate Change
PBL	planetary boundary layer
PC1	principle component of the leading mode
PM_{10}	particles less than 10 μm in diameter
$PM_{2.5}$	particles less than 2.5 μm in diameter
PRAISE	Pacific Regional Aquaculture Information Service for Education
PRD	Pearl River Delta
PSD	particle number size distribution

RAWEX	Regional Aerosol Warming Experiment
RCM	regional climate model
RH	relative humidity
SACOL	Semiarid Climate and Environment Observatory, Lanzhou University
SASM	South Asian summer monsoon
SAT	surface air temperature
SBM	spectral bin microphysics
SCHeREX	South China Heavy Rainfall Experiments
SCS	South China Sea
SDE	aerosol semidirect effect
SDM	solar dimming effect
SLP	sea level pressure
SSA	single scattering albedo
SST	sea surface temperature
SMART-COMMIT	Surface-based Mobile Atmospheric Research and Testbed-Chemical, Optical, and Microphysical Measurements of In situ Troposphere
STORM	Severe Thunderstorms Observations and Regional Modeling
SW	shortwave
TCS08	Tropical Cyclone Structure 2008
T_{min}	minimum temperature
T_{max}	maximum temperature
TOA	top-of-the-atmosphere
TP	Tibetan Plateau
TRMM	Tropical Rainfall Measuring Mission
UHI	urban heat island
UTLS	upper troposphere/lower stratosphere
WAM	West African monsoon
WCRP	World Climate Research Project
WRF	Weather Research and Forecasting
WRF-Chem	WRF model coupled with Chemistry
XSoWMWX/TiMRE	Southwest Monsoon Experiment/Terrain-influenced Monsoon Rainfall Experiment

Acknowledgments

We are grateful to the following people who provided some of the original figures used in this article: Jaehwa Lee (Figure 1), F. Song (Figure 2), J. Wu and J. Lin (Figure 6), J. Xin (Figure 7a), K. Lee (Figures 4c and 7b), A. Robock (Figure 11), S. Dey (Figure 14), V. Vinoj (Figure 18), R. Zhang (Figure 19), and Jun Matsumoto (Figure 30). The bulk of the writing was done while the lead author was on sabbatical leave at the Beijing Normal University and the Max-Planck Institutes of Germany. Major funding supports pertinent to this work have been provided by the China's National Basic Research Program on Global Change (grant 2013CB955804), National Natural Science Foundation of China (grant 91544217), U.S. National Science Foundation (AGS1534670), NOAA (NA15NWS4680011), and the U.S. Department of Energy (DESC0007171), DOE ESM Program under contract DE-AC05–76RL01830.

References

Ackerman, A. S., O. B. Toon, D. E. Stevens, A. J. Heymsfeld, V. Ramanathan, and E. J. Welton (2000), Reduction of tropical cloudiness by soot, *Science*, *288*, 1042, doi:10.1126/science.288.5468.1042.

Albrecht, B. A. (1989), Aerosols, cloud microphysics, and fractional cloudiness, *Science*, *245*, 1227–1230, doi:10.1126/science.245.4923.1227.

Allen, R. J., and S. C. Sherwood (2010), Aerosol-cloud semi-direct effect and land-sea temperature contrast in a GCM, *Geophys. Res. Lett.*, *37*, L07702, doi:10.1029/2010GL042759.

Allen, R. J., J. R. Norris, and M. Kovilakam (2014), Influence of anthropogenic aerosols and the Pacific Decadal Oscillation on tropical belt width, *Nat. Geosci.*, *7*, 270–274, doi:10.1038/NGEO2091.

An, Z. S., et al. (2015), Global monsoon dynamics and climate change, *Annu. Rev. Earth Planet. Sci.*, *43*, 29–77, doi:10.1146/annurev-earth-060313-054623.

Andreae, M. O. (2009), Correlation between cloud condensation nuclei concentration and aerosol optical thickness in remote and polluted regions, *Atmos. Chem. Phys.*, *9*, 543–556.

Andreae, M. O., D. Rosenfeld, P. Artaxo, A. A. Costa, G. P. Frank, K. M. Longo, and M. A. F. Silva-Dias (2004), Smoking rain clouds over the Amazon, *Science*, *303*, 1337–1342, doi:10.1126/science.1092779.

Aruna, K., T. V. Lakshmi Kumar, B. V. Krishna Murthy, S. S. Babu, M. VenkatRatnam, and D. NarayanaRao (2016), Short wave aerosol radiative forcing estimates over a semi urban coastal environment in south-east India and validation with surface flux measurements, *Atmos. Environ.*, *125*, 418–428.

Babu, S. S., S. K. Satheesh, and K. K. Moorthy (2002), Aerosol radiative forcing due to enhanced black carbon at an urban site in India, *Geophys. Res. Lett.*, *29*(18), 1880, doi:10.1029/2002GL015826.

Babu, S. S., K. K. Moorthy, and S. K. Satheesh (2007), Temporal heterogeneity in aerosol characteristics and the resulting radiative impact at a tropical coastal station—II: Direct short wave radiative forcing, *Ann. Geophys.*, *25*, 2309–2320.

Babu, S. S., K. K. Moorthy, R. K. Manchanda, P. R. Sinha, S. K. Satheesh, D. P. Vajja, S. Srinivasan, and V. H. A. Kumar (2011), Free tropospheric black carbon aerosol measurements using high altitude balloon: Do BC layers build 'their own homes' up in the atmosphere?, *Geophys. Res. Lett.*, *38*, L08803, doi:10.1029/2011GL046654.

Babu, S. S., M. M. Gogoi, V. H. A. Kumar, V. S. Nair, and K. K. Moorthy (2012), Radiative properties of Bay-of-Bengal aerosols: Spatial distinctiveness and source impacts, *J. Geophys. Res.*, *117*, D06213, doi:10.1029/2011JD017355.

Babu, S. S., et al. (2013), Trends in aerosol optical depth over Indian region: Potential causes and impact indicators, *J. Geophys. Res. Atmos.*, *118*, 11,794–11,806, doi:10.1002/2013JD020507.
Babu, S. S., V. S. Nair, M. M. Gogoi, and K. K. Moorthy (2016), Seasonal variation of vertical distribution of aerosol single scattering albedo over Indian sub-continent: RAWEX aircraft observations, *Atmos. Environ.*, *125*, 312–323, doi:10.1016/j.atmosenv.2015.09.041.
Badarinath, K. V. S., and K. M. Latha (2006), Direct radiative forcing from black carbon aerosols over urban environment, *Adv. Space Res.*, *37*, 2183–2188.
Bamzai, A., and L. Marx (2006), COLA AGCM simulation of the effect of anomalous spring snow over Eurasia on the Indian summer monsoon, *Q. J. R. Meteorol. Soc.*, *126*, 2575–2584, doi:10.1002/qj.49712656811.
Bamzai, A. S., and J. Shukla (1999), Relation between Eurasian snow cover, snow depth, and the Indian summer monsoon: An observational study, *J. Clim.*, *12*, 3117–3132.
Bi, J., J. Huang, Q. Fu, L. Ge, and J. Shi (2013), Field measurement of clear-sky solar irradiance in Badain Jaran Desert of northwestern China, *J. Quant. Spectros. Radiat. Transfer*, *122*, 194–207.
Bian, J., R. Yan, and H. Chen (2011), Tropospheric pollutant transport to the stratosphere by Asian summer monsoon, *Chin. J. Atmos. Sci.*, *35*(5), 897–902.
Biscaye, P. E., F. E. Grousset, A. M. Svensson, and A. Bory (2000), Eurasian air pollution reaches eastern North America, *Science*, *290*, 2258–2259.
Bollasina, M., S. Nigam, and K. M. Lau (2008), Absorbing aerosols and summer monsoon evolution over South Asia: An observational portrayal, *J. Clim.*, *21*(13), 3221–3239, doi:10.1175/2007JCLI2094.1.
Bollasina, M. A., Y. Ming, and V. Ramaswamy (2011), Anthropogenic aerosols and the weakening of the South Asian summer monsoon, *Science*, *334*, 502–505, doi:10.1126/science.1204994.
Bollasina, M. A., Y. Ming, and V. Ramaswamy (2013), Earlier onset of the Indian monsoon in the late 20th century: The role of anthropogenic aerosols, *Geophys. Res. Lett.*, *40*, 3715–3720, doi:10.1002/grl.50719.
Bollasina, M. A., Y. Ming, V. Ramaswamy, M. D. Schwarzkopf, and V. Naik (2014), Contribution of local and remote anthropogenic aerosols to the twentieth century weakening of the South Asian Monsoon, *Geophys. Res. Lett.*, *41*, 680–687, doi:10.1002/2013GL058183.
Bond, T. C., et al. (2013), Bounding the role of black carbon in the climate system: A scientific assessment, *J. Geophys. Res. Atmos.*, *118*, 5380–5552, doi:10.1002/jgrd.50171.
Boos, W., and Z. Kuang (2010), Dominant control of the South Asian monsoon by orographic insulation versus plateau heating, *Nature*, *463*, 218–222, doi:10.1038/nature08707.
Boos, W., and Z. Kuang (2013), Sensitivity of the South Asian monsoon to elevated and non-elevated heating, *Sci. Rep.*, *3*, 1192, doi:10.1038/srep01192.
Booth, B. B. B., N. J. Dunstone, P. R. Halloran, T. Andrews, and N. Bellouin (2012), Aerosols implicated as a prime driver of twentieth-century North Atlantic climate variability, *Nature*, doi:10.1038/nature10946.
Cai, W., D. Bi, J. Church, T. Cowan, M. Dix, and L. Rotstayn (2006), Pan-oceanic response to increasing anthropogenic aerosols: Impacts on the Southern Hemisphere oceanic circulation, *Geophys. Res. Lett.*, *33*, L21707, doi:10.1029/2006GL027513.
Cai, W., T. Cowan, M. Dix, L. Rotstayn, J. Ribbe, G. Shi, and S. Wijffels (2007), Anthropogenic aerosol forcing and the structure of temperature trends in the southern Indian Ocean, *Geophys. Res. Lett.*, *34*, L14611, doi:10.1029/2007GL030380.
Cai, W., T. Cowan, S. Godfrey, and S. Wijffels (2010), Simulations of processes associated with the fast warming rate of the southern midlatitude ocean, *J. Clim.*, *23*, 197–206, doi:10.1175/2009JCLI3081.1.
Chang, C.-P., B. Wang, and N.-C. Lau (2005), *The Global Monsoon System Research and Forecast*, *WMO/TD No. 1266 (TMRP Rep. 70)*, World Meteorol. Organ., Geneva, Switzerland.
Chang, C.-P., et al. (Eds.) (2010), *The Global Monsoon System Research and Forecast*, World Sci., Singapore.
Che, H., X. Zhang, Y. Li, Z. Zhou, and J. J. Qu (2007), Horizontal visibility trends in China 1981–2005, *Geophys. Res. Lett.*, *34*, L24706, doi:10.1029/2007GL031450.
Che, H., X. Zhang, S. Alfraro, B. Chatenet, L. Gomes, and J. Zhao (2009a), Aerosol optical properties and its radiative forcing over Yulin, China in 2001 and 2002, *Adv. Atmos. Sci.*, *26*, 564–576.
Che, H., et al. (2009b), Instrument calibration and aerosol optical depth validation of the China aerosol remote sensing network, *J. Geophys. Res.*, *114*, D03206, doi:10.1029/2008JD011030.
Che, H., et al. (2015), Ground-based aerosol climatology of China: Aerosol optical depth from the China Aerosol Remote Sensing Network (CARSNET) 2002–2013, *Atmos. Chem. Phys. Discuss.*, *15*, 12,715–12,776.
Che, H. Z., G. Y. Shi, X. Y. Zhang, R. Arimoto, J. Q. Zhao, L. Xu, B. Wang, and H. Z. Chen (2005), Analysis of 40 years of solar radiation data from China, 1961–2000, *Geophys. Res. Lett.*, *32*, L06803, doi:10.1029/2004GL022322.
Chen, B., and Y. Yang (2008), Remote sensing of the spatio-temporal pattern of aerosol over Taiwan Strait and its adjacent sea areas, *Acta Sci. Circumstantiae*, *28*(12), 2597–2604.
Chen, B., and Y. Yin (2014), Can we modify stratospheric water vapor by cloud seeding?, *J. Geophys. Res. Atmos.*, *119*, 1406–1418, doi:10.1002/2013JD020707.
Chen, H., and H. Wang (2015), Haze days in North China and the associated atmospheric circulations based on daily visibility data from 1960 to 2012, *J. Geophys. Res. Atmos.*, *120*, 5895–5909, doi:10.1002/2015JD023225.
Chen, L., et al. (1991a), Tentative analysis of climate change in China in last 40 years [in Chinese], *Quat. J. Appl. Meteorol.*, *2*, 164–173.
Chen, L., Q. Zhu, and H. Luo (1991b), *East Asian Monsoon*, Meteorol. Press, Beijing, China.
Chen, T., J. Guo, Z. Li, C. Zhao, H. Liu, M. Cribb, F. Wang, and J. He (2016), A CloudSat perspective on the cloud climatology and its association with aerosol perturbations in the vertical over eastern China, *J. Atmos. Sci.*, *73*, 3599–3616, doi:10.1175/JAS-D-15-0309.1.
Chen, Z. H., S. Y. Cheng, J. B. Li, X. R. Guo, W. H. Wang, and D. S. Chen (2008), Relationship between atmospheric pollution processes and synoptic pressure patterns in northern China, *Atmos. Environ.*, *42*(24), 6078–6087.
Chin, M., T. Diehl, P. Ginoux, and W. Malm (2007), Intercontinental transport of pollution and dust aerosols: Implications for regional air quality, *Atmos. Chem. Phys.*, *7*, 5501–5517.
Chin, M., R. A. Kahn, and S. E. Schwartz (Eds.) (2009), *Atmospheric Aerosols Properties and Climate Impacts, A Report by the U.S. Climate Change Science Program and the Subcommittee on Global Change Research*, Natl. Aeronaut. and Space Admin., Washington, D. C.
China National Assessment Report on Climate Change (2nd ed.) (2011), Science Press, Beijing, China.
Chung, C. E., and V. Ramanathan (2006), Weakening of north Indian SST gradients and the monsoon rainfall in India and the Sahel, *J. Clim.*, *19*, 2036–2045.
Cohen, J., and D. Rind (1991), The effect of snow cover on the climate, *J. Clim.*, *4*, 689–706.

Collier, J. C., and G. J. Zhang (2009), Aerosol direct forcing of the summer Indian monsoon as simulated by the NCAR CAM3, *Clim. Dyn.*, *32*(2–3), 313–332, doi:10.1007/s00382-008-0464-9.

Conant, W. C., J. H. Seinfeld, J. Wang, G. R. Carmichael, Y. H. Tang, I. Uno, P. J. Flatau, K. M. Markowicz, and P. K. Quinn (2003), A model for the radiative forcing during ACE-Asia derived from CIRPAS Twin Otter and R/V Ronald H. Brown data and comparison with observations, *J. Geophys. Res.*, *108*(D23), 8661, doi:10.1029/2002JD003260.

Connolly, P. J., O. Möhler, P. R. Field, H. Saathoff, R. Burgess, T. Choularton, and M. Gallagher (2009), Studies of heterogeneous freezing by three different desert dust samples, *Atmos. Chem. Phys.*, *9*, 2805–2824, doi:10.5194/acp-9-2805-2009.

Corrigan, C. E., V. Ramanathan, and J. J. Schauer (2006), Impact of monsoon transitions on the physical and optical properties of aerosols, *J. Geophys. Res.*, *111*, D18208, doi:10.1029/2005JD006370.

Cowan, T., and W. Cai (2011), The impact of Asian and non-Asian anthropogenic aerosols on 20th century Asian summer monsoon, *Geophys. Res. Lett.*, *38*, L11703, doi:10.1029/2011GL047268.

Cowan, T., and W. Cai (2013), The response of the large-scale ocean circulation to 20th century Asian and non-Asian aerosols, *Geophys. Res. Lett.*, *40*, 2761–2767, doi:10.1002/grl.50587.

Cowan, T., W. Cai, A. Purich, L. Rotstayn, and M. H. England (2013), Forcing of anthropogenic aerosols on temperature trends of the sub-thermocline southern Indian Ocean, *Sci. Rep.*, *3*, 2245, doi:10.1038/srep02245.

Deng, Z., C. Zhao, N. Ma, L. Ran, G. Zhou, D. Lu, and X. Zhou (2013), An examination of parameterizations for the CCN number concentration based on in situ measurements of aerosol activation properties in the North China Plain, *Atmos. Chem. Phys.*, *13*, 6227–6237, doi:10.5194/acp-13-6227-2013.

Devara, P. C. S., R. S. Maheskumar, P. E. Raj, G. Pandithurai, and K. K. Dani (2002), Recent trends in aerosol climatology and air pollution as inferred from multi-year lidar observations over a tropical urban station, *Int. J. Climatol.*, *22*, 435–449.

Dey, S., and L. Di Girolamo (2010), A climatology of aerosol optical and microphysical properties over the Indian subcontinent from 9 years (2000–2008) of Multiangle Imaging Spectroradiometer (MISR) data, *J. Geophys. Res.*, *115*, D15204, doi:10.1029/2009JD013395.

Dey, S., and L. Di Girolamo (2011), A decade of change in aerosol properties over the Indian subcontinent, *Geophys. Res. Lett.*, *38*, L14811, doi:10.1029/2011GL048153.

Dickerson, R. R., et al. (2007), Aircraft observations of dust and pollutants over northeast China: Insight into the meteorological mechanisms of transport, *J. Geophys. Res.*, *112*, D24S90, doi:10.1029/2007JD008999.

Ding, Y. H. (Ed.) (1994), *Monsoons Over China*, Springer, New York.

Ding, Y. H., and D. R. Sikka (2006), Synoptic systems and weather, in *The Asian Monsoon*, edited by B. Wang, pp. 171–241, Praxis, Chichester, U. K.

Ding, Y. H., G. Ren, Z. Zhao, Y. Xu, Y. Luo, Q. Li, and J. Zhang (2007), Detection, causes and projection of climate change over China: An overview of recent progress, *Adv. Atmos. Sci.*, *24*, 954–971.

Ding, Y. H., Y. Song, and J. Zhang (2015), From MONEX to the global monsoon: A review of monsoon system research, *Adv. Atmos. Sci.*, *32*, 10–31.

Dipu, S., T. V. Prabha, G. Pandithurai, J. Dudhia, G. Pfister, K. Rajesh, and B. N. Goswami (2013), Impact of elevated aerosol layer on the cloud macrophysical properties prior to monsoon onset, *Atmos. Environ.*, *70*, 454–467, doi:10.1016/j.atmosenv.2012.12.036.

Dong, L., and T. Zhou (2014), The Indian Ocean sea surface temperature warming simulated by CMIP5 models during the 20th century: Competing forcing roles of GHGs and anthropogenic aerosols, *J. Clim.*, *27*, 3348–3362.

Dong, L., T. J. Zhou, and B. Wu (2014), Indian Ocean warming during 1958–2004 simulated by a climate system model and its mechanism, *Clim. Dyn.*, *42*, 203–217.

Dubovik, O., B. Holben, T. F. Eck, A. Smirnov, Y. J. Kaufman, M. D. King, D. Tanré, and I. Slutsker (2002), Variability of absorption and optical properties of key aerosol types observed in worldwide locations, *J. Atmos. Sci.*, *59*, 590–608, doi:10.1175/1520-0469(2002)059<0590:VOAAOP>2.0.CO;2.

Dumka, U. C., S. N. Tripathi, A. Misra, D. M. Giles, T. F. Eck, R. Sagar, and B. N. Holben (2014), Latitudinal variation of aerosol properties from Indo-Gangetic Plain to central Himalayan foothills during TIGERZ campaign, *J. Geophys. Res. Atmos.*, *119*, 4750–4769, doi:10.1002/2013JD021040.

Eckhardt, S., A. Stohl, H. Wernli, P. Jams, C. Forster, and N. Spichtinger (2004), A 15-year climatology of warm conveyor belts, *J. Clim.*, *17*, 218–237.

Fan, J., R. Zhang, G. Li, and W. K. Tao (2007), Effects of aerosols and relative humidity on cumulus clouds, *J. Geophys. Res.*, *112*, D14204, doi:10.1029/2006JD008136.

Fan, J., T. Yuan, J. M. Comstock, S. Ghan, A. Khain, L. R. Leung, Z. Li, V. J. Martins, and M. Ovchinnikov (2009), Dominant role by vertical wind shear in regulating aerosol effects on deep convective clouds, *J. Geophys. Res.*, *114*, D22206, doi:10.1029/2009JD012352.

Fan, J., L. R. Leung, Z. Li, H. Morrison, H. Chen, Y. Zhou, Y. Qian, and Y. Wang (2012), Aerosol impacts on clouds and precipitation in eastern China: Results from bin and bulk microphysics, *J. Geophys. Res.*, *117*, D00K36, doi:10.1029/2011JD016537.

Fan, J., L. R. Leung, D. Rosenfeld, Q. Chen, Z. Li, J. Zhang, and H. Yan (2013), Microphysical effects determine macrophysical response for aerosol impacts on deep convective clouds, *Proc. Natl. Acad. Sci. U.S.A.*, *110*, E4581–E4590, doi:10.1073/pnas.1316830110.

Fan, J., et al. (2014), Aerosol impacts on California winter clouds and precipitation during CalWater 2011: Local pollution versus long-range transported dust, *Atmos. Chem. Phys.*, *14*, 81–101.

Fan, J., D. Rosenfeld, Y. Yang, C. Zhao, L. R. Leung, and Z. Li (2015), Substantial contribution of anthropogenic air pollution to catastrophic floods in southwest China, *Geophys. Res. Lett.*, *42*, 6066–6075, doi:10.1002/2015GL064479.

Fasullo, J. (2004), A stratified diagnosis of the Indian monsoon—Eurasian snow cover relationship, *J. Clim.*, *17*, 1110–1122.

Feingold, G., W. L. Eberhard, D. E. Veron, and M. Previdi (2003), First measurements of the Twomey indirect effect using ground-based remote sensors, *Geophys. Res. Lett.*, *30*(6), 1287, doi:10.1029/2002GL016633.

Feng, J., J. P. Li, J. L. Zhu, and H. Liao (2016), Influences of El Niño Modoki event 1994/1995 on aerosol concentrations over southern China, *J. Geophys. Res. Atmos.*, *121*, 1637–1651, doi:10.1002/2015JD023659.

Forster, P., et al. (2007), Radiative forcing of climate change, in *Climate Change 2007: The Physical Science Basis. Contribution of Working Group I to the Fourth Assessment Report of the Intergovernmental Panel on Climate Change*, edited by S. Solomon et al., pp. 130–234, Cambridge Univ. Press, Cambridge, U. K.

Freud, E., and D. Rosenfeld (2012), Linear relation between convective cloud drop number concentration and depth for rain initiation, *J. Geophys. Res.*, *117*, D02207, doi:10.1029/2011JD016457.

Fu, C. (2003), Potential impacts of human-induced land cover change on East Asia monsoon, *Global Planet. Change*, *37*, 219–229.

Fu, R., Y. Hu, J. S. Wright, J. H. Jiang, R. E. Dickinson, M. Chen, M. Filipiak, W. G. Read, J. W. Waters, and D. L. Wu (2006), Short circuit of water vapor and polluted air to the global stratosphere by convective transport over the Tibetan Plateau, *Proc. Natl. Acad. Sci. U.S.A.*, *103*(15), 5664–5669.

Gadhavi, H., and A. Jayaraman (2010), Absorbing aerosols: Contribution of biomass burning and implications for radiative forcing, *Ann. Geophys.*, *28*, 103–111.

Ganguly, D., and A. Jayaraman (2006), Physical and optical properties of aerosols over an urban location in western India: Implications for shortwave radiative forcing, *J. Geophys. Res.*, *111*, D24207, doi:10.1029/2006JD007393.
Ganguly, D., H. Gadhavi, A. Jayaraman, T. A. Rajesh, and A. Misra (2005), Single scattering albedo of aerosols over the central India: Implications for the regional aerosol radiative forcing, *Geophys. Res. Lett.*, *32*, L18803, doi:10.1029/2005GL023903.
Ganguly, D., P. J. Rasch, H. Wang, and J.-H. Yoon (2012), Climate response of the South Asian monsoon system to anthropogenic aerosols, *J. Geophys. Res.*, *117*, D13209, doi:10.1029/2012JD017508.
Gautam, R., N. C. Hsu, K. M. Lau, S. C. Tsay, and M. Kafatos (2009), Enhanced pre-monsoon warming over the Himalayan-Gangetic region from 1979 to 2007, *Geophys. Res. Lett.*, *36*, L07704, doi:10.1029/2009GL037641.
Gautam, R., et al. (2011), Accumulation of aerosols over the Indo-Gangetic plains and southern slopes of the Himalayas: Distribution, properties and radiative effects during the 2009 pre-monsoon season, *Atmos. Chem. Phys.*, *11*(24), 12,841–12,863, doi:10.5194/acp-11-12841-2011.
Ge, J., J. Huang, J. Su, J. Bi, and Q. Fu (2011), Shortwave radiative closure experiment and direct forcing of dust aerosol over northwestern China, *Geophys. Res. Lett.*, *38*, L24803, doi:10.1029/2011GL049571.
Gemmer, M., S. Becker, and T. Jiang (2004), Observed monthly precipitation trends in China 1951–2002, *Theor. Appl. Meteorol.*, *77*(1-2), 39–45, doi:10.1007/s00704-003-0018-3.
Gettelman, A., D. E. Kinnison, T. J. Dunkerton, and G. P. Brasseur (2004), Impact of monsoon circulations on the upper troposphere and lower stratosphere, *J. Geophys. Res.*, *109*, D22101, doi:10.1029/2004JD004878.
Gettelman, A., D. T. Shindell, and J. F. Lamarque (2015), Impact of aerosol radiative effects on 2000–2010 surface temperature, *Clim. Dyn.*, *45*, 2165–2179, doi:10.1007/s00382-014-2464-2.
Giles, D. M., et al. (2011), Aerosol properties over the Indo-Gangetic Plain: A mesoscale perspective from the TIGERZ experiment, *J. Geophys. Res.*, *116*, D18203, doi:10.1029/2011JD015809.
Ginoux, P., J. M. Prospero, T. E. Gill, N. C. Hsu, and M. Zhao (2012), Global-scale attribution of anthropogenic and natural dust sources and their emission rates based on MODIS Deep Blue aerosol products, *Rev. Geophys.*, *50*, RG3005, doi:10.1029/2012RG000388.
Gogoi, M. M., S. S. Babu, V. Jayachandran, K. K. Moorthy, S. K. Satheesh, M. Naja, and V. R. Kotamarthi (2015), Optical properties and CCN activity of aerosols in a high-altitude Himalayan environment: Results from RAWEX-GVAX, *J. Geophys. Res. Atmos.*, *120*, 2453–2469, doi:10.1002/2014JD022966.
Gong, D., P. J. Shi, and J. A. Wang (2004), Daily precipitation changes in the semi-arid region over northern China, *J. Arid Environ.*, *59*, 771–784, doi:10.1016/j.jaridenv.2004.02.006.
Gong, D., C. H. Ho, D. Chen, Y. Qian, Y. S. Choi, and J. Kim (2007), Weekly cycle of aerosol-meteorology interaction over China, *J. Geophys. Res.*, *112*, D22202, doi:10.1029/2007JD008888.
Gong, D., W. Wang, Y. Qian, W. Bai, Y. Guo, and R. Mao (2014), Observed holiday aerosol reduction and temperature cooling over East Asia, *J. Geophys. Res. Atmos.*, *119*, 6306–6324, doi:10.1002/2014JD021464.
Goswami, B. N. (2005), South Asia monsoon, in *Interseasonal Variability in the Atmosphere-Ocean Climate System*, edited by W. K. Lau and D. E. Waliser, pp. 19–61, Springer, Berlin Heidelberg.
Goswami, B. N., V. Venugopal, D. Sengupta, M. S. Madhusoodanan, and P. K. Xavier (2006), Increasing trend of extreme rain events over India in a warming environment, *Science*, *314*, 1442–1445, doi:10.1126/science.1132027.
Granier, C., et al. (2011), Evolution of anthropogenic and biomass burning emissions of air pollutants at global and regional scales during the 1980–2010 period, *Clim. Change*, *109*, 163–190, doi:10.1007/s10584-011-0154-1.
Gu, Y., K. N. Liou, Y. Xue, C. R. Mechoso, W. Li, and Y. Luo (2006), Climatic effects of different aerosol types in China simulated by the UCLA general circulation model, *J. Geophys. Res.*, *111*, D15201, doi:10.1029/2005JD006312.
Gunthe, S. S., et al. (2011), Cloud condensation nuclei (CCN) from fresh and aged air pollution in the megacity region of Beijing, *Atmos. Chem. Phys.*, *11*(21), 11,023–11,039, doi:10.5194/acp-11-11023-2011.
Guo, J. P., X. Y. Zhang, and Y. R. Wu (2011), Spatio-temporal variation trends of satellite-based aerosol optical depth in China, *Atmos. Environ.*, *45*, 6802–6811, doi:10.1016/j.atmosenv.2011.03.068.
Guo, J. P., M. Deng, S. S. Lee, F. Wang, Z. Li, P. Zhai, H. Liu, W. Lv, W. Yao, and X. Li (2016), Delaying precipitation and lightning by air pollution over the Pearl River Delta. Part I: Observational analyses, *J. Geophys. Res. Atmos.*, *121*, 6472–6488, doi:10.1002/2015JD023257.
Guo, L., E. J. Highwood, L. C. Shaffrey, and A. G. Turner (2013), The effect of regional changes in anthropogenic aerosols on rainfall of the East Asian Summer monsoon, *Atmos. Chem. Phys.*, *13*, 1521–1534, doi:10.5194/acp-13-1521-2013.
Guo, S., M. Hu, M. L. Zamora, J. Peng, D. Shang, J. Zheng, Z. Du, Z. Wu, M. Shao, and L. Zeng (2014), Elucidating severe urban haze formation in China, *Proc. Natl. Acad. Sci. U.S.A.*, *111*, 17,373–17,378.
Hahn, D. G., and J. Shukla (1976), An apparent relationship between Eurasian snow cover and Indian monsoon rainfall, *J. Atmos. Sci.*, *33*, 2461–2462.
Hansen, J., and L. Nazarenko (2004), Soot climate forcing via snow and ice albedos, *Proc. Natl. Acad. Sci. U.S.A.*, *101*(2), 423–428, doi:10.1073/pnas.2237157100.
Hansen, J., M. Sato, and R. Ruedy (1997), Radiative forcing and climate response, *J. Geophys. Res.*, *102*, 6831–6864, doi:10.1029/96JD03436.
Hansen, J., et al. (2005), Efficacy of climate forcings, *J. Geophys. Res.*, *110*, D18104, doi:10.1029/2005JD005776.
Hao, Z., D. Pan, and B. Yan (2007), Characteristics of the spatial distribution and monthly variation of aerosol optical thickness derived from SeaWiFS over the China Seas, *J. Mar. Sci.*, *25*(1), 80–87.
Hara, Y., K. Yumimoto, I. Uno, A. Shimizu, N. Sugimoto, Z. Liu, and D. M. Winker (2009), Asian dust outflow in the PBL and free atmosphere retrieved by NASA CALIPSO and an assimilated dust transport model, *Atmos. Chem. Phys.*, *9*(4), 1227–1239.
Hara, Y., I. Uno, A. Shimizu, N. Sugimoto, I. Matsui, K. Yumimoto, J. Kurokawa, T. Ohara, and Z. Liu (2011), Seasonal characteristics of spherical aerosol distribution in Eastern Asia: Integrated analysis using ground/space-based lidars and a chemical transport model, *SOLA*, *7*, 121–124, doi:10.2151/sola.2011-031.
Haywood, J., and O. Boucher (2000), Estimates of the direct and indirect radiative forcing due to tropospheric aerosols: A review, *Rev. Geophys.*, *38*, 513–543, doi:10.1029/1999RG000078.
Hazra, A., B. N. Goswami, and J.-P. Chen (2013), Role of interactions between aerosol radiative effect, dynamics, and cloud microphysics on transitions of monsoon intraseasonal oscillations, *J. Atmos. Sci.*, *70*, 2073–2087, doi:10.1175/JAS-D-12-0179.1.
He, B., Q. Bao, J. Li, G. Wu, Y. Liu, X. Wang, and Z. Sun (2013), Influences of external forcing changes on the summer cooling trend over East Asia, *Clim. Change*, *117*, 829–841, doi:10.1007/s10584-012-0592-4.
He, H., et al. (2012), SO_2 over central China: Measurements, numerical simulations and the tropospheric sulfur budget, *J. Geophys. Res.*, *117*, D00K37, doi:10.1029/2011JD016473.
He, Y. J., I. Uno, Z. F. Wang, P. Pochanart, J. Li, and H. Akimoto (2008), Significant impact of the East Asia monsoon on ozone seasonal behavior in the boundary layer of Eastern China and the west Pacific region, *Atmos. Chem. Phys.*, *8*(24), 7543–7555.

Ho, K. F., S. S. H. Ho, S. C. Lee, K. Kawamura, S. C. Zou, J. J. Cao, and H. M. Xu (2011), Summer and winter variations of dicarboxylic acids, fatty acids and benzoic acid in $PM_{2.5}$ in Pearl Delta River Region, China, *Atmos. Chem. Phys.*, *11*(5), 2197–2208.
Holben, B. N., et al. (1998), AERONET—A federated instrument network and data archive for aerosol characterization, *Remote Sens. Environ.*, *66*, 1–16.
Houze, R. A., Jr. (2012), Orographic effects on precipitating clouds, *Rev. Geophys.*, *50*, RG1001, doi:10.1029/2011RG000365.
Hsu, H. H., C. T. Terng, and C. T. Chen (1999), Evolution of large-scale circulation and heating during the first transition of Asian summer monsoon, *J. Clim.*, *12*, 793–810.
Hsu, N. C., S.-C. Tsay, M. D. King, and J. R. Herman (2004), Aerosol properties over bright-reflecting source regions, *IEEE Trans. Geosci. Remote Sens.*, *42*, 557–569, doi:10.1109/TGRS.2004.824067.
Hsu, N. C., C. Li, N. A. Krotkov, Q. Liang, K. Yang, and S.-C. Tsay (2012), Rapid transpacific transport in autumn observed by the A-train satellites, *J. Geophys. Res.*, *117*, D06312, doi:10.1029/2011JD016626.
Hsu, N. C., M.-J. Jeong, C. Bettenhausen, A. M. Sayer, R. Hansell, C. S. Seftor, J. Huang, and S.-C. Tsay (2013), Enhanced Deep Blue aerosol retrieval algorithm: The second generation, *J. Geophys. Res. Atmos.*, *118*, 9296–9315, doi:10.1002/jgrd.50712.
Hu, Z.-Z., S. Yang, and R. Wu (2003), Long-term climate variations in China and global warming signals, *J. Geophys. Res.*, *108*(D19), 4614, doi:10.1029/2003JD003651.
Huang, J.-P., P. Minnis, Y. Yi, Q. Tang, X. Wang, Y. Hu, Z. Liu, K. Ayers, C. Trepte, and D. Winker (2007), Summer dust aerosols detected from CALIPSO over the Tibetan Plateau, *Geophys. Res. Lett.*, *34*, L18805, doi:10.1029/2007GL029938.
Huang, J.-P., et al. (2008), An overview of the semi-arid climate and environment research observatory over the Loess Plateau, *Adv. Atmos. Sci.*, *25*(6), 906–921, doi:10.1007/s00376-008-0906-7.
Huang, J.-P., Q. Fu, J. Su, Q. Tang, P. Minnis, Y. Hu, Y. Yi, and Q. Zhao (2009), Taklimakan dust aerosol radiative heating derived from CALIPSO observations using the Fu-Liou radiation model with CERES constraints, *Atmos. Chem. Phys.*, *9*, 4011–4021, doi:10.5194/acp-9-4011-2009.
Huang, J.-P., T. Wang, W. Wang, Z. Li, and H. Yan (2014), Climate effects of dust aerosols over East Asian arid and semiarid regions, *J. Geophys. Res. Atmos.*, *119*, 11,398–11,416, doi:10.1002/2014JD021796.
Huang, R. H. (2004), Advances of the project of the formation mechanism and prediction theory of severe climatic disasters in China, *Chin. Basic Res.*, *6*, 6–16.
Huang, R. H., J. L. Chen, and G. Huang (2007), Characteristics and variations of the East Asian monsoon system and its impacts on climate disasters in China, *Adv. Atmos. Sci.*, *24*, 993–1023.
Huebert, B. J., T. Bates, P. B. Russell, G. Shi, Y. J. Kim, K. Kawamura, G. Carmichael, and T. Nakajima (2003), An overview of ACE-Asia: Strategies for quantifying the relationships between Asian aerosols and their climatic impacts, *J. Geophys. Res.*, *108*(D23), 8633, doi:10.1029/2003JD003550.
Husar, R. B., J. D. Husar, and L. Martin (2000), Distribution of continental surface aerosol extinction based on visual range data, *Atmos. Environ.*, *34*, 5067–5078.
Intergovernmental Panel on Climate Change (IPCC) (2001), *Climate Change 2001: The Scientific Basis. Contribution of Working Group I to the Third Assessment Report of the Intergovernmental Panel on Climate Change*, edited by J. T. Houghton et al., Cambridge Univ. Press, Cambridge, U. K.
Intergovernmental Panel on Climate Change (IPCC) (2007), *Climate Change 2007: The Physical Science Basis. Contribution of Working Group I to the Fourth Assessment Report of the Intergovernmental Panel on Climate Change*, edited by S. Solomon et al., Cambridge Univ. Press, Cambridge, U. K.
Intergovernmental Panel on Climate Change (IPCC) (2013), *Climate Change 2013: The Physical Science Basis, the Contribution of Working Group I to the Fifth Assessment Report of the Intergovernmental Panel on Climate Change*, edited by T. F. Stocker et al., Cambridge Univ. Press, Cambridge, U. K.
Jacob, D. J., J. H. Crawford, M. M. Kleb, V. S. Connors, R. J. Bendura, J. L. Raper, G. W. Sachse, J. C. Gille, L. Emmons, and C. L. Heald (2003), Transport and chemical evolution over the Pacific (TRACE-P) aircraft mission: Design, execution, and first results, *J. Geophys. Res.*, *108*(D20), 9000, doi:10.1029/2002JD003276.
Jacobson, M. Z. (2002), Control of fossil-fuel particulate black carbon and organic matter, possibly the most effective method of slowing global warming, *J. Geophys. Res.*, *107*(D19), 4410, doi:10.1029/2001JD001376.
Jacobson, M. Z., and Y. J. Kaufman (2006), Wind reduction by aerosol particles, *Geophys. Res. Lett.*, *33*, L24814, doi:10.1029/2006GL027838.
Jai Devi, J., S. N. Tripathi, T. Gupta, B. N. Singh, V. Gopalakrishnan, and S. Dey (2011), Observation-based 3-D view of aerosol radiative properties over Indian continental tropical convergence zone: Implications to regional climate, *Tellus, Ser. B*, *63*(5), 971–989.
Jayaraman, A., S. K. Satheesh, A. P. Mitra, and V. Ramanathan (2001), Latitude gradient in aerosol properties across the inter tropical convergence zone: Results from the joint Indo-US study onboard Sagar Kanya, *Curr. Sci.*, *80*, 128–137.
Jiang, H., H. Xue, A. Teller, G. Feingold, and Z. Levin (2006), Aerosol effects on the lifetime of shallow cumulus, *Geophys. Res. Lett.*, *33*, L14806, doi:10.1029/2006GL026024.
Jiang, M., Z. Li, B. Wan, and M. Cribb (2016), Impact of aerosols on precipitation from deep convective clouds in Eastern China, *J. Geophys. Res. Atmos.*, *121*, 9607–9620, doi:10.1002/2015JD024246.
Kahn, R. A., B. J. Gaitley, M. J. Garay, D. J. Diner, T. F. Eck, A. Smirnov, and B. N. Holben (2010), Multiangle Imaging SpectroRadiometer global aerosol product assessment by comparison with the Aerosol Robotic Network, *J. Geophys. Res.*, *115*, D23209, doi:10.1029/2010JD014601.
Kaiser, D. P. (1998), Analysis of total cloud amount over China, 1951–1994, *Geophys. Res. Lett.*, *25*, 3599–3602, doi:10.1029/98GL52784.
Kaiser, D. P. (2000), Decreasing cloudiness over China: An updated analysis examining additional variables, *Geophys. Res. Lett.*, *27*, 2193–2196, doi:10.1029/2000GL011358.
Kaiser, D. P., and Y. Qian (2002), Decreasing trends in sunshine duration over China for 1954–1998: Indication of increased haze pollution?, *Geophys. Res. Lett.*, *29*(21), 2042, doi:10.1029/2002GL016057.
Kaufman, Y. J. (1997), The effect of smoke particles on clouds and climate forcing, *Science*, *277*, 1636–1639, doi:10.1126/science.277.5332.1636.
Khain, A., A. Pokrovsky, M. Pinsky, A. Seifert, and V. Phillips (2004), Simulation of effects of atmospheric aerosols on deep turbulent convective clouds using a spectral microphysics mixed-phase cumulus cloud model. Part I: Model description and possible applications, *J. Atmos. Sci.*, *61*, 2963–2982, doi:10.1175/JAS-3350.1.
Khain, A. P. (2009), Notes on state-of-the-art investigations of aerosol effects on precipitation: A critical review, *Environ. Res. Lett.*, *4*(1), 015004, doi:10.1088/1748-9326/4/1/015004.
Kim, B.-G., M. A. Miller, S. E. Schwartz, Y. Liu, and Q. Min (2008), The role of adiabaticity in the aerosol first indirect effect, *J. Geophys. Res.*, *113*, D05210, doi:10.1029/2007JD008961.
Kim, J. H., S. S. Yum, S. Shim, W. J. Kim, M. Park, J. Kim, M. Kim, and S. C. Yoon (2014), On the submicron aerosol distributions and CCN number concentrations in and around the Korean Peninsula, *Atmos. Chem. Phys.*, *14*, 8763–8779, doi:10.5194/acp-14-8763-2014.

Kim, M.-K., W. K. M. Lau, K.-M. Kim, and W.-S. Lee (2007), A GCM study of effects of radiative forcing of sulfate aerosol on large scale circulation and rainfall in East Asia during boreal spring, *Geophys. Res. Lett.*, *34*, L24701, doi:10.1029/2007GL031683.
Kim, S. W., I. J. Choi, and S. C. Yoon (2010), A multi-year analysis of clear-sky aerosol optical properties and direct radiative forcing at Gosan, Korea (2001–2008), *Atmos. Res.*, *95*, 279–287, doi:10.1016/j.atmosres.2009.10.008.
Kim, Y., S. W. Kim, and S. C. Yoon (2014), Observation of new particle formation and growth under cloudy conditions at Gosan Climate Observatory, Korea, *Meteorol. Atmos. Phys.*, *126*, 81–90, doi:10.1007/s00703-014-0336-2.
Klimont, Z., S. J. Smith, and J. Cofala (2013), The last decade of global anthropogenic sulfur dioxide: 2000–2011 emissions, *Environ. Res. Lett.*, *8*, 014003, doi:10.1088/1748-9326/8/1/014003.
Konwar, M., R. S. Maheskumar, J. R. Kulkarni, E. Freud, B. N. Goswami, and D. Rosenfeld (2012), Aerosol control on depth of warm rain in convective clouds, *J. Geophys. Res.*, *117*, D13204, doi:10.1029/2012JD017585.
Koren, I., Y. J. Kaufman, D. Rosenfeld, L. A. Remer, and Y. Rudich (2005), Aerosol invigoration and restructuring of Atlantic convective clouds, *Geophys. Res. Lett.*, *32*, L14828, doi:10.1029/2005GL023187.
Koren, I., G. Feingold, and L. A. Remer (2010), The invigoration of deep convective clouds over the Atlantic: Aerosol effect, meteorology or retrieval artifact?, *Atmos. Chem. Phys.*, *10*, 8855–8872.
Kosaka, Y., and S. P. Xie (2013), Recent global-warming hiatus tied to equatorial Pacific surface cooling, *Nature*, *501*, 403–407, doi:10.1038/nature12534.
Krishnamurti, T. N. (1985), Summer monsoon experiment—A review, *Mon. Weather Rev.*, *113*, 1509–1626.
Krishnamurti, T. N., and H. Bhalme (1976), Oscillations of a monsoon system. Part I: Observational aspects, *J. Atmos. Sci.*, *33*, 1937–1954.
Krishnan, R., T. P. Sabin, D. C. Ayantika, A. Kitoh, M. Sugi, H. Murakami, A. G. Turner, J. M. Slingo, and K. Rajendran (2013), Will the South Asian monsoon overturning circulation stabilize any further?, *Clim. Dyn.*, *40*(1-2), 187–211, doi:10.1007/s00382-012-1317-0.
Kudo, R., A. Uchiyama, O. Ijima, N. Ohkawara, and S. Ohta (2012), Aerosol impact on the brightening in Japan, *J. Geophys. Res.*, *117*, D07208, doi:10.1029/2011JD017158.
Kumar, S., and P. C. S. Devara (2012), A long-term study of aerosol modulation of atmospheric and surface solar heating over Pune, India, *Tellus, Ser. B*, *64*, 18,420.
Kumar, R., M. C. Barth, V. S. Nair, G. G. Pfister, S. S. Babu, S. K. Satheesh, K. K. Moorthy, and G. R. Carmichael (2014), Sources of black carbon aerosols in South Asia and surrounding regions during the Integrated Campaign for Aerosols, Gases and Radiation Budget (ICARB), *Atmos. Chem. Phys.*, *14*, 30,727–30,759, doi:10.5194/acpd-14-30727-2014.18.
Lamarque, J.-F., et al. (2010), Historical (1850–2000) gridded anthropogenic and biomass burning emissions of reactive gases and aerosols: Methodology and application, *Atmos. Chem. Phys.*, *10*, 7017–7039, doi:10.5194/acp-10-7017-2010.
Lau, K. M. (2016), The aerosol-monsoon climate system of Asia: A new paradigm, *J. Meteorol. Res.*, *29*(6), 1–11, doi:10.1007/s13351-015-5999-1.
Lau, K. M., and W. Bua (1998), Mechanisms of monsoon-southern oscillation coupling: Insights from GCM experiments, *Clim. Dyn.*, *14*, 759–779.
Lau, K. M., and P. H. Chan (1986), Aspects of the 40–50 day oscillation during northern summer as inferred from outgoing longwave radiation, *Mon. Weather Rev.*, *114*, 1354–1367.
Lau, K. M., and K. M. Kim (2006), Observational relationships between aerosol and Asian monsoon rainfall, and circulation, *Geophys. Res. Lett.*, *33*, L21810, doi:10.1029/2006GL027546.
Lau, K. M., and K. M. Kim (2007), Does aerosol strengthen or weaken the Asian monsoon? in *Mountains: Witnesses of Global Change*, edited by R. Baudo, G. Tartari, and E. Vuillermoz, Elsevier, Amsterdam.
Lau, K. M., and K. M. Kim (2015), Impacts of absorbing aerosols on the Asian monsoon: An interim assessment, in *World Scientific Series on Asian-Pacific Weather and Climate*, *Clim. Change: Decadal and Beyond*, vol. 6, edited by C. P. Chang et al., World Sci., Singapore.
Lau, K. M., and M.-T. Li (1984), The monsoon of East Asia and its global associations—A survey, *Bull. Am. Meteorol. Soc.*, *65*(2), 114–125.
Lau, K. M., and H. Weng (2001), Coherent modes of global SST and summer rainfall over China: An assessment of the regional impacts of the 1997–98 El Niño, *J. Clim.*, *14*, 1294–1308, doi:10.1175/1520-0442(2001)014<1294:CMOGSA>2.0.CO;2.
Lau, K. M., and S. Yang (1997), Climatology and interannual variability of the southeast Asian summer monsoon, *Adv. Atmos. Sci.*, *14*, 141–162.
Lau, K. M., K. M. Kim, and S. Yang (2000), Dynamical and boundary forcing characteristics of regional components of the Asian summer monsoon, *J. Clim.*, *13*, 2461–2482, doi:10.1175/1520-0442(2000)013<2461:DABFCO>2.0.CO;2.
Lau, K. M., M. K. Kim, and K. M. Kim (2006), Asian summer monsoon anomalies induced by aerosol direct forcing: The role of the Tibetan Plateau, *Clim. Dyn.*, *26*, 855–864, doi:10.1007/s00382-006-0114-z.
Lau, K. M., et al. (2008), The Joint Aerosol-Monsoon Experiment: A new challenge for monsoon climate research, *Bull. Am. Meteorol. Soc.*, *89*(3), 369–383, doi:10.1175/BAMS-89-3-369.
Lau, K. M., M. Kim, K. Kim, and W. Lee (2010), Enhanced surface warming and accelerated snow melt in the Himalayas and Tibetan Plateau induced by absorbing aerosols, *Environ. Res. Lett.*, *5*(2), 025204, doi:10.1088/1748-9326/5/2/025204.
Lee, K. H., Z. Li, M. S. Wong, J. Xin, Y. Wang, W.-M. Hao, and F. Zhao (2007), Aerosol single scattering albedo estimated across China from a combination of ground and satellite measurements, *J. Geophys. Res.*, *112*, D22S15, doi:10.1029/2007JD009077.
Lee, K. H., Z. Li, M. C. Cribb, J. Liu, L. Wang, Y. Zheng, X. Xia, H. Chen, and B. Li (2010), Aerosol optical depth measurements in eastern China and a new calibration method, *J. Geophys. Res.*, *115*, D00K11, doi:10.1029/2009JD012812.
Lee, S. S., L. J. Donner, V. T. J. Phillips, and Y. Ming (2008), The dependence of aerosol effects on clouds and precipitation on cloud-system organization, shear and stability, *J. Geophys. Res.*, *113*, D16202, doi:10.1029/2007JD009224.
Lee, S. S., G. Feingold, and P. Y. Chuang (2012), Effect of aerosol on cloud-environment interactions in trade cumulus, *J. Atmos. Sci.*, *69*, 3607–3632, doi:10.1175/JAS-D-12-026.1.
Lee, S.-S., J. Guo, and Z. Li (2016), Delaying precipitation by air pollution over the Pearl River Delta. Part II: Model simulations, *J. Geophys. Res. Atmos.*, *121*, doi:10.1002/2015JD024362, in press.
Lei, Y., B. Hoskins, and J. Slingo (2014), Natural variability of summer rainfall over China in HadCM3, *Clim. Dyn.*, *42*, 417–432, doi:10.1007/s00382-013-1726-8.
Leng, C., et al. (2013), Measurements of surface cloud condensation nuclei and aerosol activity in downtown Shanghai, *Atmos. Environ.*, *69*, 354–361.
Levy, H., II, L. W. Horowitz, M. D. Schwarzkopf, Y. Ming, J.-C. Golaz, V. Naik, and V. Ramaswamy (2013), The roles of aerosol direct and indirect effects in past and future climate change, *J. Geophys. Res. Atmos.*, *118*, 4521–4532, doi:10.1002/jgrd.50192.
Levy, R. C., L. A. Remer, R. G. Kleidman, S. Mattoo, C. Ichoku, R. Kahn, and T. F. Eck (2010), Global evaluation of the Collection 5 MODIS dark-target aerosol products over land, *Atmos. Chem. Phys.*, *10*, 10,399–10,420, doi:10.5194/acp-10-10399-2010.
Li, C., and M. Yanai (1996), The onset and interannual variability of the Asian summer monsoon in relation to land-sea thermal contrast, *J. Clim.*, *9*, 358–375, doi:10.1175/1520-0442(1996)009<0358:TOAIVO>2.0.CO;2.

Li, C., N. A. Krotkov, R. R. Dickerson, Z. Li, K. Yang, and M. Chin (2010), Transport and evolution of a pollution plume from northern China: A satellite-based case study, *J. Geophys. Res.*, *115*, D00K03, doi:10.1029/2009JD012245.
Li, F., and V. Ramanathan (2002), Winter to summer monsoon variation of aerosol optical depth over the tropical Indian Ocean, *J. Geophys. Res.*, *107*(D16), 4284, doi:10.1029/2001JD000949.
Li, G., Y. Wang, K.-H. Lee, Y. Diao, and R. Zhang (2008), Increased winter precipitation over the North Pacific from 1984–1994 to 1995–2005 inferred from the Global Precipitation Climatology Project, *Geophys. Res. Lett.*, *35*, L13821, doi:10.1029/2008GL034668.
Li, H., A. Dai, T. Zhou, and J. Lu (2010a), Responses of East Asian summer monsoon to historical SST and atmospheric forcing during 1950–2000, *Clim. Dyn.*, *34*, 501–514, doi:10.1007/s00382-008-0482-7.
Li, H., L. Feng, and T. Zhou (2010b), Multi-model projection of July–August climate extreme changes over China under CO_2 doubling. Part II: Temperature, *Adv. Atmos. Sci.*, *28*(2), 448–463, doi:10.1007/s00376-010-0052-x.
Li, J. D., Z. A. Sun, M. Y. Liu, J. Li, W.-C. Wang, and G. Wu (2012), A study on sulfate optical properties and direct radiative forcing using the LASG-IAP general circulation model, *Adv. Atmos. Sci.*, *29*(6), 1185–1199.
Li, J. D., W. C. Wang, Z. A. Sun, G. Wu, H. Liao, and Y. Liu (2014), Decadal variation of East Asian radiative forcing due to anthropogenic aerosols during 1850–2100 and the role of atmospheric moisture, *Clim. Res.*, *61*, 241–257, doi:10.3354/cr01236.
Li, J. P., and Q. C. Zeng (2002), A unified monsoon index, *Geophys. Res. Lett.*, *29*(8), 1274, doi:10.1029/2001GL013874.
Li, J. P., Z. W. Wu, Z. H. Jiang, and J. H. He (2010), Can global warming strengthen the East Asian summer monsoon?, *J. Clim.*, *23*, 6696–6705.
Li, Q., et al. (2005), Convective outflow of South Asian pollution: A global CTM simulation compared with EOS MLS observations, *Geophys. Res. Lett.*, *32*, L14826, doi:10.1029/2005GL022762.
Li, Q., R. Zhang, and Y. Wang (2015), Interannual variation of the wintertime fog-haze days across central and eastern China and its relation with East Asian winter monsoon, *Int. J. Climatol.*, *36*, 346–354, doi:10.1002/joc.4350.
Li, X., M. Ting, C. Li, and N. Henderson (2015), Mechanisms of Asian summer monsoon changes in response to anthropogenic forcing in CMIP5 models, *J. Clim.*, *28*, 4107–4125.
Li, Z. (2004), Aerosol and climate: A perspective from East Asia, in *Observation, Theory, and Modeling of the Atmospheric Variability*, pp. 501–525, World Sci., Singapore.
Li, Z., et al. (2007a), Preface to special section on East Asian Studies of Tropospheric aerosols: An International Regional Experiment (EAST-AIRE), *J. Geophys. Res.*, *112*, D22S00, doi:10.1029/2007JD008853.
Li, Z., et al. (2007b), Aerosol optical properties and their radiative effects in northern China, *J. Geophys. Res.*, *112*, D22S01, doi:10.1029/2006JD007382.
Li, Z., F. Niu, K.-H. Lee, J. Xin, W.-M. Hao, B. Nordgren, Y. Wang, and P. Wang (2007c), Validation and understanding of MODIS aerosol products using ground-based measurements from the handheld sunphotometer network in China, *J. Geophys. Res.*, *112*, D22S07, doi:10.1029/2007JD008479.
Li, Z., X. Zhao, R. Kahn, M. Mishchenko, L. Remer, K.-H. Lee, M. Wang, I. Laszlo, T. Nakajima, and H. Maring (2009), Uncertainties in satellite remote sensing of aerosols and impact on monitoring its long-term trend: A review and perspective, *Ann. Geophys.*, *27*, 1–16.
Li, Z., K.-H. Lee, Y. Wang, J. Xin, and W.-M. Hao (2010), First observation-based estimates of cloud-free aerosol radiative forcing across China, *J. Geophys. Res.*, *115*, D00K18, doi:10.1029/2009JD013306.
Li, Z., et al. (2011a), East Asian Studies of Tropospheric aerosols and their Impact on Regional Climate (EAST-AIRC): An overview, *J. Geophys. Res.*, *116*, D00K34, doi:10.1029/2010JD015257.
Li, Z., F. Niu, J. Fan, Y. Liu, D. Rosenfeld, and Y. Ding (2011b), Long-term impacts of aerosols on the vertical development of clouds and precipitation, *Nat. Geosci.*, *4*(12), 888–894, doi:10.1038/ngeo1313.
Liang, F., and X. Xia (2005), Long-term trends in solar radiation and the associated climatic factors over China for 1961–2000, *Ann. Geophys.*, *23*(7), 2424–2432.
Liang, Q., L. Jaeglé, D. A. Jaffe, P. Weiss-Penzias, A. Heckman, and J. A. Snow (2004), Long-range transport of Asian pollution to the northeast Pacific: Seasonal variations and transport pathways of carbon monoxide, *J. Geophys. Res.*, *109*, D23S07, doi:10.1029/2003JD004402.
Lin, J.-T., D. Pan, and R.-X. Zhang (2013), Trend and interannual variability of Chinese air pollution since 2000 in association with socioeconomic development: A brief review, *Atmos. Oceanic Sci. Lett.*, *6*, 84–89.
Lin, J.-T., A. van Donkelaar, J. Xin, H. Che, and Y. Wang (2014), Clear-sky aerosol optical depth over East China estimated from visibility measurements and chemical transport modeling, *Atmos. Environ.*, *95*, 258–267.
Lin, L., Z. L. Wang, Y. Y. Xu, and Q. Fu (2016), Sensitivity of precipitation extremes to radiative forcing of greenhouse gases and aerosols, *Geophys. Res. Lett.*, *43*, doi:10.1002/2016GL070869.
Liu, H., D. J. Jacob, I. Bey, R. M. Yantosca, B. N. Duncan, and G. W. Sachse (2003), Transport pathways for Asian pollution outflow over the Pacific: Interannual and seasonal variations, *J. Geophys. Res.*, *108*(D20), 8786, doi:10.1029/2002JD003102.
Liu, H., T. Zhou, Y. Zhu, and Y. Lin (2012), The strengthening East Asia summer monsoon since the early 1990s, *Chin. Sci. Bull.*, *57*(13), 1553–1558.
Liu, J., and Z. Li (2014), Estimation of cloud condensation nuclei concentration from aerosol optical quantities: Influential factors and uncertainties, *Atmos. Chem. Phys.*, *14*(1), 471–483, doi:10.5194/acp-14-471-2014.
Liu, J., X. Xia, P. Wang, Z. Li, Y. Zheng, M. Cribb, and H. Chen (2007), Significant aerosol direct radiative effects during a pollution episode in northern China, *Geophys. Res. Lett.*, *34*, L23808, doi:10.1029/2007GL030953.
Liu, J., Y. Zheng, Z. Li, and M. Cribb (2011a), Analysis of cloud condensation nuclei properties at a polluted site in southeastern China during the AMF-China Campaign, *J. Geophys. Res.*, *116*, D00K35, doi:10.1029/2011JD016395.
Liu, J., Y. Zheng, Z. Li, C. Flynn, E. J. Welton, and M. Cribb (2011b), Transport, vertical structure and radiative properties of dust events in southeast China determined from ground and space sensors, *Atmos. Environ.*, *45*, 6469–6480, doi:10.1016/j.atmosenv.2011.04.031.
Liu, J., Y. Zheng, Z. Li, C. Flynn, and M. Cribb (2012), Seasonal variations of aerosol optical properties, vertical distribution and associated radiative effects in the Yangtze Delta region of China, *J. Geophys. Res.*, *117*, D00K38, doi:10.1029/2011JD016490.
Liu, L., Z. Li, X. Yang, H. Gong, C. Li, and A. Xiong (2016), The long-term trend in the diurnal temperature range over Asia and its natural and anthropogenic causes, *J. Geophys. Res. Atmos.*, *121*, 3519–3533, doi:10.1002/2015JD024549.
Liu, S. C., C.-H. Wang, C.-J. Shiu, H.-W. Chang, C.-K. Hsiao, and S.-H. Liaw (2002), Reduction in sunshine duration over Taiwan: Causes and implications terrestrial, *Atmos. Oceanic Sci.*, *13*, 523–545.
Liu, X., L. Yan, P. Yang, Z.-Y. Yin, and G. R. North (2011), Influence of Indian summer monsoon on aerosol loading in East Asia, *J. Appl. Meteorol. Climatol.*, *50*, 523–533.
Liu, Y., J. Sun, and B. Yang (2009), The effects of black carbon and sulphate aerosols in China regions on East Asia monsoons, *Tellus, Ser. B*, *61*, 642–656, doi:10.1111/j.1600-0889.2009.00427.x.
Logan, T., B. Xi, X. Dong, Z. Li, and M. Cribb (2013), Classification and investigation of Asian aerosol properties, *Atmos. Chem. Phys.*, *13*, 2253–2265, doi:10.5194/acp-13-2253-2013.

Louie, P. K. K., J. C. Chow, L. W. A. Chen, J. G. Watson, G. Leung, and D. W. M. Sin (2005), $PM_{2.5}$ chemical composition in Hong Kong: Urban and regional variations, *Sci. Total Environ.*, *338*, 267–281.
Luo, H., and M. Yanai (1984), The large-scale circulation and heat sources over the Tibetan Plateau and surrounding areas during the early summer of 1979. Part II: Heat and moisture budgets, *Mon. Weather Rev.*, *112*, 966–989.
Luo, Y., D. Lu, X. Zhou, and W. Li (2001), Characteristics of the spatial distribution and yearly variation of aerosol optical depth over China in last 30 years, *J. Geophys. Res.*, *106*, 14,501–14,513, doi:10.1029/2001JD900030.
Lyapustin, A., et al. (2011), Reduction of aerosol absorption in Beijing since 2007 from MODIS and AERONET, *Geophys. Res. Lett.*, *38*, L10803, doi:10.1029/2011GL047306.
Mahmood, R., and S.-L. Li (2011), Modeled influence of east Asian black carbon on inter-decadal shifts in east China summer rainfall, *Atmos. Oceanic Sci. Lett.*, *4*, 349–355.
Manabe, S., and T. B. Terpstra (1974), The effects of mountains on the general circulation of the atmosphere as identified by numerical experiments, *J. Atmos. Sci.*, *31*(1), 3–42.
Manoharan, V. S., R. Kotamarthi, Y. Feng, and M. P. Cadeddu (2014), Increased absorption by coarse aerosol particles over the Gangetic-Himalayan region, *Atmos. Chem. Phys.*, *14*, 1159–1165, doi:10.5194/acp-14-1159-2014.
Manoj, M. G., P. C. S. Devara, P. D. Safai, and B. N. Goswami (2011), Absorbing aerosols facilitate transition of Indian monsoon breaks to active spells, *Clim. Dyn.*, *37*, 2181–2198, doi:10.1007/s00382-010-0971-3.
Manoj, M. G., P. C. S. Devara, S. Joseph, and A. K. Sahai (2012), Aerosol indirect effect during the aberrant Indian summer monsoon breaks of 2009, *Atmos. Environ.*, *60*, 153–163, doi:10.1016/j.atmosenv.2012.06.007.
Markowicz, K. M., P. J. Flatau, A. M. Vogelmann, P. K. Quinn, and E. J. Welton (2003), Clear-sky infrared aerosol radiative forcing at the surface and the top of the atmosphere, *Q. J. R. Meteorol. Soc.*, *129*, 2927–2947, doi:10.1256/qj.02.224.
Matsumoto, J., B. Wang, J. Li, and G. Wu (2010), *The Implementation Plan for Asian Monsoon Years (AMY 2007–2012)*, 38 pp., China Meteorol. Press, Beijing.
Meehl, G. A. (1994), Influence of the land surface in the Asian summer monsoon: External conditions versus internal feedbacks, *J. Clim.*, *7*, 1033–1049.
Meehl, G. A., J. Arblaster, and W. Collins (2008), Effects of black carbon aerosols on the Indian monsoon, *J. Clim.*, *21*, 2869–2882, doi:10.1175/2007JCLI1777.1.
Menon, S., J. Hansen, L. Nazarenko, and Y. Luo (2002), Climate effects of black carbon aerosols in China and India, *Science*, *297*, 2250–2253, doi:10.1126/science.1075159.
Mi, W., Z. Li, X. Xia, B. Holben, R. Levy, F. Zhao, H. Chen, and M. Cribb (2007), Evaluation of the Moderate Resolution Imaging Spectroradiometer aerosol products at two Aerosol Robotic Network stations in China, *J. Geophys. Res.*, *112*, D22S0, doi:10.1029/2007JD008474.
Miao, Q., Z. Zhang, Y. Li, X. Qin, B. Xu, Y. Yuan, and Z. Gao (2015), Measurement of cloud condensation nuclei (CCN) and CCN closure at Mt. Huang based on hygroscopic growth factors and aerosol number-size distribution, *Atmos. Environ.*, *113*, 127–134.
Mitchell, J. F. B., T. C. Johns, J. M. Gregory, and S. F. B. Tett (1995), Climate responses to increasing levels of greenhouse gases and sulphate aerosols, *Nature*, *376*, 463–501.
Moorthy, K. K., P. R. Nair, and B. V. K. Murthy (1989), Multiwavelength solar radiometer network and features of aerosol spectral optical depth at Trivandrum, *Indian J. Radio Space Phys.*, *18*, 194–201.
Moorthy, K. K., S. S. Babu, and S. K. Satheesh (2005), Aerosol characteristics and radiative impacts over the Arabian Sea during inter-monsoon season: Results from ARMEX field campaign, *J. Atmos. Sci.*, *62*, 192–206.
Moorthy, K. K., S. K. Satheesh, S. S. Babuand, and C. B. S. Dutt (2008), Integrated Campaign for Aerosols, gases and Radiation Budget (ICARB): An overview, *J. Earth Syst. Sci.*, *117*(S1), 243–262.
Moorthy, K. K., V. S. Nair, S. S. Babu, and S. K. Satheesh (2009), Spatial and vertical heterogeneities in aerosol properties over oceanic regions around India: Implications to radiative forcing, *Q. J. R. Meteorol. Soc.*, *135*, 2131–2145, doi:10.1002/qj.525.
Moorthy, K. K., S. S. Babu, M. R. Manoj, and S. K. Satheesh (2013a), Buildup of aerosols over the Indian region, *Geophys. Res. Lett.*, *40*, 1011–1014, doi:10.1002/grl.50165.
Moorthy, K. K., S. N. Beegum, N. Srivastava, S. K. Satheesh, M. Chin, N. Blond, S. S. Babu, and S. Singh (2013b), Performance evaluation of chemistry transport models over India, *Atmos. Environ.*, *71*, 210–225.
Mu, M., and R. Zhang (2014), Addressing the issue of fog and haze: A promising way of meteorological science and technology, *Sci. China Earth Sci.*, *57*, 1–2, doi:10.1007/s11430-013-4791-2.
Nair, S., J. Sanjay, G. Pandithurai, R. S. Maheskumar, and J. R. Kulkarni (2012), On the parameterization of cloud droplet effective radius using CAIPEEX aircraft observations for warm clouds in India, *Atmos. Res.*, *108*, 104–114.
Nair, S. K., K. Rajeev, and K. Parameswaran (2003), Wintertime regional aerosol distribution and the influence of continental transport over the Indian Ocean, *J. Atmos. Sol. Terr. Phys.*, *65*(2), 149–165.
Nair, V. S., S. S. Babu, K. K. Moorthy, and S. S. Prijith (2013a), Spatial gradients in aerosol-induced atmospheric heating and surface dimming over the oceanic regions around India: Anthropogenic or natural?, *J. Clim.*, *26*, 7611–7621.
Nair, V. S., S. S. Babu, K. K. Moorthy, A. K. Sharma, A. Marinoni, and Ajai (2013b), Black carbon aerosols over the Himalayas: Direct and surface albedo forcing, *Tellus, Ser. B*, *65*, 19738, doi:10.3402/tellusb.v65i0.19738.
Nakajima, T., et al. (2003), Significance of direct and indirect radiative forcings of aerosols in the east China Sea region, *J. Geophys. Res.*, *108*(D23), 8658, doi:10.1029/2002JD003261.
Nakajima, T., et al. (2007), Overview of the atmospheric brown cloud East Asian Regional Experiment 2005 and a study of the aerosol direct radiative forcing in East Asia, *J. Geophys. Res.*, *112*, D24S91, doi:10.1029/2007JD009009.
Niemand, M., et al. (2012), A particle-surface-area-based parameterization of immersion freezing on desert dust particles, *J. Atmos. Sci.*, *69*, 3077–3091, doi:10.1175/JAS-D-11-0249.1.
Nigam, S., and M. Bollasina (2011), Reply to comment by K. M. Lau and K. M. Kim on "'Elevated heat pump' hypothesis for the aerosol-monsoon hydroclimate link: 'Grounded' in observations?", *J. Geophys. Res.*, *116*, D07204, doi:10.1029/2010JD015246.
Niranjan, K., V. Sreekanth, B. L. Madhavan, and K. K. Moorthy (2007), Aerosol physical properties and radiative forcing at the outflow region from the Indo-Gangetic plains during typical clear and hazy periods of wintertime, *Geophys. Res. Lett.*, *34*, L19805, doi:10.1029/2007GL031224.
Niu, F., and Z. Li (2012), Systematic variations of cloud top temperature and precipitation rate with aerosols over the global tropics, *Atmos. Chem. Phys.*, *12*, 8491–8498.
Niu, F., Z. Li, C. Li, K.-H. Lee, and M. Wang (2010), Increase of wintertime fog in China: Potential impacts of weakening of the Eastern Asian monsoon circulation and increasing aerosol loading, *J. Geophys. Res.*, *115*, D00K20, doi:10.1029/2009JD013484.

Ohara, T., H. Akimoto, J. Kurokawa, N. Horii, K. Yamaji, X. Yan, and T. Hayasaka (2007), An Asian emission inventory of anthropogenic emission sources for the period 1980–2020, *Atmos. Chem. Phys.*, *7*, 4419–4444.
Ohmura, A. (2009), Observed decadal variations in surface solar radiation and their causes, *J. Geophys. Res.*, *114*, D00D05, doi:10.1029/2008JD011290.
Ovchinnikov, M., A. Korolev, and J. Fan (2011), Effects of ice number concentration on dynamics of a shallow mixed-phase stratiform cloud, *J. Geophys. Res.*, *116*, D00T06, doi:10.1029/2011JD015888.
Padmakumari, B., A. K. Jaswal, and B. N. Goswami (2013), Decrease in evaporation over the Indian monsoon region: Implication on regional hydrological cycle, *Clim. Change*, *121*, 787–799, doi:10.1007/s10584-013-0957-3.
Pandithurai, G., R. T. Pinker, T. Takamura, and P. C. S. Devara (2004), Aerosol radiative forcing over a tropical urban site in India, *Geophys. Res. Lett.*, *31*, L12107, doi:10.1029/2004GL019702.
Panicker, A. S., G. Pandithurai, and S. Dipu (2010), Aerosol indirect effect during successive contrasting monsoon seasons over Indian subcontinent using MODIS data, *Atmos. Environ.*, *44*, 1937–1943, doi:10.1016/j.atmosenv.2010.02.015.
Pant, P., P. Hegde, U. C. Dumka, R. Sagar, S. K. Satheesh, K. K. Moorthy, A. Saha, and M. K. Srivastava (2006), Aerosol characteristics at a high-altitude location in central Himalayas: Optical properties and radiative forcing, *J. Geophys. Res.*, *111*, D17206, doi:10.1029/2005JD006768.
Parameswaran, K., K. O. Rose, M. Satyanarayana, and B. V. Krishna Murthy (1989), Method of analysis and preliminary results of atmospheric lidar observation at Trivandrum, *Indian J. Radio Space Phys.*, *18*, 202–209.
Park, M., W. J. Randel, L. K. Emmons, P. F. Bernath, K. A. Walker, and C. D. Boone (2008), Chemical isolation in the Asian monsoon anticyclone observed in Atmospheric Chemistry Experiment (ACE-FTS) data, *Atmos. Chem. Phys.*, *8*(3), 757–764.
Pathak, B., G. Kalita, K. Bhuyan, P. K. Bhuyan, and K. K. Moorthy (2010), Aerosol temporal characteristics and its impact on shortwave radiative forcing at a location in the northeast of India, *J. Geophys. Res.*, *115*, D19204, doi:10.1029/2009JD013462.
Peng, J., Z. Li, H. Zhang, J. Liu, and M. Cribb (2016), Systematic changes in cloud radiative forcing with aerosol loading for deep clouds in the tropics, *J. Atmos. Sci.*, *73*, 231–249, doi:10.1175/JAS-D-15-0080.1.
Penner, J. E., et al. (2001), Aerosols, their direct and indirect effects, in *Climate Change 2001: The Scientific Basis. Contribution of Working Group I to the Third Assessment Report of the Intergovernmental Panel on Climate Change*, edited by J. T. Houghton et al., pp. 289–348, Cambridge Univ. Press, Cambridge, U. K.
Pielke, R., et al. (2009), Climate change: The need to consider human forcing besides greenhouse gases, *Eos Trans. AGU*, *90*, 413, doi:10.1029/2009EO450008.
Prabha, T. V., A. Khain, R. S. Maheshkumar, G. Pandithurai, J. R. Kulkarni, M. Konwar, and B. N. Goswami (2011), Microphysics of pre-monsoon and monsoon clouds as seen from in situ measurements during the Cloud Aerosol Interaction and Precipitation Enhancement Experiment (CAIPEEX), *J. Atmos. Sci.*, *68*(9), 1882–1901.
Prabha, T. V., S. Patade, G. Pandithurai, A. Khain, D. Axisa, P. Pradeep-Kumar, R. S. Maheshkumar, J. R. Kulkarni, and B. N. Goswami (2012), Spectral width of premonsoon and monsoon clouds over Indo-Gangetic valley, *J. Geophys. Res.*, *117*, D20205, doi:10.1029/2011JD016837.
Prijith, S. S., S. S. Babu, N. B. Lakshmi, S. K. Satheesh, and K. K. Moorthy (2016), Meridional gradients in aerosol vertical distribution over Indian Mainland: Observations and model simulations, *Atmos. Environ.*, *125*, 337–345, doi:10.1016/j.atmosenv.2015.10.066.
Qian, Y., L. R. Leung, S. J. Ghan, and F. Giorgi (2003), Regional climate effects of aerosols over China: Modeling and observation, *Tellus, Ser. B*, *55*, 914–934, doi:10.1046/j.1435-6935.2003.00070.x.
Qian, Y., D. P. Kaiser, L. R. Leung, and M. Xu (2006), More frequent cloud-free sky and less surface solar radiation in China from 1955 to 2000, *Geophys. Res. Lett.*, *33*, L01812, doi:10.1029/2005GL024586.
Qian, Y., D. Gong, J. Fan, L. R. Leung, R. Bennartz, D. Chen, and W. Wang (2009), Heavy pollution suppresses light rain in China: Observations and modeling, *J. Geophys. Res.*, *114*, D00K02, doi:10.1029/2008JD011575.
Qian, Y., M. Flanner, L. Leung, and W. Wang (2011), Sensitivity studies on the impacts of Tibetan Plateau snowpack pollution on the Asian hydrological cycle and monsoon climate, *Atmos. Chem. Phys.*, *11*(5), 1929–1948, doi:10.5194/acp-11-1929-2011.
Qian, Y., C. N. Long, H. Wang, J. M. Comstock, S. A. McFarlane, and S. Xie (2012), Evaluation of cloud fraction and its radiative effect simulated by IPCC AR4 global models against ARM surface observations, *Atmos. Chem. Phys.*, *12*(4), 1785–1810, doi:10.5194/acp-12-1785-2012.
Qian, Y., T. Yasunnari, S. Doherty, M. G. Flanner, W. K. M. Lau, J. Ming, H. Wang, M. Wang, S. G. Warren, and R. Zhang (2014), Light-absorbing particles in snow and ice: Measurement and modeling of climatic and hydrological impact, *Adv. Atmos. Sci.*, *32*, 64–91.
Qin, Y., C. K. Chan, and L. Y. Chan (1997), Characteristics of chemical compositions of atmospheric aerosols in Hong Kong: Spatial and seasonal distributions, *Sci. Total Environ.*, *206*, 25–37.
Qiu, J., and L. Yang (2000), Variation characteristics of atmospheric aerosol optical depth and visibility in northern China during 1980–1994, *Atmos. Environ.*, *34*, 603–609.
Ramachandran, S. (2005), Premonsoon shortwave aerosol radiative forcings over the Arabian Sea and tropical Indian Ocean: Yearly and monthly mean variabilities, *J. Geophys. Res.*, *110*, D07207, doi:10.1029/2004JD005563.
Ramachandran, S., R. Rengarajan, A. Jayaraman, M. M. Sarin, and S. K. Das (2006), Aerosol radiative forcing during clear, hazy, and foggy conditions over a continental polluted location in north India, *J. Geophys. Res.*, *111*, D20214, doi:10.1029/2006JD007142.
Ramage, C. S. (1971), *Monsoon Meteorology*, 296 pp., Academic Press, New York.
Ramanathan, V., and G. Carmichael (2008), Global and regional climate changes due to black carbon, *Nat. Geosci.*, *1*, 221–227, doi:10.1038/ngeo156.
Ramanathan, V., and Y. Feng (2009), Air pollution, greenhouse gases and climate change: Global and regional perspectives, *Atmos. Environ.*, *43*, 37–50, doi:10.1016/j.atmosenv.2008.09.063.
Ramanathan, V., P. J. Crutzen, J. T. Kiehl, and D. Rosenfeld (2001a), Aerosols, climate, and the hydrological cycle, *Science*, *294*, 2119–2124, doi:10.1126/science.1064034.
Ramanathan, V., et al. (2001b), The Indian Ocean Experiment: An integrated analysis of the climate forcing and effects of the great Indo-Asian haze, *J. Geophys. Res.*, *106*, 28,371–28,398, doi:10.1029/2001JD900133.
Ramanathan, V., C. Chung, D. Kim, T. Bettge, L. Buja, J. T. Kiehl, W. M. Washington, Q. Fu, D. R. Sikka, and M. Wild (2005), Atmospheric brown clouds: Impacts on South Asian climate and hydrological cycle, *Proc. Natl. Acad. Sci. U.S.A.*, *102*, 5326–5333, doi:10.1073/pnas.0500656102.
Ramanathan, V., et al. (2007), Atmospheric brown clouds: Hemispherical and regional variations in long-range transport, absorption, and radiative forcing, *J. Geophys. Res.*, *112*, D22S21, doi:10.1029/2006JD008124.
Randel, W. J., M. Park, L. Emmons, D. Kinnison, P. Bernath, K. A. Walker, C. Boone, and H. Pumphrey (2010), Asian monsoon transport of pollution to the stratosphere, *Science*, *328*, 611–613.

Randles, C. A., and V. Ramaswamy (2008), Absorbing aerosols over Asia: A Geophysical Fluid Dynamics Laboratory general circulation model sensitivity study of model response to aerosol optical depth and aerosol absorption, *J. Geophys. Res.*, *113*, D21203, doi:10.1029/2008JD010140.

Remer, L. A., S. Mattoo, R. C. Levy, and L. A. Munchak (2013), MODIS 3 km aerosol product: Algorithm and global perspective, *Atmos. Meas. Tech.*, *6*, 1829–1844, doi:10.5194/amt-6-1829-2013.

Ren, G., J. Guo, M. Xu, Z. Chu, L. Zhang, X. Zou, Q. Li, and X. Liu (2005), Climate changes of mainland China over the past half century, *Acta Meteorol. Sin.*, *63*(6), 942–956 (in Chinese).

Robock, A., M. Mu, K. Vinnikov, and D. Robinson (2003), Land surface conditions over Eurasia and Indian summer monsoon rainfall, *J. Geophys. Res.*, *108*(D4), 4131, doi:10.1029/2002JD002286.

Rose, D., A. Nowak, P. Achtert, A. Wiedensohler, M. Hu, M. Shao, Y. Zhang, M. O. Andreae, and U. Pöschl (2010), Cloud condensation nuclei in polluted air and biomass burning smoke near the mega-city Guangzhou, China—Part 1: Size-resolved measurements and implications for the modeling of aerosol particle hygroscopicity and CCN activity, *Atmos. Chem. Phys.*, *10*, 3365–3383, doi:10.5194/acp-10-3365-2010.

Rose, D., et al. (2011), Cloud condensation nuclei in polluted air and biomass burning smoke near the mega-city Guangzhou, China—Part 2: Size-resolved aerosol chemical composition, diurnal cycles, and externally mixed weakly CCN-active soot particles, *Atmos. Chem. Phys.*, *11*, 2817–2836, doi:10.5194/acp-11-2817-2011.

Rosenfeld, D. (2000), Suppression of rain and snow by urban and industrial air pollution, *Science*, *287*, 1793–1796, doi:10.1126/science.287.5459.1793.

Rosenfeld, D., J. Dai, X. Yu, Z. Yao, X. Xu, X. Yang, and C. Du (2007), Inverse relations between amounts of air pollution and orographic precipitation, *Science*, *315*, 1396–1398, doi:10.1126/science.1137949.

Rosenfeld, D., U. Lohmann, G. B. Raga, C. D. O'Dowd, M. Kulmala, S. Fuzzi, A. Reissell, and M. O. Andreae (2008), Flood or drought: How do aerosols affect precipitation?, *Science*, *321*, 1309–1313, doi:10.1126/science.1160606.

Rosenfeld, D., G. Liu, X. Yu, Y. Zhu, J. Dai, X. Xu, and Z. Yue (2014), High resolution (375 m) cloud microstructure as seen from the NPP/VIIRS satellite imager, *Atmos. Chem. Phys.*, *14*, 2479–2496, doi:10.5194/acp-14-2479-2014.

Rosenfeld, D., et al. (2016), Satellite retrieval of cloud condensation nuclei concentrations by using clouds as CCN chambers, *Proc. Natl. Acad. Sci. U.S.A.*, *113*, 5828–5834, doi:10.1073/pnas.1514044113.

Sankar Rao, M., K. M. Lau, and S. Yang (1996), On the relationship between snow cover over Eurasia and the Asian summer monsoon, *Int. J. Climatol.*, *16*, 605–616.

Satheesh, S. K. (2002), Radiative forcing by aerosols over Bay of Bengal region, *Geophys. Res. Lett.*, *29*(22), 2083, doi:10.1029/2002GL015334.

Satheesh, S. K., and V. Ramanathan (2000), Large differences in tropical aerosol forcing at the top of the atmosphere and Earth's surface, *Nature*, *405*, 60–63, doi:10.1038/35011039.

Satheesh, S. K., K. Krishna Moorthy, S. S. Babu, V. Vinoj, and C. B. S. Dutt (2008), Climate implications of large warming by elevated aerosol over India, *Geophys. Res. Lett.*, *35*, L19809, doi:10.1029/2008GL034944.

Schwartz, S. E. (1996), The whitehouse effect: Shortwave radiative forcing of climate by anthropogenic aerosols: An overview, *J. Aerosol Sci.*, *27*, 359–382, doi:10.1016/0021-8502(95)00533-1.

Shahid, M. Z., H. Liao, J. P. Li, I. Shahid, A. Lodhi, and M. Mansha (2015), Seasonal variations of aerosols in Pakistan: Contributions of domestic anthropogenic emissions and transboundary transport, *Aerosol Air Qual. Res.*, *15*, 1580–1600, doi:10.4209/aaqr.2014.12.0332.

Shi, G.-Y., T. Hayasaka, A. Ohmura, Z.-H. Chen, B. Wang, J.-Q. Zhao, H.-Z. Che, and L. Xu (2008), Data quality assessment and the long-term trend of ground solar radiation in China, *J. Appl. Meteorol. Climatol.*, *47*, 1006–1016, doi:10.1175/2007JAMC1493.1.

Shimizu, A., N. Sugimoto, I. Matsui, K. Arao, I. Uno, T. Murayama, N. Kagawa, K. Aoki, A. Uchiyama, and A. Yamazaki (2004), Continuous observations of Asian dust and other aerosols by polarization lidar in China and Japan during ACE-Asia, *J. Geophys. Res.*, *109*, D19S17, doi:10.1029/2002JD003253.

Sikka, D. R. (1980), Some aspects of the large scale fluctuations of summer monsoon rainfall over India in relationship to fluctuations in the planetary and regional scale 2 parameters, *Proc. Indian Acad. Sci. U.S.A.*, *89*, 179–195.

Simmonds, I., D. H. Bi, and P. Hope (1999), Atmospheric water vapor flux and its association with rainfall over China in summer, *J. Clim.*, *12*, 1353–1367.

Singh, S. K., K. Soni, T. Bano, R. S. Tanwar, S. Nath, and B. C. Arya (2010), Clear-sky direct aerosol radiative forcing variations over mega-city Delhi, *Ann. Geophys.*, *28*, 1157–1166, doi:10.5194/angeo-28-1157-2010.

Skamarock, W. C., J. B. Klemp, J. Dudhia, D. O. Gill, D. M. Barker, W. Wang, and J. G. Powers (2005), A description of the advanced research WRF version 2, *NCAR Tech. Note NCAR/TN-468+STR*, 88 pp., Natl. Cent. for Atmos. Res., Boulder, Colo.

Solmon, F., V. S. Nair, and M. Mallet (2015), Increasing Arabian dust activity and the Indian summer monsoon, *Atmos. Chem. Phys.*, *15*, 8051–8064.

Song, F., T. Zhou, and Y. Qian (2014), Responses of East Asian summer monsoon to natural and anthropogenic forcings in the 17 latest CMIP5 models, *Geophys. Res. Lett.*, *41*, 596–603, doi:10.1002/2013GL058705.

Sotiropoulou, R. E. P., A. Nenes, P. J. Adams, and J. H. Seinfeld (2007), Cloud condensation nuclei prediction error from application of Köhler theory: Importance for the aerosol indirect effect, *J. Geophys. Res.*, *112*, D12202, doi:10.1029/2006JD007834.

Sreekanth, V., K. Niranjan, and B. L. Madhavan (2007), Radiative forcing of black carbon over eastern India, *Geophys. Res. Lett.*, *34*, L17818, doi:10.1029/2007GL030377.

Stohl, A. (2001), A 1-year Lagrangian "climatology" of airstreams in the Northern Hemisphere troposphere and lowermost stratosphere, *J. Geophys. Res.*, *106*, 7263–7279.

Stott, P. A., J. F. B. Mitchell, M. R. Allen, T. L. Delworth, J. M. Gregory, G. A. Meehl, and B. D. Santer (2006), Observational constraints on past attributable warming and predictions of future global warming, *J. Clim.*, *19*, 3055–3069.

Sugimoto, N., A Shimizu, T. Nishizawa, I. Matsui, Y. Jin, P. Khatri, H. Irie, T. Takamura, K. Aoki, and B. Thana (2015), Aerosol characteristics in Phimai, Thailand determined by continuous observation with a polarization sensitive Mie-Raman lidar and a sky radiometer, *Environ. Res. Lett.*, *10*(6), 065003, doi:10.1088/1748-9326/10/6/065003.

Sun, L., X. Xia, P. Wang, and Y. Fei (2014), Do aerosols impact ground observation of total cloud cover over the North China Plain?, *Global Planet. Change*, *117*, 91–95, doi:10.1016/j.gloplacha.2014.03.009.

Takami, A., T. Miyoshi, A. Shimono, and S. Hatakeyama (2005), Chemical composition of fine aerosol measured by AMS at Fukue Island, Japan during APEX period, *Atmos. Environ.*, *39*, 4913–4924.

Takemura, T., T. Nakajima, A. Higurashi, S. Ohta, and N. Sugimoto (2003), Aerosol distributions and radiative forcing over the Asian-Pacific region simulated by Spectral Radiation-Transport Model for Aerosol Species (SPRINTARS), *J. Geophys. Res.*, *108*(D23), 8659, doi:10.1029/2002JD003210.

Tang, J. P., P. Wang, L. J. Mickley, X. Xia, H. Liao, X. Yue, L. Sun, and J. Xia (2013), Positive relationship between liquid cloud droplet effective radius and aerosol optical depth over Eastern China from satellite data, *Atmos. Environ.*, *84*, 244–253, doi:10.1016/j.atmosenv.2013.08.024.

Tang, W. J., K. Yang, J. Qin, C. C. K. Cheng, and J. He (2011), Solar radiation trend across China in recent decades: A revisit with quality-controlled data, *Atmos. Chem. Phys.*, *11*(1), 393–406.
Tao, W.-K., X. Li, A. Khain, T. Matsui, S. Lang, and J. Simpson (2007), Role of atmospheric aerosol concentration on deep convective precipitation: Cloud-resolving model simulations, *J. Geophys. Res.*, *112*, D24S18, doi:10.1029/2007JD008728.
Tett, S. F. B., et al. (2002), Estimation of natural and anthropogenic contributions to twentieth century temperature change, *J. Geophys. Res.*, *107*(D16), 4306, doi:10.1029/2000JD000028.
Trenary, L. L., and W. Han (2013), Local and remote forcing of decadal sea level and thermocline depth variability in the South Indian Ocean, *J. Geophys. Res. Oceans*, *118*, 381–398, doi:10.1029/2012JC008317.
Tripathi, S. N., S. Dey, V. Tare, and S. K. Satheesh (2005), Aerosol black carbon radiative forcing at an industrial city in northern India, *Geophys. Res. Lett.*, *32*, doi:10.1029/2005GL022515.
Twomey, S. (1977), The influence of pollution on the shortwave albedo of clouds, *J. Atmos. Sci.*, *34*, 1150–1152, doi:10.1175/1520-0469(1977)034<1149:TIOPOT>2.0.CO;2.
Uno, I., *et al.* (2003), Regional chemical weather forecasting system CFORS: Model descriptions and analysis of surface observations at Japanese island stations during the ACE-Asia experiment, *J. Geophys. Res.*, *108*(D23), 8668, doi:10.1029/2002JD002845.
van Curen, R. A., and T. A. Cahill (2002), Asian aerosols in North America: Frequency and concentration of fine dust, *J. Geophys. Res.*, *107*(D24), 4804, doi:10.1029/2002JD002204.
van Donkelaar, A., et al. (2008), Analysis of aircraft and satellite measurements from the Intercontinental Chemical Transport Experiment (INTEX-B) to quantify long-range transport of East Asian sulfur to Canada, *Atmos. Chem. Phys.*, *8*, 2999–3014.
Vernekar, A. D., J. Zhou, and J. Shukla (1995), The effect of Eurasian snow cover on the Indian monsoon, *J. Clim.*, *8*, 248–266.
Vinoj, V., P. J. Rasch, H. Wang, J. Yoon, P. Ma, and K. Landu (2014), Short-term modulation of Indian summer monsoon rainfall by West Asian dust, *Nat. Geosci.*, *7*, 308–313, doi:10.1038/NGEO2107.
Wang, B. (1994), Climatic regimes of tropical convection and rainfall, *J. Clim.*, *7*, 1109–1118.
Wang, B. (2006), *The Asian Monsoon*, Praxis Ltd., Chichester, U. K.
Wang, B., and Q. Ding (2008), The global monsoon: Major modes of annual variations in the tropics, *Dyn. Atmos. Oceans*, *44*(3–4), 165–183, doi:10.1016/j.dynatmoce.2007.05.002.
Wang, B., and L. Ho (2002), Rainy season of the Asian-Pacific summer monsoon, *J. Clim.*, *15*, 386–398.
Wang, B., S. C. Clemons, and P. Liu (2003), Contrasting the Indian and East Asian monsoons: Implications on geologic timescales, *Mar. Geol.*, *201*, 5–21.
Wang, B., Q. Bao, B. Hoskins, G. Wu, and Y. Liu (2008), Tibetan Plateau warming and precipitation change in East Asia, *Geophys. Res. Lett.*, *35*, L14702, doi:10.1029/2008GL034330.
Wang, B., F. Huang, Z. Wu, J. Yang, X. Fu, and K. Kikuchi (2009), Multi-scale climate variability of the South China Sea monsoon: A review, *Dyn. Atmos. Oceans*, *47*, 15–37, doi:10.1016/j.dynatmoce.2008.09.004.
Wang, B., Q. Ding, and J. Liu (2010), Concept of global monsoon, in *The Global Monsoon System Research and Forecast*, pp. 3–14, World Sci., Hackensack, N. J.
Wang, H. J., S. P. He, and J. P. Liu (2013), Present and future relationship between the East Asian winter monsoon and ENSO: Results of CMIP5, *J. Geophys. Res. Oceans*, *118*, 5222–5237, doi:10.1002/jgrc.20332.
Wang, H. J., H. P. Chen, and J. P. Liu (2015), Arctic sea ice decline intensified haze pollution in eastern China, *Atmos. Oceanic Sci. Lett.*, *8*(1), 1–9, doi:10.3878/AOSL20140081.
Wang, J., J. A. Dale, K. E. Pickering, Z. Li, and H. He (2016), Impact of aerosol direct effect on East Asian air quality during the EAST-AIRE campaign, *J. Geophys. Res. Atmos.*, *121*, 6534–6554, doi:10.1002/2016JD025108.
Wang, K. C. (2014), Measurement biases explain discrepancies between the observed and simulated decadal variability of surface incident solar radiation, *Sci. Rep.*, *4*, 6144, doi:10.1038/srep06144.
Wang, K. C., and R. E. Dickinson (2013), Contribution of solar radiation to decadal temperature variability over land, *Proc. Natl. Acad. Sci. U.S.A.*, *110*(37), 14,877–14,882.
Wang, K. C., R. E. Dickinson, and S. L. Liang (2009), Clear sky visibility has decrease over land globally from 1973 to 2007, *Science*, *323*, 1468–1470, doi:10.1126/science.1167549.
Wang, K. C., R. E. Dickinson, M. Wild, and S. Liang (2010a), Evidence for decadal variation in global terrestrial evapotranspiration between 1982 and 2002: 1. Model development, *J. Geophys. Res.*, *115*, D20112, doi:10.1029/2009JD013671.
Wang, K. C., R. E. Dickinson, M. Wild, and S. Liang (2010b), Evidence for decadal variation in global terrestrial evapotranspiration between 1982 and 2002: 2. Results, *J. Geophys. Res.*, *115*, D20113, doi:10.1029/2010JD013847.
Wang, K. C., R. E. Dickinson, M. Wild, and S. Liang (2012a), Atmospheric impacts on climatic variability of surface incident solar radiation, *Atmos. Chem. Phys.*, *12*(20), 9581–9592.
Wang, K. C., R. E. Dickinson, L. Su, and K. E. Trenberth (2012b), Contrasting trends of mass and optical properties of aerosols over the Northern Hemisphere from 1992 to 2011, *Atmos. Chem. Phys.*, *12*(19), 9387–9398.
Wang, Q. Y., Z. L. Wang, and H. Zhang (2016), Impact of anthropogenic aerosols from global, East Asian, and non-East Asian sources on East Asian summer monsoon system, *Atmos. Res.*, *183*, 224–236.
Wang, R., et al. (2014), Trend in global black carbon emissions from 1960 to 2007, *Environ. Sci. Technol.*, *48*, 6780–6787, doi:10.1021/es5021422.
Wang, S. W., and D. Z. Ye (1993), Analysis of the global warming during the last one hundred years, in *Climate Variability*, edited by D. Ye et al, pp. 23–32, China Meteorol. Press, Beijing.
Wang, T., H. J. Wang, O. H. Otterå, Y. Q. Gao, L. L. Suo, T. Furevik, and L. Yu (2013), Anthropogenic agent implicated as a prime driver of shift in precipitation in eastern China in the late 1970s, *Atmos. Chem. Phys.*, *13*, 12,433–12,450.
Wang, X., J. Huang, R. Zhang, B. Chen, and J. Bi (2010), Surface measurements of aerosol properties over northwest China during ARM China 2008 deployment, *J. Geophys. Res.*, *115*, D00K27, doi:10.1029/2009JD013467.
Wang, X. Y., and K. C. Wang (2014), Estimation of atmospheric mixing layer height from radiosonde data, *Atmos. Meas. Tech.*, *7*(6), 1701–1709.
Wang, Y., and L. Zhou (2005), Observed trends in extreme precipitation events in China during 1961–2001 and the associated changes in large-scale circulation, *Geophys. Res. Lett.*, *32*, L09707, doi:10.1029/2005GL022574.
Wang, Y., Q. Wan, W. Meng, F. Liao, H. Tan, and R. Zhang (2011), Long-term impacts of aerosols on precipitation and lightning over the Pearl River Delta megacity area in China, *Atmos. Chem. Phys.*, *11*, 12,421–12,436, doi:10.5194/acp-11-12421-2011.
Wang, Y., A. Khalizov, M. Levy, and R. Zhang (2013), New directions: Light absorbing aerosols and their atmospheric impacts, *Atmos. Environ.*, *81*, 713–715, doi:10.1016/j.atmosenv.2013.09.034.
Wang, Y., R. Zhang, and R. Saravanan (2014a), Asian pollution climatically modulates mid-latitude cyclones following hierarchical modelling and observational analysis, *Nat. Commun.*, *4*, 3098, doi:10.1038/ncomms4098.

Wang, Y., M. Wang, R. Zhang, S. J. Ghan, Y. Lin, J. Hu, B. Pan, M. Levy, J. Jiang, and M. J. Molina (2014b), Assessing the effects of anthropogenic aerosols on Pacific storm track using a multi-scale global climate model, *Proc. Natl. Acad. Sci. U.S.A.*, *111*(19), 6894–6899.
Wang, Z. L., H. Zhang, and X. Shen (2011), Radiative forcing and climate response due to black carbon in snow and ice, *Adv. Atmos. Sci.*, *28*(6), 1336–1344.
Wang, Z. L., H. Zhang, X. W. Jing, and X. D. Wei (2013a), Effect of non-spherical dust aerosol on its direct radiative forcing, *Atmos. Res.*, *120-121*, 112–126, doi:10.1016/j.atmosres.2012.08.006.
Wang, Z. L., H. Zhang, J. Li, X. Jing, and P. Lu (2013b), Radiative forcing and climate response due to the presence of black carbon in cloud droplets, *J. Geophys. Res. Atmos.*, *118*, 3662–3675, doi:10.1002/jgrd.50312.
Wang, Z. L., H. Zhang, and X. Y. Zhang (2016a), Projected response of East Asian summer monsoon system to future reductions in emissions of anthropogenic aerosols and their precursors, *Clim. Dyn.*, *47*(5), 1455–1468.
Wang, Z. L., L. Lin, M. Yang, and Y. Xu (2016b), The effect of future reduction in aerosol emissions on climate extremes in China, *Clim. Dyn.*, doi:10.1007/s00382-016-3003-0.
Warren, S. G., and W. J. Wiscombe (1980), A model for the spectral albedo of snow. II: Snow containing atmospheric aerosols, *J. Atmos. Sci.*, *37*(12), 2734–2745.
Warren, S. G., R. M. Eastman, and C. J. Hahn (2007), A survey of changes in cloud cover and cloud types over land from surface observations, 1971–96, *J. Clim.*, *20*(4), 717–738.
Webster, P. J. (1987), The variable and interactive monsoon, in *Monsoon*, edited by J. Fein and P. Stephens, pp. 269–330, John Wiley, Hoboken, N. J.
Webster, P. J., V. O. Magaña, T. N. Palmer, J. Shukla, R. A. Tomas, M. Yanai, and T. Yasunari (1998), Monsoons: Processes, predictability, and the prospects for prediction, *J. Geophys. Res.*, *103*, 14,451–14,510, doi:10.1029/97JC02719.
Wiedensohler, A., et al. (2009), Rapid aerosol particle growth and increase of cloud condensation nucleus activity by secondary aerosol formation and condensation: A case study for regional air pollution in northeastern China, *J. Geophys. Res.*, *114*, D00G08, doi:10.1029/2008JD010884.
Wilcox, L. J., E. J. Highwood, and N. J. Dunstone (2013), The influence of anthropogenic aerosol on multi-decadal variations of historical global climate, *Environ. Res. Lett.*, *8*, 024033, doi:10.1088/1748-9326/8/2/024033.
Wild, M., B. Trüssel, A. Ohmura, C. N. Long, G. K. Langlo, E. G. Dutton, and A. Tsvetkov (2009), Global dimming and brightening: An update beyond 2000, *J. Geophys. Res.*, *114*, D00D13, doi:10.1029/2008JD011382.
Wilkening, K. E., L. A. Barrie, and M. Engle (2000), Trans-Pacific air pollution, *Science*, *290*, 65–67.
Wu, G., and Y. Zhang (1998), Tibetan Plateau forcing and the timing of the monsoon onset over South Asia and the South China Sea, *Mon. Weather Rev.*, *126*(4), 913–927.
Wu, G., Y. Liu, Q. Zhang, A. Duan, T. Wang, R. Wan, X. Liu, W. Li, Z. Wang, and X. Liang (2007), The influence of mechanical and thermal forcing by the Tibetan Plateau on Asian climate, *J. Hydrometeorol.*, *8*, 770–789, doi:10.1175/JHM609.1.
Wu, G. X., Y. M. Liu, B. W. Dong, X. Y. Liang, A. M. Duan, Q. Bao, and J. J. Yu (2012a), Revisiting Asian monsoon formation and change associated with Tibetan Plateau forcing: I. Formation, *Clim. Dyn.*, *39*(5), 1169–1181, doi:10.1007/s00382-012-1334-z.
Wu, G. X., Y. M. Liu, B. He, Q. Bao, A. M. Duan, and F. F. Jin (2012b), Thermal controls on the Asian summer monsoon, *Sci. Rep.*, *2*, 404, doi:10.1038/srep00404.
Wu, G. X., Y. Guan, Y. M. Liu, J. H. Yan, and J. Y. Mao (2012c), Air–sea interaction and formation of the Asian summer monsoon onset vortex over the Bay of Bengal, *Clim. Dyn.*, *38*, 261–279, doi:10.1007/s00382-010-0978-9.
Wu, G. X., Y. Liu, B. He, Q. Bao, A. Duan, and F. F. Jin (2012d), Thermal controls on the Asian summer monsoon, *Sci. Rep.*, *2*, 404, doi:10.1038/srep00404.
Wu, G. X., A. M. Duan, Y. M. Liu, J. Yan, B. Liu, S. Ren, Y. Zhang, T. Wang, X. Liang, and Y. Guan (2013), Recent advances in the study on the dynamics of the Asian summer monsoon onset, *Chin. J. Atmos. Sci.*, *37*(2), 211–228.
Wu, G. X., A. M. Duan, Y. M. Liu, J. Y. Mao, R. C. Ren, Q. Bao, B. He, B. Q. Liu, and W. T. Hu (2014), Recent progress in the study of Tibetan Plateau climate dynamics, *Natl. Sci. Rev.*, doi:10.1093/nsr/nwu045.
Wu, J., C. B. Fu, and L. Y. Zhang (2012), Trends of visibility on sunny days in China in the recent 50 years, *Atmos. Environ.*, *55*, 339–346, doi:10.1016/j.atmosenv.2012.03.037.
Wu, J., J. Luo, L. Zhang, L. Xia, D. Zhao, and J. Tang (2014), Improvement of aerosol optical depth retrieval using visibility data in China during the past 50 years, *J. Geophys. Res. Atmos.*, *119*, 13,370–13,387, doi:10.1002/2014JD021550.
Wu, L., H. Su, and J. H. Jiang (2013), Regional simulation of aerosol impacts on precipitation during the East Asian summer monsoon, *J. Geophys. Res. Atmos.*, *118*, 6454–6467, doi:10.1002/jgrd.50527.
Wu, R., and B. P. Kirtman (2007), Observed relationship of spring and summer East Asian rainfall with winter and spring Eurasian snow, *J. Clim.*, *20*, 1285–1304, doi:10.1175/JCLI4068.1.
Wu, T. W., and Z. A. Qian (2003), The relation between the Tibetan winter snow and the Asian summer monsoon and rainfall: An observational investigation, *J. Clim.*, *16*(12), 2038–2051.
Wu, Y., J. Zhu, H. Che, X. Xia, and R. Zhang (2015), Column-integrated aerosol optical properties and direct radiative forcing based on sun photometer measurements at a semi-arid rural site in Northeast China, *Atmos. Res.*, *157*, 56-65.
Xia, X. (2010), Spatiotemporal changes in sunshine duration and cloud amount as well as their relationship in China during 1954–2005, *J. Geophys. Res.*, *115*, D00K06, doi:10.1029/2009JD012879.
Xia, X. (2012), Significant decreasing cloud cover during 1954–2995 due to more clear-sky days and less overcast days in China and its relation to aerosol, *Ann. Geophys.*, *30*(3), 573–582.
Xia, X. (2013), Variability and trend of diurnal temperature range in China and their relationship to total cloud cover and sunshine duration, *Ann. Geophys.*, *31*(5), 795–804.
Xia, X., and X. Zong (2009), Shortwave versus longwave direct radiative forcing by Taklimakan dust aerosols, *Geophys. Res. Lett.*, *36*, L07803, doi:10.1029/2009GL037237.
Xia, X., Z. Li, B. Holben, P. Wang, T. Eck, H. Chen, M. Cribb, and Y. Zhao (2007a), Aerosol optical properties and radiative effects in the Yangtze Delta region of China, *J. Geophys. Res.*, *112*, D22S12, doi:10.1029/2007JD008859.
Xia, X., Z. Li, P. Wang, H. Chen, and M. Cribb (2007b), Estimation of aerosol effects on surface irradiance based on measurements and radiative transfer model simulations in northern China, *J. Geophys. Res.*, *112*, D22S10, doi:10.1029/2006JD008337.
Xia, X., H. Chen, Z. Li, P. Wang, and J. Wang (2007c), Significant reduction of surface solar irradiance induced by aerosols in a suburban region in northeastern China, *J. Geophys. Res.*, *112*, D22S02, doi:10.1029/2006JD007562.
Xia, X., H. Chen, P. Goloub, W. Zhang, B. Chatenet, and P. Wang (2007d), A compilation of aerosol optical properties and calculation of direct radiative forcing over an urban region in northern China, *J. Geophys. Res.*, *112*, D12203, doi:10.1029/2006JD008119.

Xia, X., et al. (2016), Ground-based remote sensing of aerosol climatology in China: Aerosol optical properties, direct radiative effect and its parameterization, *Atmos. Environ.*, *124*, 243–251.
Xin, J., et al. (2007), Aerosol optical depth (AOD) and Ångstrom exponent of aerosols observed by the Chinese Sun Hazemeter Network from August 2004 to September 2005, *J. Geophys. Res.*, *112*, D05203, doi:10.1029/2006JD007075.
Xu, M., C. P. Chang, C. Fu, Y. Qi, A. Robock, D. Robinson, and H. M. Zhang (2006), Steady decline of east Asian monsoon winds, 1969–2000: Evidence from direct ground measurements of wind speed, *J. Geophys. Res.*, *111*, D24111, doi:10.1029/2006JD007337.
Xu, X., C. Lu, X. Shi, and S. Gao (2008), World water tower: An atmospheric perspective, *Geophys. Res. Lett.*, *35*, L20815, doi:10.1029/2008GL035867.
Xu, X., C. Lu, X. Shi, and Y. Ding (2010), The large-scale topography of China: A factor for seasonal march of the Meiyu-Baiu-Changma in East Asia, *J. Geophys. Res.*, *115*, D02110, doi:10.1029/2009JD012444.
Xu, X., X. Shi, and C. Lu (2012), *Theory and Application for Warning and Prediction of Disastrous Weather Downstream From the Tibetan Plateau*, Nova Sci. Publ., New York.
Xu, X., C. Lu, Y. Ding, X. Shi, Y. Guo, and W. Zhu (2013), What is the relationship between China warm-season precipitation and the change of apparent heat source over the Tibetan Plateau?, *Atmos. Sci. Lett.*, *14*(4), 227–234, doi:10.1002/asl2.444.
Yamaguchi, Y., and T. Takemura (2011), Time evolution of observational time of smog and Asian dust [in Japanese], *Tenki*, *58*, 965–968.
Yan, H., Z. Li, J. Huang, M. Cribb, and J. Liu (2014), Long-term aerosol-mediated changes in cloud radiative forcing of deep clouds at the top and bottom of the atmosphere over the Southern Great Plains, *Atmos. Chem. Phys.*, *14*, 7113–7124, doi:10.5194/acp-14-7113-2014.
Yan, L., X. Liu, P. Yang, Z.-Y. Yin, and G. R. North (2011), Study of the impact of summer monsoon circulation on spatial distribution of aerosols in East Asia based on numerical simulations, *J. Appl. Meteorol. Climatol.*, *50*(11), 2270–2282.
Yanai, M., and G.-X. Wu (2006), Effects of the Tibetan Plateau, in *The Asian Monsoon*, edited by B. Wang, pp. 513–549, Praxis Ltd., Chichester, U. K.
Yanai, M., C. Li, and Z. Song (1992), Seasonal heating of the Tibetan Plateau and its effects on the evolution of the Asian summer monsoon, *J. Meteorol. Soc. Jpn.*, *70*(1B), 319–351.
Yang, S., and K. M. Lau (1998), Influence of SST and ground wetness on the Asian summer monsoon, *J. Clim.*, *11*, 3230–3246.
Yang, X., Z. Yao, Z. Li, and T. Fan (2013a), Heavy air pollution suppresses summer thunderstorms in central China, *J. Atmos. Sol. Terr. Phys.*, *95–96*, 28–40, doi:10.1016/j.jastp.2012.12.023.
Yang, X., M. Ferrat, and Z. Li (2013b), New evidence of orographic precipitation suppression by aerosols in central China, *Meteorol. Atmos. Phys.*, *119*, 17–29, doi:10.1007/s00703-012-0221-9.
Yang, X., and Z. Li (2014), Increases in thunderstorm activity and relationships with air pollution in southeast China, *J. Geophys. Res. Atmos.*, *119*, 1835–1844, doi:10.1002/2013JD021224.
Yang, X., Z. Li, L. Liu, and L. Zhou (2016), Distinct impact of aerosol type on the weekly cycles of thunderstorms in China, *Geophys. Res. Lett.*, *43*, 8760–8768, doi:10.1002/2016GL070375.
Yang, Y., J. Fan, L. R. Leung, C. Zhao, Z. Li, and D. Rosenfeld (2016), Mechanisms contributing to suppressed precipitation in Mt. Hua of central China. Part I: Mountain valley circulation, *J. Atmos. Sci.*, *73*(3), 1351–1366, doi:10.1175/JAS-D-15-0233.1.
Yasunari, T. J., R. D. Koster, W. K. M. Lau, and K.-M. Kim (2015), Impact of snow darkening via dust, black carbon, and organic carbon on boreal spring climate in the Earth system, *J. Geophys. Res. Atmos.*, *120*, 5485–5503, doi:10.1002/2014JD022977.
Ye, D., S. Tao, and M. Li (1958), The seasonal sudden change of atmospheric circulation in June and October, *Acta Meteorol. Sin.*, *29*(4), 249–263.
Ye, J., W. Li, L. Li, and F. Zhang (2013), "North drying and south wetting" summer precipitation trend over China and its potential linkage with aerosol loading, *Atmos. Res.*, *125-126*, 12–19, doi:10.1016/j.atmosres.2013.01.007.
Yeh, T. C., S. W. Lo, and P. C. Chu (1957), On the heat balance and circulation structure in troposphere over Tibetan Plateau, *Acta Meteorol. Sin.*, *28*, 108–121 (in Chinese).
Yeh, T.-C., et al. (1979), *Meteorology of Qinhai- Xizhang (Tibetan) Plateau* [in Chinese], Science, Beijing.
Yin, Y., Q. Chen, L. Jin, B. Chen, S. Zhu, and X. Zhang (2012), The effects of deep convection on the concentration and size distribution of aerosol particles within the upper troposphere: A case study, *J. Geophys. Res.*, *117*, D22202, doi:10.1029/2012JD017827.
Yoon, C. H., J. G. Won, A. H. Omar, S. W. Kim, and B. J. Sohn (2005), Estimation of the radiative forcing by key aerosol types in worldwide locations using a column model and AERONET data, *Atmos. Environ.*, *39*, 6620–6630.
Yu, H., S. C. Liu, and R. E. Dickinson (2002), Radiative effects of aerosols on the evolution of the atmospheric boundary layer, *J. Geophys. Res.*, *107*(D12), 4142, doi:10.1029/2001JD00075.
Yu, H., et al. (2006), A review of measurement-based assessments of the aerosol direct radiative effect and forcing, *Atmos. Chem. Phys.*, *6*, 613–666, doi:10.5194/acp-6-613-2006.
Yu, H., L. A. Remer, M. Chin, H. Bian, R. G. Kleidman, and T. Diehl (2008), A satellite-based assessment of transpacific transport of pollution aerosol, *J. Geophys. Res.*, *113*, D14S12, doi:10.1029/2007JD009349.
Yu, H., L. A. Remer, M. Chin, H. Bian, Q. Tan, T. Yuan, and Y. Zhang (2012), Aerosols from overseas rival domestic emissions over North America, *Science*, *337*, 566–569.
Yu, R., B. Wang, and T. Zhou (2004), Tropospheric cooling and summer monsoon weakening trend over East Asia, *Geophys. Res. Lett.*, *31*, L22212, doi:10.1029/2004GL021270.
Yu, S., V. K. Saxena, and Z. Zhao (2001), A comparison of signals of regional aerosol-induced forcing in eastern China and the southeastern United States, *Geophys. Res. Lett.*, *28*, 713–716, doi:10.1029/2000GL011834.
Yuan, T., Z. Li, R. Zhang, and J. Fan (2008), Increase of cloud droplet size with aerosol optical depth: An observation and modeling study, *J. Geophys. Res.*, *113*, D04201, doi:10.1029/2007JD008632.
Yue, D. L., et al. (2011), Potential contribution of new particle formation to cloud condensation nuclei in Beijing, *Atmos. Environ.*, *45*, 6070–6077.
Yum, S. S., G. Roberts, J. Kim, K. Song, and D. Kim (2007), Submicron aerosol size distributions and cloud condensation nuclei concentrations measured at Gosan, Korea, during the Atmospheric Brown Clouds–East Asian Regional Experiment 2005, *J. Geophys. Res.*, *112*, D22S32, doi:10.1029/2006JD008212.
Yun, K.-S., K.-H. Seo, and K.-J. Ha (2008), Relationship between ENSO and northward propagating ISO in the East Asian summer monsoon system, *J. Geophys. Res.*, *113*, D14120, doi:10.1029/2008JD009901.
Zeng, Q. C. (2005), About King Shun's poem "Southerly wind" [in Chinese], *Clim. Environ. Res.*, *10*, 283–84.
Zhai, P., and F. Ren (1997), Changes in maximum and minimum temperatures of the past 40 years over China [in Chinese], *Acta Meteorol. Sin.*, *55*(4), 418–429.
Zhai, P., and F. Ren (1999), On changes of China's maximum and minimum temperature in 1951–1990, *Acta Meteorol. Sin.*, *13*, 190–278.

Zhai, P., X. Zhang, H. Wan, and X. Pan (2005), Trends in total precipitation and frequency of daily precipitation extremes over China, *J. Clim.*, *18*, 1096–1108, doi:10.1175/JCLI-3318.1.
Zhang, B., et al. (2014), Optical properties and radiative forcing of urban aerosols in Nanjing, China, *Atmos. Environ.*, *83*, 43–52.
Zhang, F., et al. (2014), Aerosol hygroscopicity and cloud condensation nuclei activity during the AC3Exp campaign: Implications for cloud condensation nuclei parameterization, *Atmos. Chem. Phys.*, *14*, 13,423–13,437.
Zhang, F., Z. Li, Y. Li, Y. Sun, Z. Wang, L. Sun, M. Cribb, C. Zhao, P. Li, and Q. Wang (2016), Challenges of parameterizing CCN due to changes in particle physicochemical properties: Implications from observations at a suburban site in China, *Atmos. Chem. Phys.*, *15*, 16,141–16,174.
Zhang, H., Z. Wang, P. Guo, and Z. Wang (2009), A modeling study of the effects of direct radiative forcing due to carbonaceous aerosol on the climate in East Asia, *Adv. Atmos. Sci.*, *26*, 57–66, doi:10.1007/s00376-009-0057-5.
Zhang, H., et al. (2012), Simulation of direct radiative forcing of aerosols and their effects on East Asian climate using an interactive AGCM-aerosol coupled system, *Clim. Dyn.*, *38*, 1675–1693, doi:10.1007/s00382-011-1131-0.
Zhang, H., Q. Yin, T. Nakajima, N. Mukai Makiko, P. Lu, and J. He (2013), Influence of changes in solar radiation on surface temperature in China, *Acta Meteorol. Sin.*, *27*(1), 87–97, doi:10.1007/s13351-013-0109-8.
Zhang, H., C. Zhou, Z. Wang, S. Zhao, and J. Li (2015), The influence of different black carbon and sulfate mixing methods on their optical and radiative properties, *J. Quant. Spectrosc. Radiat. Transfer*, *161*, 105–116, doi:10.1016/j.jqsrt.2015.04.002.
Zhang, L., H. Liao, and J. P. Li (2010a), Impacts of Asian summer monsoon on seasonal and interannual variations of aerosols over eastern China, *J. Geophys. Res.*, *115*, D00K05, doi:10.1029/2009JD012299.
Zhang, L., H. Liao, and J. P. Li (2010b), Impact of the southeast Asian summer monsoon strength on the outflow of aerosols from South Asia, *Ann. Geophys.*, *28*, 277–287.
Zhang, L., and T. Li (2016), Relative roles of anthropogenic aerosols and greenhouse gases in land and oceanic monsoon changes during past 156 years in CMIP5 models, *Geophys. Res. Lett.*, *43*, 5295–5301, doi:10.1002/2016GL069282.
Zhang, Q., J. Meng, J. Quan, Y. Gao, D. Zhao, P. Chen, and H. He (2012), Impact of aerosol composition on cloud condensation nuclei activity, *Atmos. Chem. Phys.*, *12*, 3783–3790, doi:10.5194/acp-12-3783-2012.
Zhang, R. (2001), Relations of water vapor transports from Indian monsoon with those over East Asia and the summer rainfall in China, *Adv. Atmos. Sci.*, *18*, 1005–1017.
Zhang, R., G. Li, J. Fan, D. L. Wu, and M. J. Molina (2007), Intensification of Pacific storm track linked to Asian pollution, *Proc. Natl. Acad. Sci. U.S.A.*, *104*(13), 5295–5299.
Zhang, R., A. F. Khalizov, L. Wang, M. Hu, and W. Xu (2012), Nucleation and growth of nanoparticles in the atmosphere, *Chem. Rev.*, *112*, 1957–2011, doi:10.1021/cr2001756.
Zhang, R. H., Q. Li, and R. N. Zhang (2014), Meteorological conditions for the persistent severe fog and haze event over eastern China in January 2013, *Sci. China Earth Sci.*, *57*, 26–35, doi:10.1007/s11430-013-4774-3.
Zhang, X. Y., Y. Q. Wang, X. C. Zhang, W. Guo, T. Niu, S. L. Gong, Y. Yin, P. Zhao, J. L. Jin, and M. Yu (2008), Aerosol monitoring at multiple locations in China: Contributions of EC and dust to aerosol light absorption, *Tellus, Ser. B*, *60*, 647–656, doi:10.1111/j.1600-0889.2008.00359.
Zhang, Y., T. Li, B. Wang, and G. X. Wu (2002), Onset of the summer monsoon over the Indochina Peninsula: Climatology and interannual variations, *J. Clim.*, *15*(11), 3206–3221.
Zhao, C., X. Tie, and Y. Lin (2006), A possible positive feedback of reduction of precipitation and increase in aerosols over eastern central China, *Geophys. Res. Lett.*, *33*, L11814, doi:10.1029/2006GL025959.
Zhao, C., Y. Wang, Q. Yang, R. Fu, D. Cunnold, and Y. Choi (2010), Impact of East Asian summer monsoon on the air quality over China: View from space, *J. Geophys. Res.*, *115*, D09301, doi:10.1029/2009JD012745.
Zhao, P., Z. Zhou, and J. Liu (2007), Variability of Tibetan spring snow and its associations with the hemispheric extratropical circulation and East Asian summer monsoon rainfall: An observational investigation, *J. Clim.*, *20*, 3942–3955, doi:10.1175/JCLI4205.1.
Zheng, Y., D. Rosenfeld, and Z. Li (2015), Satellite inference of thermals and cloud base updraft speeds based on retrieved surface and cloud base temperatures, *J. Atmos. Sci.*, doi:10.1175/JAS-D-14-0283.1.
Zhou, L., R. E. Dickinson, Y. Tian, J. Fang, Q. Li, R. K. Kaufmann, C. J. Tucker, and R. B. Myneni (2004), Evidence for a significant urbanization effect on climate in China, *Proc. Natl. Acad. Sci. U.S.A.*, *101*, 9540–9544, doi:10.1073/pnas.0400357101.
Zhou, L., R. G. Wu, and R. H. Huang (2010), Variability of surface sensible heat flux over northwest China, *Atmos. Oceanic Sci. Lett.*, *3*(2), 75–80.
Zhou, T., and R. Yu (2005), Atmospheric water vapor transport associated with typical anomalous summer rainfall patterns in China, *J. Geophys. Res.*, *110*, D08104, doi:10.1029/2004JD005413.
Zhou, T., and R. Yu (2006), Twentieth century surface air temperature over China and the globe simulated by coupled climate models, *J. Clim.*, *19*, 5843–5858.
Zhou, T., D. Gong, J. Li, and B. Li (2009), Detecting and understanding the multi-decadal variability of the East Asian Summer Monsoon—Recent progress and state of affairs, *Meteorol. Z.*, *18*, 455–467, doi:10.1127/0941-2948/2009/0396.
Zhou, Y., J. Jiang, A. Huang, M. La, Y. Zhao, and L. Zhang (2013), Possible contribution of heavy pollution to the decadal change of rainfall over eastern China during the summer monsoon season, *Environ. Res. Lett.*, *8*, 044024, doi:10.1088/1748-9326/8/4/044024.
Zhu, J., H. Liao, and J. Li (2012), Increases in aerosol concentrations over eastern China due to the decadal-scale weakening of the East Asian summer monsoon, *Geophys. Res. Lett.*, *39*, L09809, doi:10.1029/2012GL051428.
Zhu, Y. L., H. J. Wang, W. Zhou, and J. H. Ma (2011), Recent changes in the summer precipitation pattern in East China and the background circulation, *Clim. Dyn.*, *36*, 1463–1473, doi:10.1007/s00382-010-0852-9.
Zhu, Y., D. Rosenfeld, X. Yu, and Z. Li (2015), Separating aerosol microphysical effects and satellite measurement artifacts of the relationships between warm rain onset height and aerosol optical depth, *J. Geophys. Res. Atmos.*, *120*, 7726–7736, doi:10.1002/2015JD023547.